Summer 2014

# ABCB11 functions with B1 and B19 to regulate rootward auxin transport

Jesica Elyse Reemmer
*Purdue University*

# PURDUE UNIVERSITY
## GRADUATE SCHOOL
### Thesis/Dissertation Acceptance

This is to certify that the thesis/dissertation prepared

By  Jesica Elyse Reemmer

Entitled
ABCB11 FUNCTIONS WITH B1 AND B19 TO REGULATE ROOTWORD AUXIN TRANSPORT

For the degree of     Master of Science

Is approved by the final examining committee:

Angus Murphy                                        Wendy Peer

Christine Hrycyna

To the best of my knowledge and as understood by the student in the *Thesis/Dissertation Agreement. Publication Delay, and Certification/Disclaimer (Graduate School Form 32)*, this thesis/dissertation adheres to the provisions of Purdue University's "Policy on Integrity in Research" and the use of copyrighted material.

Angus Murphy

Approved by Major Professor(s): _____

Approved by: Robert Joly                                              07/22/2014

Head of the Department Graduate Program                    Date

ABCB11 FUNCTIONS WITH B1 AND B19 TO REGULATE ROOTWARD AUXIN
TRANSPORT


A Thesis

Submitted to the Faculty

of

Purdue University

by

Jesica Elyse Reemmer




In Partial Fulfillment of the

Requirements for the Degree

of

Master of Science




August 2014

Purdue University

West Lafayette, Indiana

For the simple joy of bubbles.

ACKNOWLEDGEMENTS

TABLE OF CONTENTS

LIST OF FIGURES

# ABSTRACT

Reemmer, Jesica Elyse M.S., Purdue University, August 2014. ABCB11 functions with B1 and B19 to regulate rootward auxin transport. Major Professor: Angus Murphy.

Auxin transport is essential for the architecture and development of erect plants. In a network of transporters directing auxin flows, ATP-Binding Cassette (ABC) transporters are a ubiquitous family of proteins that actively transport important substrates, including auxins, across the plasma membrane. ABCB1 and ABCB19 have been shown to account for the majority of rootward auxin transport, but residual fluxes to the root tip in Arabidopsis *b1b19* double mutants implies the involvement of at least one additional auxin transporter in this process. Of specific interest, the severe dwarfism seen in *abcb1abcb19* is strikingly reminiscent of that seen in mutants defective in the F̲K̲506-b̲inding p̲rotein 42 (FKBP42), known as T̲W̲ISTED D̲WARF1 (TWD1). FKBPs function in the maturation and stabilization of proteins, and biochemical evidence indicates that TWD1 functions in ABCB protein maturation and activation in particular. However, although *b1b19* largely phenocopies *twd1*, the relative severity of the *twd1* phenotype further suggests TWD1 activity may regulate the missing rootward auxin transporter. A broad screen including 12 ABCBs now reveals that ABCB11 acts in concert with ABCB1 and ABCB19 in long-distance transport, with an additional role in basipetal auxin transport in leaf tissues. Support for this conclusion comes from analyses of *ABCB11* expression, ABCB11 protein localization and interaction, growth phenotypes of *b11* single and *abcb1b19b11* triple mutants, and auxin transport and accumulation mediated by ABCB11. The comparative analysis of the *ABCB* knock-out lines with *twd1-3* now provides the means to deconvolute the relationship between auxin, ABCB transporters and FKBP42, as well as the mechanisms leading to the phenotypes seen in the *abcb* and *twd1* mutants. My work thus concludes both that B11 mediates long-distance rootward auxin efflux and that such function by ABCB transporters is crucial to describing the *twd* phenotype. Future uses of this work include the possibility of customizing plant architecture through the manipulation of substrate specificity and transport directionality of ABCB transporters.

PREFACE

The work described in this thesis details the characterization of Arabidopsis ABCB11 along with ABCB21 (hereafter B11 and B21) in the pursuit of detailing an integrated map of auxin transporters and their activities. Completing such a systemic auxin transport map will provide a clearer understanding of which ABCB proteins function in auxin transport in plants, provide new insights into the evolution of auxin transport in plants, and suggest the physiological roles of the remaining ABCB transporters. B11 was initially identified as a member of the B subgroup of ABC transporters and was suspected as a potential auxin transporter based on homology to known proteins family members. Primary SDS-PAGE analysis found B11 to be enriched in detergent resistant membrane fractions, implying that it functions at the plasma membrane along with other members of the auxin transport family (Borner et al., 2005). It has also been shown through B11 promoter fusion that expression is found in phloem and xylem parenchyma, cortex, and epidermis, and this implicates B11 in rootward auxin transport in inflorescences, though no claim of significant reduction of auxin transport could be yet be made (Kaneda et al., 2011).

In efforts to complete the whole story of auxin transport, a clever screen leveraging the clustering sequence similarity of the ABCB family genes was conducted by Dr. Haibing Yang. Artificial micro RNA interference (RNAi) technology was employed to generate multiple knock-downs of paralogous ABCBs. These lines could then be tested for phenotypic characteristics typical of auxin transport disruption. Using this approach, B11 was successfully identified as a new player in rootward, long-range auxin transport. This work is described in the first section of the experimental results.

It was also found that ABCB21 showed great promise for further exploration. B21 is a close homolog of ABCB4, but unlike B4, which is root specific (Santelia et al., 2005; Terasaka et al., 2005; Kubeš et al., 2012), B21 was reported to both regulate rootward auxin transport in the mature seedling root and also be expressed in the shoot (Kamimoto et al., 2012). B21 has also already been shown to function as a concentration-dependent uptake/efflux transporter, similar to

B4 in *Saccharomyces cerevisiae* expression assays (Kamimoto et al., 2012). Based on these results, B21 was advanced as a primary candidate for FKBP42-mediated rootward auxin transport as well. However, this research was undertaken in tandem by graduate colleague Mark Jenness in a project separate from my work.

The work presented in the main experimental section makes considerable use of phenotypic comparison between the *twd1-3* mutant and mutant lines constructed to lack multiple ABCB transporters.  The inspiration for this approach arose from previously published observations of the double mutant *abcb1abcb19* (Geisler et al., 2003). Knocking out both auxin transporters ABCB1 and 19 led to a dwarfed phenotype that was strikingly reminiscent of that seen in *twd1-3*. Although *b1b19* largely phenocopies *twd1*, the relative severity of the *twd1* phenotype argues that additional transporters might also be regulated by TWD1 activity.  Thus, the subsequent crossing of *b1b19* with *b11* alleles was initiated by Dr. Nicola Carraro.  I inherited this seed stock and was responsible for extensive backcrossing and genotyping at the outset of the project. Guided by preliminary phenotypic data gathered by Dr. Carraro and Carolina Zamorano Montanez, I set out to characterize the progeny triple mutants. To do so, I began by examining the seedling root phenotypes and conducted extensive observation of the influence of media and light conditions on the severity of observed phenotypes. I also accumulated photographic data of adult phenotypes including a close inspection of leaf size and number.  A comparison of the epidermal cells at the tip of the leaves, where leaf expansion takes place, revealed that *b1b19*, *twd1-3* and both *b11* triple mutants have strongly reduced cell sizes. This provides preliminary suggestion that the smaller leaves result from a decrease in cell size and not from a reduction in total cell count. An investigation of leaf cell size was initiated to further document the curling leaf phenotype, but was delegated to be continued as part of a separate project by colleague Changxu Pang.  Further study of adult phenotypic characterization, particularly of the inflorescence and phyllotactic patterning of the axillary buds was conducted by Dr. Wiebke Tapken after the conclusion of my research.

Alongside establishing a clear phenotypic effect, I further pursued the characterization of the B11 protein through molecular work. I began by visualizing the GFP tagged expression pattern *in planta* of the B11 promoter region, cloned by Dr. Nicola Carraro as a continuation of previous results of promoter fusions visualized by GUS staining published in Kaneda et al., 2011. In addition to mapping the expression of the B11 promoter fusion, I also tested the auxin sensitivity of the B11 promoter.  However, auxin treatments of 10-100 nM NAA solutions

produced no noticeable increase in signal was observed and suggested that ABCB11 may not be regulated by an auxin-sensitive promoter or that such a factor is distally located.

I began my own molecular work by managing to successfully clone the entire B11 CDS into a functional plasmid, a task that had previously resulted in a number of failures. Mutagenesis was employed for the correction of transcription errors with experienced advice provided by Mark Jenness. With this construct, I was able to shuttle the B11 sequence into appropriate destination vectors to express the B11 protein in *Schizosaccharomyces pombe* yeast cells. This allowed me to more closely analyze the transport capacity and capabilities of the ABCB11 protein via a $^{3}$H-IAA transport assay. $^{3}$H-benzoic acid transport assays were also conducted in the same heterologous system by Mark Jenness as a comparison of substrate specificity.

To demonstrate the subcellular localization of the whole B11 protein, I also designed a complete genomic construct with a CFP tag for visualization. The genomic sequence of *ABCB11*, including its native promoter region (-1933 bp), was amplified from *Arabidopsis* genomic DNA for transformation. Due to the length of the full genomic sequence, the insertion was no trivial feat, but was successfully introduced into the Gateway system and transformed into *Agrobacterium tumefaciens*. It was seen that the transient expression of *ABCB11* in the pavement cells of infiltrated *Nicotiana benthamiana* tobacco leaves overlapped with plasma membrane marker FM4-64, suggesting ABCB11 indeed functions as a membrane transporter. I further continued to transform this construct into Col-0 to produce a stable transformant. Initial attempts to visualize a stable expression of native ABCB11 in *Arabidopsis* seedlings yielded negative results, but future attempts may yield clearer results for further study.

My final project was to initiate the creation of an AtABCB11 specific antibody for immunological studies. Peptide sequence was custom synthesized by ThermoScientific based on my design, including a single mismatched substitution of Isoleucine amino acid (from native glutamic acid) to reduce sequence similarity with other ABCB family members and increase specificity for ABCB11 binding. Peptide was conjugated to Keyhole Limpet Hemocyanin and transferred to collaborators Anna Olek and Amber Chase for injection into chickens. From shipments of return eggs of five to seven weeks after initial injection, I created a stock of stabilized IgY as well as aliquots of concentrated antibody via affinity purification. Optimization of concentration and technique will hopefully find these stocks as useful tools for future research.

This thesis was an effort to better understand the function of B11 and how it functions as a factor within the auxin transport pathway. The use of genetic, biochemistry and molecular biology tools has facilitated the characterization of B11. The completed map could be instrumental in introducing additional transporters to manipulate auxin concentration in cases where modification of a target plant genome is impractical, but genetic transformation is possible. The implications of this work is tremendously exciting and it is my hope that this research may be used in future agronomic techniques to improve yields of both crop and biofuel feedstocks.

LITERATURE REVIEW

# Intercellular Transport of Auxin

Jesica Reemmer and Angus Murphy

Abstract

Auxin is an essential hormone that regulates both programmed and plastic plant development. The mechanisms that regulate auxin metabolism, transport and signal transduction are well characterized, although important unresolved questions remain. A unique feature of auxin-regulated plant development is that it involves a combination of cellular perception with polarized auxin gradients across groups of cells, tissues, and organs. Plants achieve these polarized auxin gradients via site-specific synthesis followed by directed and polar patterning of transport components in individual cells. These streams are primarily mediated by three functionally distinct plasma membrane transporter families. Apical–basal and organogenic patterning is largely defined by the polar efflux activities of full-length PIN-FORMED (PIN) facilitators. Dynamic auxin uptake into directed streams is mediated by the AUXIN RESISTANT 1 (AUX1) and LIKE AUX1 (LAX) symporters. Finally, long-distance transport streams are motivated by the ATP-BINDING CASSETTE subfamily B (ABCB) active transporters that continually pump across the plasma membrane and prevent reuptake of exported auxin. Multiple accessory proteins regulate auxin transporter activity and interactions with subcellular environments. The current understanding of cellular transport of auxin will be reviewed in this chapter.

_____

J. Reemmer
Department of Horticulture and Landscape Architecture, Purdue University, West Lafayette, IN 47907, USA

A. Murphy (*)
Department of Horticulture and Landscape Architecture, Purdue University, West Lafayette, IN 47907, USA

Department of Plant Science and Landscape Architecture, University of Maryland, College Park, MD 20742, USA
e-mail: asmurphy@umd.edu
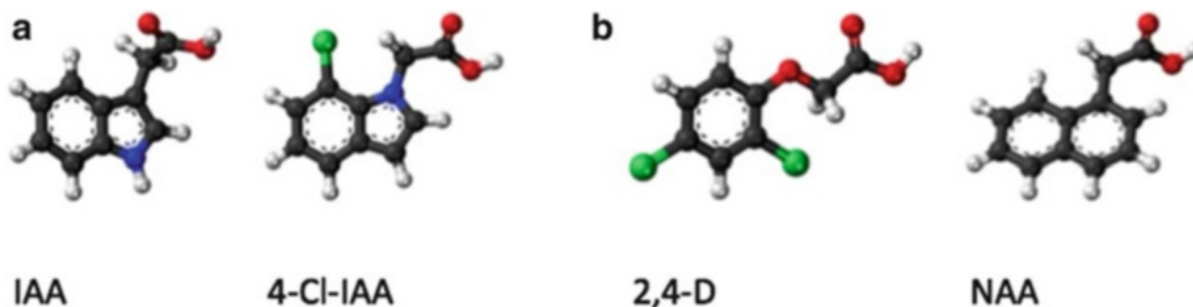
Fig. 5.1 Molecular structures of auxin. IAA and 4-Cl-IAA are endogenous auxins (a), whereas 2,4-D (2,4-dichlorophenoxyacetic acid) and naphtalene-1-acetic acid (NAA) are synthetically produced (b). The synthetic auxins 2,4-D and NAA exhibit chemical traits, such as greater resistance to metabolism or higher rates of diffusion into cells, that make them useful tools for auxin transport studies.

## 1 Introduction

Auxins are indolic plant hormones that function in regulation of cell division and elongation, polar growth, organogenesis, determination of shoot and root architecture, and tropic responses to gravity and light (reviewed in Teale et al. 2006; Benjamins and Scheres 2008). The word auxin is derived from the Greek word "auxein," meaning "to grow/increase" (Kögl and Haagen-Smith 1931). Naturally occurring auxins contain an indole and carboxylic acid group. The most abundant and developmentally important natural auxin is indole-3-acetic acid (IAA), although 4-chloro-indole acetic acid (4-Cl-IAA) is also found in some species (Fig. 5.1a). Synthetic auxins mimic IAA in structure and spacing of the carboxylic acid moiety (Fig. 5.1b).

IAA is produced primarily by multistep conversion of the aminoacyl precursor tryptophan synthesized from chorismate in the chloroplast (Radwanski and Last 1995). In Arabidopsis, tryptophan is converted to indole-3-pyruvic acid (IPA) by TRYPTOPHAN AMINOTRANSFERASE of ARABIDOPSIS 1 (TAA1), also known as TRANSPORT INHIBITOR RESPONSE 2 (TIR2) (Yamada et al. 2009; Tao et al. 2008; Stepanova et al. 2008; see Chap. 2). The second, and rate limiting, step of this pathway is the conversion of IPA to IAA by YUCCA, which catalyzes the oxidative decarboxylation of α-keto acids, including IPA and phenyl pyruvate (PPA) in Arabidopsis (Dai et al. 2013). In the model plant Arabidopsis, the biosynthetic pathway that generates indole glucosinolate as defense compounds also contributes to IAA pools (Sugawara et al. 2009).

Auxins are produced in the shoot apex and other sites of cell division and differentiation (Ljung et al. 2001, 2005; Bhalerao et al. 2002; Cheng et al. 2006, 2007; Stepanova et al. 2008; Tao et al. 2008; Petersson et al. 2009). Emergent evidence of localized auxin production stands in contrast to traditional models in which auxin was thought to be synthesized almost exclusively in the shoot apex and transported to sites of action (Ljung et al. 2001, 2005; Bhalerao et al. 2002; Petersson et al. 2009). Simultaneous elucidation of auxin transport mechanisms over the past 15 years has largely supported models of more distributed synthesis at the expense of shoot apical source models (reviewed in Peer et al. 2011). In particular, closely linked localized synthesis and polar auxin gradients involved in organogenesis have emerged as largely distinct from long-distance auxin transport streams.

When free auxin reaches a cell, two temporally distinct sets of responses may be observed (see Chap. 6). The earliest cell elongation responses to auxin may involve non-transcriptional events. AUXIN-BINDING PROTEIN 1 (ABP1) is a putative auxin receptor localized to the ER and cell periphery and may perceive auxin levels outside of the cell (Löbler and Klämbt 1985; Peer et al. 2013). However, transcriptional activation of genes containing auxin response promoter elements requires derepression of trans-acting Auxin Response Factor (ARF) proteins by the TIR1/ AFB-AUX/IAA co-receptor system (Guilfoyle et al. 1986; Theologis et al. 1985). Auxin binding to the TIR1/AFB F-box ubiquitin ligase subunit and an AUX/IAA co-receptor promotes AUX/IAA degradation to derepress ARF activation of auxin responsive genes expression (Dharmasiri et al. 2005; Kepinski and Leyser 2005). The S-Phase Kinase-Associated Protein 2A (SKP2A) is a similar F-box protein whose function has been found to be additive to the effects of *tir1-1* (del Pozo et al. 2002; Jurado et al. 2010). SKP2A has a different target, however, and its rapid degradation of key regulators of cell cycle control suggests SKP2A mediates auxin- responsive cell cycle control (del Pozo et al. 2006; Jurado et al. 2008).

A unique aspect of auxin-dependent growth regulation is that the polarity and concentration of the auxin transport stream imparts vital information that the system can recognize. As early as 1880, Darwin described the unknown transmission of "some influence" as the agent of seedling bending in response to light (Darwin 1880). Though delayed by nearly 50 years, the theory of lateral auxin relocalization as a mechanism for bending was almost immediately proposed by both Cholodny and Went once the phytohormone auxin was discovered (Cholodny 1927; Went and Thimann 1937). The asymmetric distribution of auxin in this relocalization is responsible for differential

cell elongation and the reorientation of growth evidenced in both photo- and gravitropic responses (see Chap. 16).

Another result of lateral relocalization is uneven accumulation of auxin into local maxima and minima. It is through these concentration differences that auxin sets the blueprint for plant development. These gradients are found to be essential for both the embryonic development of apical–basal polarity (see Chap. 9) and the continued patterning of organogenesis (Reinhardt et al. 2003).

## 2 Cellular Auxin Transport

### 2.1 Cellular Auxin Import Is Motivated by Chemiosmotic Gradients

Cellular uptake and efflux of auxin is motivated by a combination of chemiosmotic forces and ATP hydrolysis. IAA is a weak acid with a pKa of approximately 4.85. In the acidic (pH 5.5) conditions of the apoplast, only a small fraction (a calculated 17 %) of auxin molecules are proton associated (Rubery and Sheldrake 1974; Raven 1975). While protonated auxin preferentially diffuses into the cell membrane, 83% of the auxin pool remains unavailable to lipophilic diffusion in its dissociated form (IAA-). Additionally, cells must be able to selectively take up auxin in competition with other organic acids, and adjust for incorporation of the already limited pool of auxin into other tissues. Thus, in order to meet developmental demands, there is a distinct need for protein importers to actively recruit the traveling auxin signal. In *Arabidopsis*, this transport is carried out by the high- affinity auxin influx transporter AUX1 and its LAX protein family members (Goto et al. 1987; Parry et al. 2001). These permease-like proteins function by harnessing the potential of the proton gradient to drive passive anionic symport of deprotonated IAA at the plasma membrane (Yang et al. 2006).

The importance of symport-driven uptake in enhancing transport streams is observed in *aux1* mutants or transformants wherein AUX/LAX genes are uniformly expressed in all cells of a tissue. Increased uptake activity increases the total auxin found in transport streams, and decreased activity results in decreased concentration of auxin in provascular and vascular tissues compared to wild-type plants (Marchant et al. 2002; Kramer 2004). AUX1 activity in lateral root cap cells has been shown to be essential to uptake of auxin from the root apex into directed

transport streams in the root epidermis that direct gravitropic responses (Swarup et al. 2001; Kleine-Vehn et al. 2006).

In *Arabidopsis*, the three closely related LAX proteins also function in auxin uptake. Comparison of gene structure revealed well-conserved exon/intron boundaries indicative of origination from a common ancestor through gene duplication, but regulation of subcellular trafficking and spatial expression patterns of the LAXs differ considerably from AUX1 (Parry et al. 2001; Bainbridge et al. 2008; Swarup et al. 2008; Jones et al. 2009; Péret et al. 2012). For instance, AUX1 intracellular targeting is regulated by AXR4, which encodes a putative endoplasmic reticulum (ER) chaperone thought to facilitate the correct folding of AUX1 and its export from ER to Golgi (Dharmasiri et al. 2006). However, LAX2 and LAX3 fail to target to the plasma membrane in AUX1-expressing cells, suggesting they may need their own specific ER chaperones (Péret et al. 2012). Mutations have member-specific effects on auxin-related phenotypes as well. Both mutant aux1 and lax3 plants show comparable reduced lateral root emergence. However, *aux1* shows a reduced level of lateral root primordia, whereas *lax3* actually has a threefold increase in primordia compared to the wild type (Swarup et al. 2008). This suggests distinct functional roles for the different family members. However, all three LAX proteins have been shown to retain an auxin influx carrier function, albeit with varying transport specificities, that strongly suggests subfunctionalization (Yang et al. 2006; Swarup et al. 2008; Pe ́ret et al. 2012).

## 2.2 Polar Auxin Transport Defines Local Concentration Gradients

Once inside the neutral conditions of the cytosol, auxin is deprotonated to its polar anionic form ($IAA^-$). This precludes auxin from diffusing back through the lipophilic cell membrane and, unless aided by exporters, auxin remains trapped in the cytosol. In a unique system, auxin can be transported cell to cell in a polar fashion. This short-range directional transport is not only a method of export, but the key to building the patterned auxin gradients crucial in developing tissues (Rubery and Sheldrake 1974; Raven 1975; Zažímalová et al. 2010).

PIN-FORMED (PIN) efflux facilitators derive their name from the striking phenotype of *pin1* mutants in which the inflorescences do not form floral organs and remain bare pin-like stems (Goto et al. 1987). In addition to PIN1, seven other PIN genes are present in the genome of the model species *Arabidopsis*. Studies of plasma membrane-localized, "long" PINs (PIN1, 2, 3, 4, and 7) have shown distinct roles for individual members of the family. PIN1, 4, and 7 are vital in maintaining the polar auxin streams necessary for organogenesis and development along with

AUX1/LAX influx carriers (Reinhardt et al. 2003; Bainbridge et al. 2008). PIN2 activity is crucial to gravitropism and the reflux of auxin at the root tip (Chen et al. 1998; Müller et al. 1998; Friml et al. 2004; Rahman et al. 2010). PIN3 has a restrictive effect on auxin streams important for directional growth (Friml et al. 2002). However, mutational studies reveal that despite their apparent special- ties, PINs largely have redundant functions; the loss of a single PIN protein can be compensated for by the ectopic activities of the other PIN family members (Blilou et al. 2005; Vieten et al. 2005). By mutating multiple PIN gene family members, greater phenotypic and developmental defects can be induced in systems such as embryonic development, root patterning, and lateral root initiation (Benkova et al. 2003; Friml et al. 2003; Blilou et al. 2005). Interestingly, application of the auxin efflux inhibitor naphthylphthalamic acid (NPA) can mimic these effects. The fact that NPA produces these mutant phenotypes indicates a function in the proximity of PINs and has long made NPA a useful tool in studying altered development (Katekar and Geissler 1977).

One of the key purposes of directing local auxin concentrations is the creation of the auxin maxima necessary for organogenesis (see Chaps. 10–12). The auxin streams created by joint AUX/LAX uptake and PIN efflux form the architectural patterns of new organs at the shoot apical meristem (Vernoux et al 2010). Interestingly, a plant lacking the function of all four members of the AUX/LAX auxin influx/transporters is still viable and moderately fertile, although its architecture is significantly altered (Bainbridge et al. 2008). Similarly, while auxin efflux transport proteins ABCB1 and ABCB19 can be visualized in developing embryos, knocking out their function did not result in observable defect to development (Mravec et al. 2008). Treating a double mutant of *pin1* and *aux1* with auxin discovered one clue as to how fertility is maintained in the face of such mutations. Auxin treatment resulted in very large, fused organs at the apex rather than single flowers being produced (Reinhardt et al. 2003). This suggests that AUX1 may be involved in the positioning of organs and restricting their boundaries, thus ensuring that sufficient auxin remains in the necessary layers of the SAM (Reinhardt et al. 2003). Furthermore, these observations imply that the function of concentrating auxin at a maximum is shared, with input from ABCB efflux transporters acting redundantly (Noh et al. 2001).

*2.3 ABCB Efflux Transporters Maintain Long-Distance Streams of Auxin*

Long-range transport of IAA is needed to generate auxin pools in sink tissues, which are important for such developmental processes as stimulating lateral roots and shoot branching. This transport can be accomplished via the phloem vasculature, as is the common route for metabolites.

The best-known member of the B subfamily of ATP-Binding Cassette (ABC) transporters is human ABCB1 (MULTIDRUG RESISTANT 1/PHOSPHO- GLYCOPROTEIN 1), which has been extensively studied for its role in increased resistance to chemotherapeutic agents in breast, brain, and colon cancer cells (Luckie et al. 2003). However, it was apparent that plant homologues of human ABCB1 are not promiscuous drug transporters, and, while applicable in mammalian systems, the use of the multidrug resistance (MDR) nomenclature for this subgroup of proteins has been discontinued (Sidler et al. 1998). The *Arabidopsis thaliana* ABC subfamily B comprises 21 members; four proteins to date clearly mediate high-specificity auxin transport, and a number of highly homologous proteins are thought to mediate auxin transport to some degree (Kamimoto 2012). While both the PIN and AUX/LAX families have been extensively studied in terms of gene expression and protein localization, ABCB proteins are not as well characterized. Phylogenetic and structural analyses indicate that the subclass of ABCB transporters function in auxin transport across plant species, and many studies have focused on the representative ABCB1 and 19 proteins of *Arabidopsis* (reviewed in Blakeslee et al. 2005; Verrier et al. 2008).

ABCB1 was discovered in the attempt to identify proteins conferring broad- spectrum herbicide resistance. Mammalian cells with increased expression of ATP-driven efflux pumps can gain resistance to a wide variety of cytotoxic drugs, and it had been proposed that a similar system might exist in plants (Dudler and Hertig 1992). Instead, it was found that overexpression of AtABCB1 resulted in elongation of seedling hypocotyls when grown under dim light, whereas antisense lines exhibited reduced elongation of the hypocotyls (Sidler et al. 1998). These phenotypes are similar to those witnessed after treating wild-type plants with low concentrations of auxin or an auxin transport inhibitor, for the overexpressor and antisense line, respectively. Further studies revealed that AtABCB1 is localized at the plasma membrane in nonpolar distributions at the shoot and root apices and is predominantly found with polar localization above the root apex. Its expression in both yeast and mammalian systems displays increased efflux of IAA and active synthetic 1-NAA, and *in planta* oxidative breakdown products of IAA

are effluxed as well (Geisler et al. 2005). ABCB1 genes also have auxin transport function in other plant species. In maize, the P-glycoprotein *brachytic2* (*br2*) mutation shares 67 % identity with AtABCB1 and results in dwarfed plants with shortened lower stalk internodes (Leng and Vineyard 1951; Stein 1955; Noh et al. 2001). The mutant gene *dwarf3* similarly results in dwarfed sorghum, a close relation to maize in both genomic organization and plant form (Mullet et al. 2002). While specific phenotypes vary between species, it has been confirmed that both *brachytic2* and *dwarf3* mutant phenotypes result from loss-of-function mutations to ABCB1 genes and display reductions in long-distance transport of auxin (Multani et al. 2003; Bailly et al. 2012). The collective evidence suggests that ABCB1 functions primarily in regions of high auxin concentration to accelerate vectorial transport and maintain long-distance auxin transport streams in combination with PIN and other ABCB family members (Bandyopadhyay et al. 2007).

*Arabidopsis* ABCB19 was quickly linked to its closest homologue *Arabidopsis* ABCB1 (Noh et al. 2001). Both AtABCB1 and AtABCB19 exhibit remarkable structural similarity to the mammalian ABCB1 multidrug resistance transporter known for very broad substrate specificity. However, both AtABCB1 and AtABCB19 exhibit relatively high specificity for auxin as a transport substrate (Titapiwatanakun et al. 2009; Yang and Murphy 2009). Phenotypic analyses of *abcb19* showed epinastic cotyledons, abnormally wrinkled leaves, reduced apical dominance, partial dwarfism, and reduced basipetal polar auxin transport in hypocotyls and inflorescences, all of which are phenotypes consistent with altered auxin response and/or transport. These defects were synergistically enhanced in the double mutant *abcb1abcb19*, suggesting some functional redundancy between these efflux transporters (Noh et al. 2001; Geisler et al. 2003, 2005). Comparison of expression domains revealed that ABCB19 maintains whole-plant auxin flow from the shoot to root apices, whereas ABCB1 function is more restricted to the shoot apex (Geisler et al. 2005). In addition, ABCB19 appears to function in the regulation of differential growth in response to light and gravity stimulation, and it is the substrate target for photoreceptor kinase PHOTOTROPIN1 (PHOT1) (Liscum and Briggs 1995; Noh et al. 2001, 2003; Lin and Wang 2005; Lewis et al. 2007; Wu et al. 2007; Nagashima et al. 2008). Phosphorylation of ABCB19 halts auxin efflux activity, which increases auxin levels at and above the site of inhibition. This action is an early step in the eventual unilateral growth that causes the bend seen in phototropism (Christie et al. 2011).
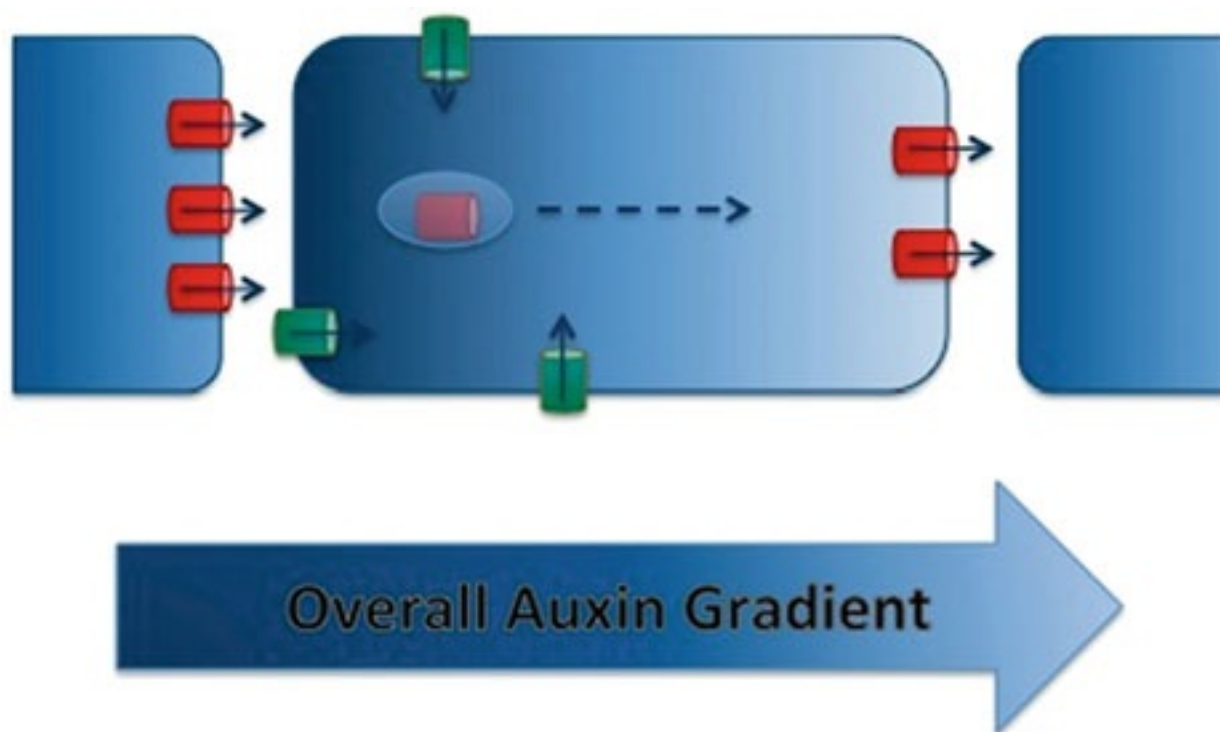
Fig. 5.2 Micropolar auxin gradients. In addition to the auxin gradient at the tissue level, auxin gradients can be thought of to exist within individual cells. This gradient (higher auxin concentration in darker blue) may interact with vesicular trafficking as a way for individual cells to perceive this auxin gradient. Red cylinders denote PIN exporters, green cylinders AUX/LAX importers. Solid black arrows denote auxin transport, broken arrow possible vesicular movement.

## 2.4 Canalization and the Amplification of Streams by PIN Proteins

The notion that auxin and polarity are linked dates back to classic histological studies on developing vascular cells (Sachs 1969). The canalization hypothesis was put forward by Sachs, and later mathematically formulated by Mitchison, as a proposal that a positive feedback exists between the flow of the signal molecule and the capacity for its flow (Sachs 1969; Mitchison 1980). Further experimentation employing an antibody against export protein PIN1 revealed the occurrence of upregulation and relocalization away from the site of exogenous auxin application (Sauer et al. 2006). Studies of such experimental responses strongly suggest that auxin, or a secondary signal produced in response to auxin, is transported into the cell and directs canalization by regulating the polarity of PIN positioning in some cell types. This idea was expanded to include the hypothesis that cells could effectively monitor the auxin concentration in their surrounding environment and respond by pumping auxin toward neighboring cells against a

concentration gradient (Fig. 5.2). To test this hypothesis, computer simulation was employed to handle the hundreds of complex interactions that would occur in such a scenario (Jönsson et al. 2006; Smith et al. 2006). Using theoretical parameters, the canalization hypothesis was shown to amplify small auxin fluxes and generate physiologically plausible results in phyllotactic patterning and vein formation in some tissues (Scarpella et al. 2006; Sauer et al. 2006).

Interesting observations arise from computational modeling. In the attempt to describe PIN allocation and function, two radically different, but conditionally functional, models have been defined that yield discrepant functional conclusions in different locations. In meristematic tissues, PINs act to sense local auxin concentrations, yet in inner tissues a mechanism of flux sensing is called for (Jönsson et al. 2006; Smith et al. 2006; Scarpella et al. 2006; Sauer et al. 2006). Therefore, simplistic models of transport are not sufficient to fully describe the complexities that arise in the actual *in planta* scenario. Boundaries such as cell walls can pose issues that have significant effects on the expected design of a system (Stoma et al. 2008; Bayer et al. 2009). The topologic effect of networks of intracellular compartments can have an appreciable effect on cytoplasmic auxin concentration through sequestration; merely averaging over a cell volume would result in an inappropriate rate constant for describing auxin flux (Merks et al. 2007; Hosek et al. 2012). While computational models provide powerful insights and direction for further research, it is necessary to consider that some of their conclusions may diverge from *in planta* auxin patterns.

## 2.5 PIN Polarity Is Regulated by Phosphorylation

PIN function is influenced by the phosphorylation of kinases in the AGC family (named for homology to mammalian cAMP-dependent protein kinase A, cGMP-dependent protein kinase G, and phospholipid-dependent protein kinase C). This family includes members such as PINOID (PID) kinase, D6 PROTEIN KINASE (D6PK), WAVY ROOT GROWTH 1 (WAG1), WAG2, and PHOTOTROPIN 1 (PHOT1) and PHOT2 (Sakai et al. 2001; Dhonukshe et al. 2010; Huang et al. 2010). Although the mechanisms for the PHOT blue light receptors and the WAG root growth regulators have not been fully elucidated, their corresponding tropisms may be the result of changes in auxin response or transport (Harper et al. 2000; Esmon et al. 2006; Santner and Watson 2006).

PID was previously proposed to be responsible for the phosphorylation of PIN proteins, as it was observed that *pid* mutants phenocopy the pin1 mutant phenotype. From overexpression studies, it was further seen that phosphorylation by PID leads to a basal to apical localization shift of at least PIN1, PIN2, and PIN4 in root cortex and lateral root cap cells (Friml et al. 2003). Shifts triggered by this PID kinase can be reverted by increasing the expression of PP2A, a gene whose product is a subunit of a compound phosphatase. This suggests that PIN polarity is at least in part controlled by PID-dependent phosphorylation (Michniewicz et al. 2007). Another group of kinases, D6PK and its three D6PK-LIKE homologues, have more recently been shown to phosphorylate and directly activate PIN proteins (Zourelidou et al. 2009; Willige et al. 2013). D6PKs colocalize at the basal ends of cells with PINs that mediate rootward auxin transport. However, D6PK does not colocalize with PIN2 in epidermal root cells and, thus, does not appear to regulate PIN2 activity. This is consistent with auxin efflux activity exhibited by PIN2, but not PIN1, 3, or 7 when heterologously expressed in Saccharomyces cerevisiae (Yang and Murphy 2009), where a D6PK ortholog has not been identified. Expression, abundance, localization, and biochemical activity of D6PK are insensitive to auxin and NPA, although the genes are expressed strongly at the sites of lateral root initiation (Zourelidou et al. 2009). Consistent with direct regulation of PIN transport activity, neither loss of function nor overexpression of D6PK causes alteration in PIN polarity. Seedlings of overexpression studies show other differences: D6PK seedlings having defects in lateral root formation, while PID seedlings exhibit agravitropic growth and meristem collapse (Benjamins et al. 2001; Friml et al. 2004).

## 2.6 PIN Proteins Interact with ABP1

Of the long PINs, all are trafficked by dynamic cellular mechanisms (reviewed in Grunewald and Friml 2010). The clathrin-mediated endocytosis of PIN proteins is positively regulated by ABP1. ABP1 normally functions in the recruitment of clathrin to the plasma membrane. However, when ABP1 is bound by auxin, its signaling is blocked. This leads to a reduced internalization of PINs by clathrin- mediated endocytosis. The effect of auxin binding is thus the enhancement of auxin efflux transport (Robert et al. 2010). ABP1 also activates the Rho GTPase ROP6 and its effector RIC1. RIC1 promotes cytoskeletal organization by physically interacting with the microtubules-severing protein KATANIN1 (KTN1) (Fu et al. 2005, 2009; Lin et al. 2013). In this way, the auxin signaling pathway is linked to the regulation of microtubule organization and physically promotes cell elongation.

## 2.7 *In Silico* Modeling of ABCB Proteins Suggests Exclusion

The aforementioned auxin transport mechanisms mainly address the shuttling of auxin discretely to and from the apoplast and cytoplasm of the cell. As efflux transporters, ABCB proteins have two well-studied binding sites in the central pocket through which cytoplasmic auxin can be exported from the cell. Early models of plant ABCBs were designed by threading their sequences on the crystal structure of the Sav1866 bacterial ABC transporter in the closed conformation (Dawson and Locher 2006; Yang and Murphy 2009). Further insight came from the publication and validation of the crystal structure of murine ABCB1 (MmABCB1) in the open conformation (Aller et al. 2009). New structural models identified kingdom-specific candidate substrate-binding regions and suggested an early evolutionary divergence of plant and mammalian ABCBs. While the two experimentally validated IAA substrate-binding sites identified in models based on the closed Sav1866 structure are present in open configuration models, an additional binding site within the outer leaflet was also uncovered (Bailly et al. 2012) (Fig. 5.3a).

This finding led to an elegant development in the conceptualization of auxin transport. Auxin is an amphipathic molecule, and a significant amount of anionic auxin is found partially inserted in the lipid bilayer. A mechanism for the removal of this auxin is thus necessary, particularly in cells such as those adjoining vascular tissues where the apoplastic concentration of auxin is high, and reuptake must be prevented to maintain transport flow (Mravec et al. 2008; Titapiwatanakun et al. 2009; Matsuda et al. 2011). AtABCB1 and AtABCB19 have been shown to function primarily in such exclusion of IAA from cellular membranes (Blakeslee et al. 2007; Wu et al. 2007; Mravec et al. 2008; Bailly et al. 2012). With the rise of vascular plants, PINs appear to have emerged to provide an additional vectorial factor for the control of organogenesis and tropic responses while ABCBs maintained long-distance transport in increasingly longer and complex shoots and roots (Blakeslee et al. 2007; Titapiwatanakun et al. 2009).

## *2.8 ABCB Trafficking and Maturation*

Similar to what is seen with AXR4 and AUX1, folding, trafficking, and activation of ABCB1, ABCB4, and ABCB19 is dependent on the co-chaperone immunophilin-like FK506-BINDING PROTEIN 42/TWISTED DWARF 1 (FKBP42/TWD1) (Bouchard et al. 2006; Bailly et al. 2008; Wu et al. 2010). TWD1 was originally biochemically identified in plasma membrane (PM) fractions and has been shown to be distributed to the endoplasmic reticulum (ER) and tonoplast as well (Murphy et al. 2002; Kamphausen et al. 2002; Geisler et al. 2003). TWD1 acts at the ER surface to fold and activate ABCBs, but appears to function at the PM to maintain ABCB activity
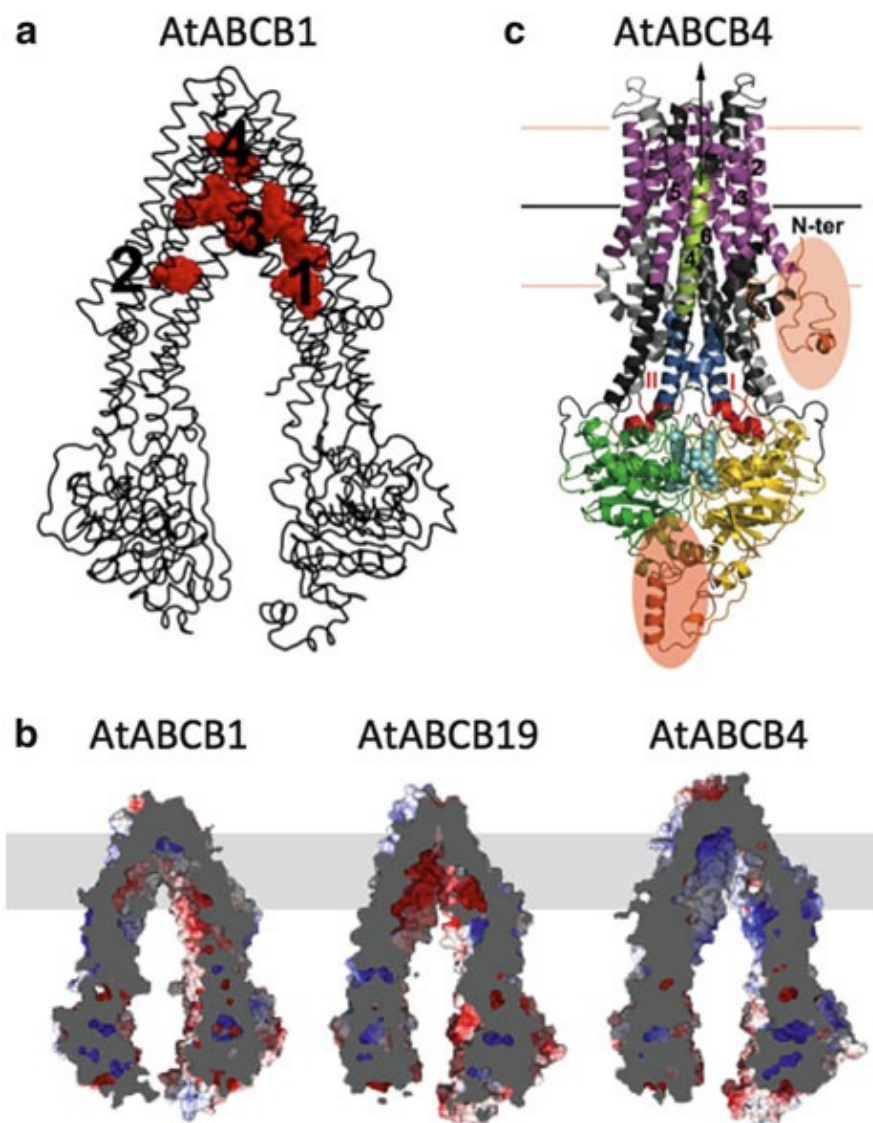
Fig. 5.3 ABCB transporter *in silico* models. (a) Red mesh indicates IAA docking poses for AtABCB1 threaded on MmABCB1 in the open conformation. Site 3 reveals a new region of auxin binding potential that may account for exporter membrane exclusion ability (Bailly et al. 2012). (b) Electrostatic potentials between *Arabidopsis* ABCB proteins in cut view. The predominantly positive surface of the transport chamber of AtABCB4 suggests an evolution of transport specialization (Yang and Murphy 2009). (c) AtABCB4 has additional unique domains as compared to AtABCB exporters. N-terminal coiled-coil domain and linker domain between NBD1 and TMD2 are highlighted in red. TMH4 highlighted in green is shifted down off the membrane plane. These adjustments could be sufficient to alter the regulation and direction of auxin transport (Bailly et al. 2012)

as well (Bailly et al. 2008; Wu et al. 2010; Henrichs et al. 2012; Wang et al. 2013). Although ABCB1, ABCB4, and ABCB19 are largely trapped at the ER in the absence of TWD1, a percentage of all three transporters still reside at the PM (Titapiwatanakun et al. 2009; Wu et al. 2010; Wang et al. 2013). However, TWD1 also colocalizes widely with the lateral marker PEN3/ABCG36 and partially with nonpolar PM proteins and BRI1- GFP (Langowski et al. 2010; Ruzicka et al. 2010; Wang et al. 2013) suggesting other potential interactions.

In attempting to determine the mechanism of activation of ABCB activity by TWD1, TWD1 was found to interact with the PINOID AGC kinase that alters ABCB1 activity by protein phosphorylation (Henrichs et al. 2012). In addition, the plasma membrane localization of TWD1 provides a mechanism to minimize apoplastic reflux in tissues where high auxin contents exist, thus addressing the need to separate shoot- and rootward auxin streams in opposing root tissues and leaf epidermal cells (Geisler et al. 2005; Matsuda et al. 2011). This idea is further in agreement with the acid growth theory prediction of auxin-stimulated lateral proton extrusion for axial cell expansion (Hager 2003). Finally, the severity of the twd1 phenotype in comparison to the *abcb1abcb19* double mutant argues that additional transporters might also be regulated by TWD1 activity.

## 2.9 Membrane Lipids Define Functional Environments

Regardless of the site of TWD1 activation, ABCB transporters must be trafficked to the plasma membrane to function properly. Sphingolipids are essential to establishing a rigid membrane environment to maintain native structure necessary for protein validation and vesicular packaging. Fluorescently labeled ABCB19, for instance, is impaired in its ability to reach the plasma membrane in tsc10a mutant plants (Yang et al. 2013). The tsc10a mutants are deficient in a key enzyme in sphingolipid biosynthesis, and a loss of this function results in epinastic cotyledon development, altered flowering patterns, and reduced hypocotyl elongation phenotypes reminiscent of *abcb19* mutants (Chao et al. 2011). In particular, very long chain fatty acid sphingolipids (VLCFA-SL) are essential for proper development (Markham et al. 2011).

Co-localization experiments showed that inhibiting the synthesis of sphingolipids, either because of the tsc10a mutation or treatment with fumonisin B1 (FB1), results in ABCB19 retention in the ER and the Golgi apparatus and failure to reach the PM. Additionally, fluorescently labeled ABCB19 already present on the membrane accumulates intracellularly after treatment with 1-phenyl-2- hexadecanoylamino-3-morpholino-1-propanol (PPMP) or fumonisin B1 (FB1), both

inhibitors of the synthesis of the sphingolipid ceramide (Yang et al. 2013). These observations suggest sphingolipids are of particular importance at multiple points of ABCB trafficking and maintenance at the plasma membrane.

Once positioned at the plasma membrane, sterols are required to create the correct lipid composition of the plasma membrane environment to allow for the conformational changes associated with transport action. Cell membranes are necessary not only as the boundaries of living units, but also as the critical sites for interactions. The removal of sterols by methyl-beta-cyclodextrin (MβCD) induces the removal of ABCB19 from the plasma membrane. The removal is only partial, although it seems to have a distinct effect on ABCB19, as marker protein PLASMA MEMBRANE INTRINSIC PROTEIN 2A (PIP2-GFP) has no loss of signal at the plasma membrane under the same treatment conditions (Yang et al. 2013). Addition of cholesterol to ABCB19, however, enhances transport activity (Titapiwatanakun et al. 2009). This suggests that ABCB19 recruits sterols to its environment to increase its stability and functioning. It has already been shown that ABC family members are capable of transferring these sterols as well (Tarling and Edwards 2011). With the knowledge that Type 4 P-type ATPases catalyze the translocation of phospholipids between the cytosolic and apoplastic sides of the plasma membrane, it is conceivable that ABCB19 may catalyze a similar flipping action (Tanaka et al. 2011). In keeping with the idea that the third modeled auxin-binding site of ABCB transporters is less specific, this site has been suggested to flip substrates wrapped by lipids to the outer leaflet during the change to the outward-facing conformation (Aller et al. 2009; Bailly et al. 2012).

In *Arabidopsis*, sphingolipids and sterols have been shown to contribute to trafficking of PIN1 and AUX1 in their respective membrane domains as well (Carland et al. 2002; Willemsen et al. 2003; Men et al. 2008; Pan et al. 2009; Roudier et al. 2010; Markham et al. 2011). It is well documented that ABCB19 has a profound effect on the stabilization of PIN1 at the PM; PIN and ABCB proteins function together, and ABCB19 is actually required for PIN1 retention in those membranes (Blakeslee et al. 2007; Mravec et al. 2008; Titapiwatanakun et al. 2009; Yang et al. 2013). Observations of this web of interactions point to the existence of an interactive and dynamic environment that allows multiple facets of regulation to exert control over particular stimuli.

**3 Homeostasis**

As further components of fine-tuning auxin transport, homeostatic transport and subcellular compartmentalization have developed. Among the ABCB and PIN efflux transporters, there are proteins that diverged in function from their family members to play more conditional refining roles. Reversible transporters can be employed to keep auxin levels constant or augment its uptake in cell types where importers are not present (Swarup et al. 2001; Jones et al. 2009; Yang and Murphy 2009). Intracellular partitioning can both influence the effective cytoplasmic concentration and expose auxin molecules to various enzymatic environments for conjugation or degradation.

*3.1 Conditional ABCB Transport Responds to Auxin Concentration*

ABCB4 was originally identified as the most similar *Arabidopsis* homologue to the *Coptis japonica* ATP-dependent berberine influx transporter CjMDR1 (71 % amino acid identity) (Shitan et al. 2003). Despite the fact that *Arabidopsis* does not produce any isoquinoline alkaloids, this homology is greater than the 60 % amino acid sequence identity ABCB4 shares with ABCB1 (Terasaka et al. 2005). The sequence of ABCB4 was also predicted to diverge substantially from other ABCB efflux proteins in the loop region adjoining the first conserved nucleotide-binding domain as well as in a unique coiled-coil interactive domain at its N-terminus (Terasaka et al. 2005). Compilation of characterization data revealed that ABCB4 is a root-specific transporter that functions in shootward epidermal transport of auxin from the root apex, primary and lateral root elongation, and regulation of auxin movement into root hair cells. However, early studies often led to incongruent results that were tissue specific and highly dependent on growth and treatment conditions (Santelia et al. 2005; Terasaka et al. 2005; Cho et al. 2007; Lewis et al. 2007). Despite the fact that ABCB4 belongs to a family of active transporters primarily known for their efflux action, ABCB4 auxin efflux is conditional, mediating import at very low IAA concentrations but reversing rapidly to stronger export activity with increased internal IAA levels (Yang and Murphy 2009; Kim et al. 2010; Kubes et al. 2012). This homeostatic role is consistent with the need to balance auxin streams in root epidermal cells and would be expected as a plasma membrane complement to short PIN function at the ER (Mravec et al. 2009; Ding et al. 2012; see below and Chap. 4).

*3.2 In Silico Modeling Supports ABCB Homeostatic Function*

ABC transporters, regardless of the direction in which they transport substrates, have a basic conserved structure of two transmembrane domains (TMDs) and two nucleotide-binding domains (NBDs) (Dawson and Locher 2006). Using these NBDs, ATP is expended in a "power stroke" that drives the rearrangement of the TMDs between open and closed conformations (Hopfner et al. 2000). But confined to this general structure, from where does the capacity for import arise? Indeed, AtABCB4 has a closer alignment with efflux transporters MmABCB1 and Sav1866 than with other ABC importers (Bailly et al. 2012). The explanation lies in the differences between the charge potentials of the binding pocket. When AtABCB1 faces the cytosol, it presents an environment that is predominantly negative at the opening of the cavity and weakens in charge nearer the interior binding regions. AtABCB19 also displays a similar distribution of negative to neutral electrostatic potentials. Strikingly, AtABCB4 presents the opposite charge, having a neutral to positive electrostatic surface spanning the entire binding pocket (Bailly et al. 2012) (Fig. 5.3b). This strongly suggests that these proteins have significantly diverged and adopted specialized functions. A model could be proposed in which ABCB4, due to its altered binding potential, does not engage auxin when cytoplasmic concentrations are low but rather switches conformation to export either other cargo or remains independent of substrate entirely (Procko et al. 2009). This would result in empty auxin-binding sites being exposed to the apoplast, and a net uptake activity could result upon restoration to the open, cytosolic-facing conformation (Aller et al. 2009). This scenario would account for auxin efflux activity when challenged with greater concentration of cytosolic auxin, as well as the observed lack of saturable influx kinetics (Dawson and Locher 2006; Yang and Murphy 2009). In addition to electrostatic potential differences, ABCB4 displays three other notable structural traits that are not present in ABCB1 or ABCB19. A shift in the hydrophobic region of transmembrane helix 4 would change its positioning in respect to the plasma membrane and thus significantly alter the distances and interactions between the second intercellular loop and its NBD, resulting in altered binding and transport properties (Yang and Murphy 2009). Docking simulations also identified two additional coiled coil domains for ABCB4, one of which is shared with ABCB14 guard cell malate importer and CjMDR1 putative berberine importer (Shitan et al. 2003; Lee et al. 2008; Yang and Murphy 2009) (Figs. 5.3c). These N-terminal domains may be interaction sites in which other proteins could further shift the positioning of the transmembrane helices.

In addition to the activities of ABCB4, it was expected that another protein would share this conditional function. Most plant ABCB members exist with a paralog, and ABCB21 indeed shares 68% nucleotide identity and 79% amino acid identity with ABCB4. These proteins are grouped in clade II of the phylogenic tree of P-glycoproteins, which is distinct from clade I where ABCB1 and ABCB19 are classified (Knöller et al. 2010). Characterization of ABCB21 revealed an NPA-sensitive, plasma membrane-localized auxin transporter with strong expression in the abaxial side of cotyledons, junctions of aerial lateral organs, and root pericycle cells adjacent to the protoxylem poles. However, likeness of ABCB21 auxin transport to that of ABCB4 was not as strong as anticipated, as time course experiments with low concentration (300 nM) of IAA showed a different pattern of seedling response to exogenously added IAA. This suggests a different physiological role for ABCB21 from that of ABCB4. When cytoplasmic IAA concentration was increased by preloading IAA into yeast cells however, IAA uptake activity by ABCB21 was abolished. This same effect is seen in the activity of ABCB4 and suggests that ABCB21 also functions as a facultative auxin transporter in plant cells (Kamimoto et al. 2012).

### 3.3 "Short" PIN and PIN-Like Proteins Act in ER Compartmentalization of Auxin

In contrast to "long" PIN plasma membrane efflux facilitators, PIN5, 6, and 8 encode "short" proteins with a reduced or absent central hydrophilic loop (see Chap. 4). Unlike their longer, plasma membrane-localized family members, short PINs reside in endomembrane structures where they are hypothesized to function in the homeostatic compartmentalization of auxin (Mravec et al. 2009). This sequestration within the ER would both reduce the pool of auxin available for cell-to-cell transport and alter intracellular perception and nuclear signaling. Although the motive force for auxin efflux via short PINs is not known, recent studies have unveiled the important implications of their activity. Overexpression of PIN5, for example, leads to a dramatic shift in the profile of auxin metabolites. Upon induction of overexpressed PIN5, levels of free IAA and IAA-glucosyl ester nearly vanish, while there is increased accumulation of amino acid–auxin conjugates (Mravec et al. 2009). This implicates an unexpected role for PIN5 in controlling the metabolic fate of intracellular auxin.
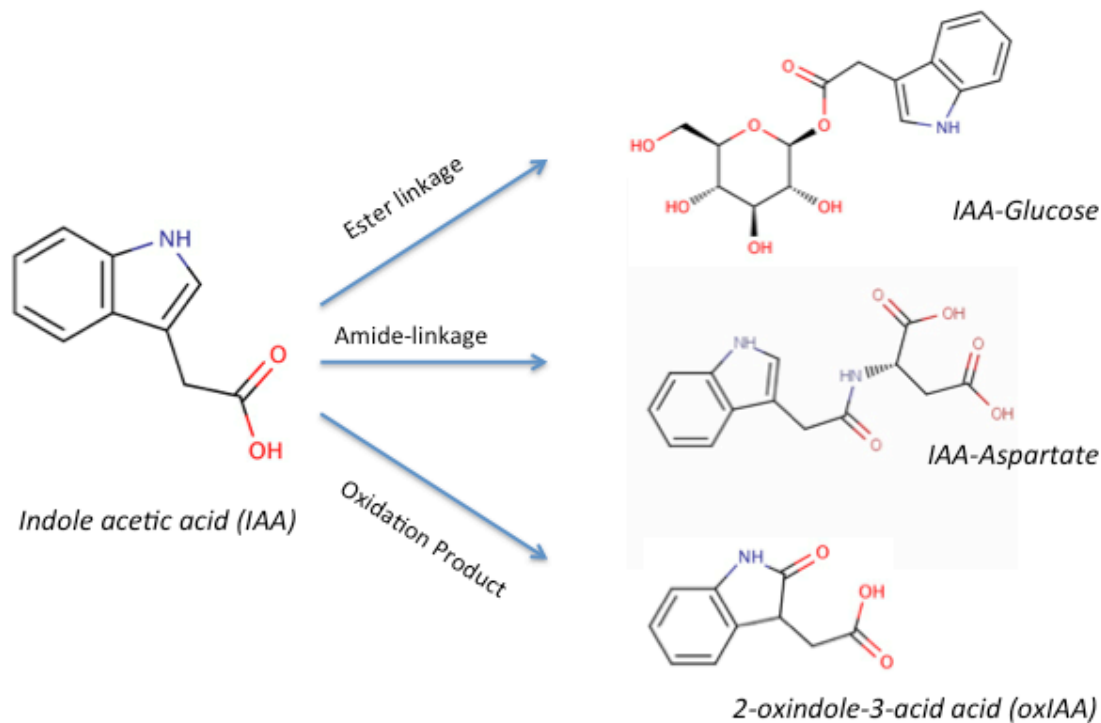
Fig. 5.4. Inactivation of auxin. To attenuate the signal, auxin can undergo reversible or irreversible modification. Conjugates of auxin are found mainly in one of three forms: ester-linked to sugars, amide-linked to amino acids, or amide-linked to peptides or proteins. Many conjugation products can be hydrolyzed to reactivate auxin. Other modifications, such as oxidation, are terminal.

On the other hand, PIN6 and PIN8 have been shown to act antagonistically to PIN5 in directional auxin efflux (Ding et al. 2012; Sawchuk et al. 2013). In contrast to PIN5 overexpression studies, when PIN8 is overexpressed, elevated levels of free IAA and ester-conjugated IAA are observed (Dal Bosco et al. 2012). It is yet unknown how these complementary activities are regulated, although varying hypotheses have been proposed. One suggestion is that PIN6 and PIN8 may serve to move auxin from the lumen of the ER to the nucleus for signaling and thus regulate auxin- dependent transcriptional activity (Dal Bosco et al. 2012). Alternatively, these PINs could have different affinities for alternate auxins or auxin conjugates and form a more complex regulatory network for control of intracellular auxin levels (Sawchuk et al. 2013). Characterization of these PINs points to the possibility of highly specialized and conditional functions. PIN8 has been shown to specifically accumulate in pollen and functions in the development of the pollen tube and auxin homeostasis of the male gametophyte (Ganguly et al.

2010; Ding et al. 2012; Dal Bosco et al. 2012). PIN6 has been shown to act in floral development in *Arabidopsis* and maintains the auxin homeostasis required for proper nectary function (Bender et al. 2013). Studies of vein patterning and defects have led to the conclusions that PIN6 can act redundantly with PIN8 (Sawchuk et al. 2013).

A complicating factor is that *in silico* analyses indicate that some members of the PIN-LIKES (PILS) family exhibit a topology that would include a central hydrophilic loop similar to that of the PIN family (see Chap. 4). Characterization of these seven family members revealed that PILS localize to the ER and stimulate intra- cellular auxin accumulation, potentially contributing to the regulation of auxin metabolism via compartmentalization. The decreased levels of free IAA in PILS2 and PILS5 overexpressors and increase of auxin conjugates in double mutant pils2pils5 are reminiscent of similarly altered PIN5 activity (Barbez et al. 2012).

## 4 Rectification: The Oxidation of Auxin Irreversibly Terminates Auxin Transport and Signaling

Ultimately, auxin that has been transported from cell to cell must be redirected or catabolized to terminate response processes in destination cells. Auxin can be reversibly conjugated for temporary inactivation or can be eliminated from the system via irreversible catabolism (Fig. 5.4). The metabolites oxIAA and oxIAA-hexose (oxIAA-Hex) are the major degradation products of IAA and are not transported in polar streams (Östin et al. 1998; Kai et al. 2007; Novák et al. 2012; Kubeš et al. 2012). These oxidation products are terminally inactivated and no longer induce the expression of auxin-responsive genes, as tested with auxin-inducible reporters DR5rev:GFP and 2XD0:GUS (Peer et al. 2013). However, addition of oxIAA does activate IAA transport mediated by ABCB1 and 4 (Geisler et al. 2005; Kubeš et al. 2012; Peer et al. 2013).

## 5 Conclusions

In conclusion, the phytohormone auxin is found to function in a tremendously complex system that requires a profusion of interacting proteins and specifically defined lipid environments to be synthesized, perceived, and (particularly) transported. The level of refinement required to transport auxin distinctly for diverse plans such as polar gradients, organogenic concentrations, long-distance sinks, and intracellular sequestration is staggering. While we have a conceptual

blueprint of auxin cellular transport to guide our research, the complexity of the cellular transport systems makes direct measurements difficult. Compartmentalization of auxin has an unaccounted influence on effective concentrations that will greatly impact the results of intercellular transport models.

Compared to the well-defined ATP-driven export activity of ABCB proteins and the H+ symport activity of AUX1/LAX proteins, PIN function remains ill defined at the molecular level. Currently, there exist no crystal structures for PIN proteins or their close homologues, and the best conceptual models available are inspired by distantly related microbial transporters (Galvan-Ampudia and Offringa 2007; Peer and Murphy 2007). Determining the true structure of PIN proteins may shed some light on putative substrates capable of maintaining a sufficient gradient for this purpose.

# References

Aller SG, Yu J, Ward A, Weng Y, Chittaboina S, Zhuo R, Harrell PM, Trinh YT, Zhang Q, Urbatsch IL, Chang G (2009) Structure of P-glycoprotein reveals a molecular basis for poly- specific drug binding. Science 323:1718–1722

Bailly A, Sovero V, Vincenzetti V, Santelia D, Bartnik D, Koenig BW, Mancuso S, Martinoia E, Geisler M (2008) Modulation of P-glycoproteins by auxin transport inhibitors is mediated by interaction with immunophilins. J Biol Chem 283:21817–21826

Bailly A, Yang H, Martinoia E, Geisler M, Murphy AS (2012) Plant lessons: exploring ABCB functionality through structural modeling. Front Plant Sci 2:108

Bainbridge K, Guyomarch S, Bayer E, Swarup R, Bennett M, Mandel T, Kuhlemeier C (2008) Auxin influx carriers stabilize phyllotactic patterning. Genes Dev 22:810–823

Bandyopadhyay A, Blakeslee JJ, Lee OR, Mravec J, Sauer M, Titapiwatanakun B, Makam SN, Bouchard R, Geisler M, Martinoia E, Friml J, Peer WA, Murphy AS (2007) Interactions of PIN and PGP auxin transport mechanisms. Biochem Soc Trans 35:137–141

Barbez E, Kubeš M, Rolčík J, Béziat C, Pěnčík A, Wang B, Rosquete MR, Zhu J, Dobrev PI, Lee Y, Zažímalová E, Petrášek J, Geisler M, Friml J, Kleine-Vehn J (2012) A novel putative auxin carrier family regulates intracellular auxin homeostasis in plants. Nature 485:119–122

Bayer EM, Smith RS, Mandel T, Nakayama N, Sauer M, Prusinkiewicz P, Kuhlemeier C (2009) Integration of transport-based models for phyllotaxis and midvein formation. Genes Dev 23:373–384

Bender RL, Fekete ML, Klinkenberg PM, Hampton M, Bauer B, Malecha M, Lindgren K, Maki JA, Perera MA, Nikolau BJ, Carter CJ (2013) PIN6 is required for nectary auxin response and short stamen development. Plant J 74:893-904

Benjamins R, Scheres B (2008) Auxin: the looping star in plant development. Annu Rev Plant Biol 59:443–465

Benjamins R, Quint A, Weijers D, Hooykaas P, Offringa R (2001) The PINOID protein kinase regulates organ development in Arabidopsis by enhancing polar auxin transport. Development 128:4057–4067

Benkova E, Michniewicz M, Sauer M, Teichmann T, Seifertova D, Jurgens G, Friml J (2003) Local, efflux-dependent auxin gradients as a common module for plant organ formation. Cell 115:591–602

Bhalerao RP, Eklof J, Ljung K, Marchant A, Bennett M, Sandberg G (2002) Shoot-derived auxin is essential for early lateral root emergence in Arabidopsis seedlings. Plant J 29:325–332

Blakeslee JJ, Peer WA, Murphy AS (2005) Auxin transport. Curr Opin Plant Biol 8:494–500 Blakeslee JJ, Bandyopadhyay A, Lee OR, Mravec J, Titapiwatanakun B, Sauer M, Makam SN, Cheng Y, Bouchard R, Adamec J, Geisler M, Nagashima A, Sakai T, Martinoia E, Friml J, Peer WA, Murphy AS (2007) Interactions among PIN-FORMED and P-glycoprotein auxin transporters in Arabidopsis. Plant Cell 19:131–147

Blilou I, Xu J, Wildwater M, Willemsen V, Paponov I, Friml J, Heidstra R, Aida M, Palme K, Scheres B (2005) The PIN auxin efflux facilitator network controls growth and patterning in Arabidopsis roots. Nature 433:39–44

Bouchard R, Bailly A, Blakeslee JJ, Oehring SC, Vincenzetti V, Lee OR, Paponov I, Palme K, Mancuso S, Murphy AS, Schulz B, Geisler M (2006) Immunophilin-like TWISTED DWARF1 modulates auxin efflux activities of Arabidopsis P-glycoproteins. J Biol Chem 281:30603– 30612

Carland FM, Fujioka S, Takatsuto S, Yoshida S, Nelson T (2002) The identification of CVP1 reveals a role for sterols in vascular patterning. Plant Cell 14:2045–2058

Chao DY, Gable K, Chen M, Baxter I, Dietrich CR, Cahoon EB, Guerinot ML, Lahner B, Lu S, Markham JE, Morrissey J, Han G, Gupta SD, Harmon JM, Jaworski JG, Dunn TM, Salt DE (2011) Sphingolipids in the root play an important role in regulating the leaf ionome in Arabidopsis thaliana. Plant Cell 23:1061–1081

Chen R, Hilson P, Sedbrook J, Rosen E, Caspar T, Masson PH (1998) The Arabidopsis thaliana AGRAVITROPIC 1 gene encodes a component of the polar-auxin-transport efflux carrier. Proc Natl Acad Sci 95:15112–15117

Cheng Y, Dai X, Zhao Y (2006) Auxin biosynthesis by the YUCCA flavin monooxygenases controls the formation of floral organs and vascular tissues in Arabidopsis. Genes Dev 20:1790–1799

Cheng Y, Dai X, Zhao Y (2007) Auxin synthesized by the YUCCA flavin monooxygenases is essential for embryogenesis and leaf formation in Arabidopsis. Plant Cell 19:2430–2439

Cho M, Lee SH, Cho HT (2007) P-Glycoprotein4 displays auxin efflux transporter like action in Arabidopsis root hair cells and tobacco cells. Plant Cell 19:3930–3943

Cholodny N (1927) Wuchshormone und Tropismen bei den Pflanzen. Biol Zent Bl 47:604–626 Christie JM, Yang H, Richter GL, Sullivan S, Thomson CE, Lin J, Titapiwatanakun B, Ennis M, Kaiserli E, Lee OR, Adamec J, Peer WA, Murphy AS (2011) phot1 inhibition of ABCB19 primes lateral auxin fluxes in the shoot apex required for phototropism. PLoS Biol 9:e1001076

Dai X, Mashiguchi K, Chen Q, Kasahara H, Kamiya Y, Ojha S, DuBois J, Ballou D, Zhao Y (2013) The biochemical mechanism of auxin biosynthesis by an Arabidopsis YUCCA flavin-containing monooxygenase. J Biol Chem 288:1448–1457

Dal Bosco C, Dovzhenko A, Liu X, Woerner N, Rensch T, Eismann M, Eimer S, Hegermann J, Paponov IA, Ruperti B, Heberle-Bors E, Touraev A, Cohen JD, Palme K (2012) The endoplasmic reticulum localized PIN8 is a pollen-specific auxin carrier involved in intracellular auxin homeostasis. Plant J 71:860-870

Darwin C (1880) The power of movement in plants. John Murray, London, p 474

Dawson RJ, Locher KP (2006) Structure of a bacterial multidrug ABC transporter. Nature 443:180–185

Del Pozo JC, Boniotti MB, Gutierrez C (2002) Arabidopsis E2Fc functions in cell division and is degraded by the ubiquitin-SCF(AtSKP2) pathway in response to light. Plant Cell 14:3057– 3071

Del Pozo JC, Diaz-Trivino S, Cisneros N, Gutierrez C (2006) The balance between cell division and endoreplication depends on E2FC- DPB, transcription factors regulated by the ubiquitin– SCFSKP2A pathway in Arabidopsis. Plant Cell 18:2224–2235

Dharmasiri N, Dharmasiri S, Estelle M (2005) The F-box protein TIR1 is an auxin receptor. Nature 435:441–445

Dharmasiri S, Swarup R, Mockaitis K, Dharmasiri N, Singh SK, Kowalchyk M, Marchant A, Mills S, Sandberg G, Bennett MJ, Estelle M (2006) AXR4 is required for localization of the auxin influx facilitator AUX1. Science 312:1218–1220

Dhonukshe P, Huang F, Galvan-Ampudia CS, Mahonen AP, Kleine-Vehn J, Xu J, Quint A, Prasad K, Friml J, Scheres B, Offringa R (2010) Plasma membrane-bound AGC3 kinases phosphorylate PIN auxin carriers at TPRXS(N/S) motifs to direct apical PIN recycling. Development 137:3245–3255

Ding Z, Wang B, Moreno I, Duplakova N, Simon S, Carraro N, Reemmer J, Pencik A, Chen X, Tejos R, Skupa P, Pollmann S, Mravec J, Petrasek J, Zažímalová E, Honys D, Rolcik J, Murphy A, Orellana A, Geisler M, Friml J (2012) ER-localized auxin transporter PIN8 regulates auxin homeostasis and male gametophyte development in Arabidopsis. Nat Commun 3:941

Dudler R, Hertig C (1992) Structure of an mdr-like gene from Arabidopsis thaliana: evolutionary implications. J Biol Chem 267:5882–5888

Esmon CA, Tinsley AG, Ljung K, Sandberg G, Hearne LB, Liscum E (2006) A gradient of auxin and auxin-dependent transcription precedes tropic growth responses. Proc Natl Acad Sci USA 103:236–241

Friml J, Wisniewska J, Benkova E, Mendgen K, Palme K (2002) Lateral relocation of auxin efflux regulator PIN3 mediates tropism in Arabidopsis. Nature 415:806–809

Friml J, Vieten A, Sauer M, Weijers D, Schwarz H, Hamann T, Offringa R, Ju̇rgens G (2003) Efflux-dependent auxin gradients establish the apical-basal axis of Arabidopsis. Nature 426:147–153

Friml J, Yang X, Michniewicz M, Weijers D, Quint A, Tietz O, Benjamins R, Ouwerkerk PB, Ljung K, Sandberg G, Hooykaas PJ, Palme K, Offringa R (2004) A PINOID-dependent binary switch in apical-basal PIN polar targeting directs auxin efflux. Science 306:862–865

Fu Y, Gu Y, Zheng Z, Wasteneys G, Yang Z (2005) Arabidopsis interdigitating cell growth requires two antagonistic pathways with opposing action on cell morphogenesis. Cell 120:687– 700

Fu Y, Xu T, Zhu L, Wen M, Yang Z (2009) A ROP GTPase signaling pathway controls cortical microtubule ordering and cell expansion in Arabidopsis. Curr Biol 19:1827–1832

Galvan-Ampudia CS, Offringa R (2007) Plant evolution: AGC kinases tell the auxin tale. Trends Plant Sci 12:541–547

Ganguly A, Lee SH, Cho M, Lee OR, Yoo H, Cho HT (2010) Differential auxin-transporting activities of PIN-FORMED proteins in Arabidopsis root hair cells. Plant Physiol 153:1046– 1061

Geisler M, Kolukisaoglu HU, Bouchard R, Billion K, Berger J, Saal B, Frangne N, Koncz- Kalman Z, Koncz C, Dudler R, Blakeslee JJ, Murphy AS, Martinoia E, Schulz B (2003) TWISTED DWARF1, a unique plasma membrane-anchored immunophilin-like protein, inter- acts with Arabidopsis multidrug resistance-like transporters AtPGP1 and AtPGP19. Mol Biol Cell 14:4238–4249

Geisler M, Blakeslee JJ, Bouchard R, Lee OR, Vincenzetti V, Bandyopadhyay A, Titapiwatanakun B, Peer WA, Bailly A, Richards EL, Ejendal KF, Smith AP, Baroux C, Grossniklaus U, Muller A, Hrycyna CA, Dudler R, Murphy AS, Martinoia E (2005) Cellular efflux of auxin catalyzed by the Arabidopsis MDR/PGP transporter AtPGP1. Plant J 44:179–194

Goto N, Starke M, Kranz AR (1987) Effect of gibberellins on flower development of the pin-formed mutant of Arabidopsis thaliana. Arabidopsis Inf Serv 23:66–71

Grunewald W, Friml J (2010) The march of the PINs: developmental plasticity by dynamic polar targeting in plant cells. EMBO J 29:2700–2714

Guilfoyle TJ, Suzich JA, Lindberg M (1986) Synthesis of 5S rRNA and putative tRNAs in nuclei isolated from wheat embryos. Plant Mol Biol 7:95–104

Hager A (2003) Role of the plasma membrane H+-ATPase in auxin-induced elongation growth: historical and new aspects. J Plant Res 116:483–505

Harper RM, Stowe-Evans EL, Luesse DR, Muto H, Tatematsu K, Watahiki MK, Yamamoto K, Liscum E (2000) The NPH4 locus encodes the auxin response factor ARF7, a conditional regulator of differential growth in aerial Arabidopsis tissue. Plant Cell 12:757–770

Henrichs S, Wang B, Fukao Y, Zhu J, Charrier L, Bailly A, Oehring SC, Linnert M, Weiwad M, Endler A, Nanni P, Pollmann S, Mancuso S, Schulz A, Geisler M (2012) Regulation of ABCB1/PGP1-catalysed auxin transport by linker phosphorylation. EMBO J 31:2965–2980

Hopfner KP, Karcher A, Shin DS, Craig L, Arthur LM, Carney JP, Tainer JA (2000) Structural biology of Rad50 ATPase: ATP-driven conformational control in DNA double-strand break repair and the ABC-ATPase superfamily. Cell 101:789–800

Hosek P, Kubes M, Lankova M, Dobrev PI, Klima P, Kohoutova M, Petrasek J, Hoyerova K, Jirina M, Zažímalová E (2012) Auxin transport at cellular level: new insights supported by mathematical modelling. J Exp Bot 63:3815–3827

Huang F, Zago MK, Abas L, van Marion A, Galvan-Ampudia CS, Offringa R (2010) Phosphorylation of conserved PIN motifs directs Arabidopsis PIN1 polarity and auxin transport. PlantCell 22:1129–1142

Jones AR, Kramer EM, Knox K, Swarup R, Bennett MJ, Lazarus CM, Leyser HM, Grierson CS (2009) Auxin transport through non-hair cells sustains root-hair development. Nat Cell Biol 11:78–84

Jonsson H, Heisler MG, Shapiro BE, Meyerowitz EM, Mjolsness E (2006) An auxin-driven polarized transport model for phyllotaxis. Proc Natl Acad Sci USA 103:1633–1638

Jurado S, Diaz-Trivino S, Abraham Z, Manzano C, Gutierrez C, del Pozo C (2008) SKP2A, an F-box protein that regulates cell division, is degraded via the ubiquitin pathway. Plant J 53:828–841

Jurado S, Abraham Z, Manzano C, Lopez-Torrejon G, Pacios LF, Del Pozo JC (2010) The Arabidopsis cell cycle F-box protein SKP2A binds to auxin. Plant Cell 22:3891–3904

Kai K, Horita J, Wakasa K, Miyagawa H (2007) Three oxidative metabolites of indole-3-acetic acid from Arabidopsis thaliana. Phytochemistry 68:1651–1663Kamimoto Y, Terasaka K, Hamamoto M,

Takanashi K, Fukuda S, Shitan N, Sugiyama A, Suzuki H, Shibata D, Wang B, Pollmann S, Geisler M, Yazaki K (2012) Arabidopsis ABCB21 is a facultative auxin importer/exporter regulated by cytoplasmic auxin concentration. Plant Cell Physiol 53:2090–2100

Kamphausen T, Fanghänel J, Neumann D, Schulz B, Rahfeld JU (2002) Characterization of Arabidopsis thaliana AtFKBP42 that is membrane-bound and interacts with Hsp90. Plant J 32:263–276

Katekar GK, Geissler AE (1977) Auxin transport inhibitors. III. Chemical requirements of a class of auxin transport inhibitors. Plant Physiol 60:826–829

Kepinski S, Leyser O (2005) The Arabidopsis F-box protein TIR1 is an auxin receptor. Nature 435:446–451

Kim JY, Henrichs S, Bailly A, Vincenzetti V, Sovero V, Mancuso S, Pollmann S, Kim D, Geisler M, Nam HG (2010) Identification of an ABCB/P-glycoprotein-specific inhibitor of auxin transport by chemical genomics. J Biol Chem 285:23309–23317

Kleine-Vehn J, Dhonukshe P, Swarup R, Bennett M, Friml J (2006) Subcellular trafficking of the Arabidopsis auxin influx carrier AUX1 uses a novel pathway distinct from PIN1. Plant Cell 18:3171–3181

Knöller AS, Blakeslee JJ, Richards EL, Peer WA, Murphy AS (2010) Brachytic2/ZmABCB1 functions in IAA export from intercalary meristems. J Exp Bot 61:3689–3696

Kögl F, Haagen-Smith AJ (1931) Über die Chemie des Wuchsstoffs K. Akad. Wetenschap. Amsterdam. Proc Sect Sci 34:1411–1416

Kramer EM (2004) PIN and AUX/LAX proteins: their role in auxin accumulation. Trends Plant Sci 9:578–582

Kubeš M, Yang H, Richter GL, Cheng Y, Mlodzinska E, Wang X, Blakeslee JJ, Carraro N, Petrasek J, Zažímalová E, Hoyerova K, Peer WA, Murphy AS (2012) The Arabidopsis concentration- dependent influx/efflux transporter ABCB4 regulates cellular auxin levels in the root epidermis. Plant J 69:640–654

Langowski L, Ruzicka K, Naramoto S, Kleine-Vehn J, Friml J (2010) Trafficking to the outer polar domain defines the root-soil interface. Curr Biol 20:904–908

Lee M, Choi Y, Burla B, Kim YY, Jeon B, Maeshima M, Yoo JY, Martinoia E, Lee Y (2008) The ABC transporter AtABCB14 is a malate importer and modulates stomatal response to CO2. Nat Cell Biol 10:1217–1223

Leng ER, Vineyard ML (1951) Dwarf and short plants. Maize Genet Coop Newsl 25:31–32 Lewis DR, Miller ND, Splitt BL, Wu G, Spalding EP (2007) Separating the roles of acropetal and basipetal auxin transport on gravitropism with mutations in two Arabidopsis multidrug resistance-like ABC transporter genes. Plant Cell 19:1838–1850

Lin R, Wang H (2005) Two homologous ATP-binding cassette transporter proteins, AtMDR1 and AtPGP1, regulate Arabidopsis photomorphogenesis and root development by mediating polar auxin transport. Plant Physiol 138:949–964

Lin D, Cao L, Zhou Z, Zhu L, Ehrhardt D, Yang Z, Fu Y (2013) Rho GTPase signaling activates microtubule severing to promote microtubule ordering in Arabidopsis. Curr Biol 23:290–297

Liscum E, Briggs WR (1995) Mutations in the NPH1 locus of Arabidopsis disrupt the perception of phototropic stimuli. Plant Cell 7:473–485

Ljung K, Östin A, Lioussanne L, Sandberg G (2001) Developmental regulation of indole-3-acetic acid turnover in Scots pine seedlings. Plant Physiol 125:464–475

Ljung K, Hull AK, Celenza J, Yamada M, Estelle M, Normanly J, Sandberg G (2005) Sites and regulation of auxin biosynthesis in Arabidopsis roots. Plant Cell 17:1090–1104

Löbler M, Klämbt D (1985) Auxin-binding protein from coleoptile membranes of corn (Zea mays L.). I. Purification by immunological methods and characterization. J Biol Chem 260:9848–9853

Luckie DB, Wilterding JH, Krha M, Krouse ME (2003) CFTR and MDR: ABC transporters with homologous structure but divergent function. Curr Genomics 4:225–235

Ludwig-Müller J (2000) Indole-3-butyric acid in plant growth and development. Plant Growth Regul 32:219–230

Marchant A, Bhalerao R, Casimiro I, Eklof J, Casero PJ, Bennett M, Sandberg G (2002) AUX1 promotes lateral root formation by facilitating indole-3-acetic acid distribution between sink and source tissues in the Arabidopsis seedling. Plant Cell 14:589–597

Markham JE, Molino D, Gissot L, Bellec Y, Hematy K, Marion J, Belcram K, Palauqui JC, Satiat-Jeunemaitre B, Faure JD (2011) Sphingolipids containing very-long-chain fatty acids define a secretory pathway for specific polar plasma membrane protein targeting in Arabidopsis. Plant Cell 23:2362–2378

Matsuda S, Kajizuka T, Kadota A, Nishimura T, Koshiba T (2011) NPH3- and PGP-like genes are exclusively expressed in the apical tip region essential for blue-light perception and lateral auxin transport in maize coleoptiles. J Exp Bot 62:3459–3466

Men S, Boutte Y, Ikeda Y, Li X, Palme K, Stierhof YD, Hartmann MA, Moritz T, Grebe M (2008) Sterol-dependent endocytosis mediates post-cytokinetic acquisition of PIN2 auxin efflux carrier polarity. Nat Cell Biol 10:237–244

Merks RMH, Van de Peer Y, Inzé D, Beemster GTS (2007) Canalization without flux sensors: a traveling-wave hypothesis. Trends Plant Sci 12:384–390

Michniewicz M, Zago MK, Abas L, Weijers D, Schweighofer A, Meskiene I, Heisler MG, Ohno C, Zhang J, Huang F, Schwab R, Weigel D, Meyerowitz EM, Luschnig C, Offringa R, Friml J (2007) Antagonistic regulation of PIN phosphorylation by PP2A and PINOID directs auxin flux. Cell 130:1044–1056

Mitchison GJ (1980) A model for vein formation in higher plants. Proc R Soc Lond B Boil Sci 207:79–109

Mravec J, Kubes M, Bielach A, Gaykova V, Petrasek J, Skupa P, Chand S, Benkova E, Zažímalová E, Friml J (2008) Interaction of PIN and PGP transport mechanisms in auxin distribution-dependent development. Development 135:3345–3354

Mravec J, Sku̇pa P, Bailly A, Hoyerová K, Krecek P, Bielach A, Petrásek J, Zhang J, Gaykova V, Stierhof YD, Dobrev PI, Schwarzerová K, Rolcık J, Seifertová D, Luschnig C, Benkova E, Zažímalová E, Geisler M, Friml J (2009) Subcellular homeostasis of phytohormone auxin is mediated by the ER-localized PIN5 transporter. Nature 459:1136–1140

Mu̇ller A, Guan C, Galweiler L, Tanzler P, Huijser P, Marchant A, Parry G, Bennett M, Wisman E, Palme K (1998) AtPIN2 defines a locus of Arabidopsis for root gravitropism control. EMBO J 17:6903–6911

Mullet JE, Klein RR, Klein PE (2002) Sorghum bicolor—an important species for comparative grass genomics and a source of beneficial genes for agriculture. Curr Opin Plant Biol 5:118– 121

Multani DS, Briggs SP, Chamberlin MA, Blakeslee JJ, Murphy AS, Johal GS (2003) Loss of an MDR transporter in compact stalks of maize br2 and sorghum dw3 mutants. Science 302:81– 84

Murphy AS, Hoogner KR, Peer WA, Taiz L (2002) Identification, purification, and molecular cloning of N-1-naphthylphthalmic acid-binding plasma membrane-associated aminopeptidases from Arabidopsis. Plant Physiol 128:935–950

Nagashima A, Suzuki G, Uehara Y, Saji K, Furukawa T, Koshiba T, Sekimoto M, Fujioka S, Kuroha T, Kojima M, Sakakibara H, Fujisawa N, Okada K, Sakai T (2008) Phytochromes and cryptochromes regulate the differential growth of Arabidopsis hypocotyls in both a PGP19- dependent and a PGP19-independent manner. Plant J 53:516–529

Noh B, Murphy AS, Spalding EP (2001) Multidrug resistance-like genes of Arabidopsis required for auxin transport and auxin-mediated development. Plant Cell 13:2441–2454

Noh B, Bandyopadhyay A, Peer WA, Spalding EP, Murphy AS (2003) Enhanced gravi- and phototropism in plant mdr mutants mislocalizing the auxin efflux protein PIN1. Nature 423:999–1002

Novák O, Hényková E, Sairanen I, Kowalczyk M, Pospısil T, Ljung K (2012) Tissue-specific profiling of the Arabidopsis thaliana auxin metabolome. Plant J 72:523–536

Östin A, Kowalyczk M, Bhalerao RP, Sandberg G (1998) Metabolism of indole-3-acetic acid in Arabidopsis. Plant Physiol 118:285–296

Pan J, Fujioka S, Peng J, Chen J, Li G, Chen R (2009) The E3 ubiquitin ligase SCFTIR1/AFB and membrane sterols play key roles in auxin regulation of endocytosis, recycling, and plasma membrane accumulation of the auxin efflux transporter PIN2 in Arabidopsis thaliana. Plant Cell 21:568–580

Parry G, Delbarre A, Marchant A, Swarup R, Napier R, Perrot-Rechenmann C, Bennett MJ (2001) Novel auxin transport inhibitors phenocopy the auxin influx carrier mutation aux1. Plant J 25:399–406

Peer WA, Murphy AS (2007) Flavonoids and auxin transport: modulators or regulators? Trends Plant Sci 12:556–563

Peer WA, Blakeslee JJ, Yang H, Murphy AS (2011) Seven things we think we know about auxin transport. Mol Plant 4:487–504

Peer WA, Cheng Y, Murphy AS (2013) Evidence of oxidative attenuation of auxin signalling. J Exp Bot 64:2629–2639

Peret B, Swarup K, Ferguson A, Seth M, Yang Y, Dhondt S, James N, Casimiro I, Perry P, Syed A, Yang H, Reemmer J, Venison E, Howells C, Perez-Amador MA, Yun J, Alonso J, Beemster GT, Laplaze L, Murphy A, Bennett MJ, Nielsen E, Swarup R (2012) AUX/LAX genes encode a family of auxin influx transporters that perform distinct functions during Arabidopsis development. Plant Cell 24:2874–2885

Petersson SV, Johansson AI, Kowalczyk M, Makoveychuk A, Wang JY, Moritz T, Grebe M, Benfey PN, Sandberg G, Ljung K (2009) An auxin gradient and maximum in the Arabidopsis root apex shown by high-resolution cell-specific analysis of IAA distribution and synthesis. Plant Cell 21:1659–1668

Procko E, O'Mara ML, Bennett WFD, Tieleman DP, Gaudet R (2009) The mechanism of ABC transporters: general lessons from structural and functional studies of an antigenic peptide transporter. FASEB J 23:1287–1302

Radwanski ER, Last RL (1995) Tryptophan biosynthesis and metabolism: biochemical and molecular genetics. Plant Cell 7:921–934

Rahman A, Takahashi M, Shibasaki K, Wu S, Inaba T, Tsurumi S, Baskin TI (2010) Gravitropism of Arabidopsis thaliana roots requires the polarization of PIN2 toward the root tip in meriste- matic cortical cells. Plant Cell 22:1762–1776

Raven JA (1975) Transport of indoleacetic acid in plant cells in relation to pH and electrical potential gradients, and its significance for polar IAA transport. New Phytol 74:163–172

Reinhardt D, Pesce ER, Stieger P, Mandel T, Baltensperger K, Bennett M, Traas J, Friml J, Kuhlemeier C (2003) Regulation of phyllotaxis by polar auxin transport. Nature 426:255–260

Robert S, Kleine-Vehn J, Barbez E, Sauer M, Paciorek T, Baster P, Vanneste S, Zhang J, Simon S, Covanova M, Hayashi K, Dhonukshe P, Yang Z, Bednarek SY, Jones AM, Luschnig C, Aniento F, Zažímalová E, Friml J (2010) ABP1 mediates auxin inhibition of clathrin-dependent endocytosis in Arabidopsis. Cell 143:111–121

Roudier F, Gissot L, Beaudoin F, Haslam R, Michaelson L, Marion J, Molino D, Lima A, Bach L, Morin H, Tellier F, Palauqui JC, Bellec Y, Renne C, Miquel M, Dacosta M, Vignard J, Rochat C, Markham JE, Moreau P, Napier J, Faure JD (2010) Very-long-chain fatty acids are involved in polar auxin transport and developmental patterning in Arabidopsis. Plant Cell 22:364–375

Rubery PH, Sheldrake AR (1974) Carrier-mediated auxin transport. Planta 118:101–121

Ruzicka K, Strader LC, Bailly A, Yang H, Blakeslee J, Langowski L, Nejedla E, Fujita H, Itoh H, Syono K, Hejatko J, Gray WM, Martinoia E, Geisler M, Bartel B, Murphy AS, Friml J (2010) Arabidopsis PIS1 encodes the ABCG37 transporter of the auxinic compounds including the auxin precursor indole-3-butyric acid. Proc Natl Acad Sci USA 107:10749–10753

Sachs T (1969) Polarity and the induction of organized vascular tissues. Ann Bot Lond 33:263

Sakai T, Kagawa T, Kasahara M, Swartz TE, Christie JM, Briggs WR, Wada M, Okada K (2001) Arabidopsis nph1 and npl1: Blue light receptors that mediate both phototropism and chloroplast relocation. Proc Natl Acad Sci USA 98:6969–6974

Santelia D, Vincenzetti V, Azzarello E, Bovet L, Fukao Y, Duchtig P, Mancuso S, Martinoia E, Geisler M (2005) MDR-like ABC transporter AtPGP4 is involved in auxin-mediated lateral root and root hair development. FEBS Lett 579:5399–5406

Santner AA, Watson JC (2006) The WAG1 and WAG2 protein kinases negatively regulate root waving in Arabidopsis. Plant J 45:752–764

Sauer M, Balla J, Luschnig C, Wisniewska J, Reinohl V, Friml J, Benkova E (2006) Canalization of auxin flow by Aux/IAA-ARF-dependent feedback regulation of PIN polarity. Genes Dev 20:2902–2911

Sawchuk MG, Edgar A, Scarpella E (2013) Patterning of leaf vein networks by convergent auxin transport pathways. PLoS Genet 9:e1003294

Scarpella E, Marcos D, Friml J, Berleth T (2006) Control of leaf vascular patterning by polar auxin transport. Genes Dev 20:1015–1027

Shitan N, Bazin I, Dan K, Obata K, Kigawa K, Ueda K, Sato F, Forestier C, Yazaki K (2003) Involvement of CjMDR1, a plant multidrug-resistance-type ATP-binding cassette protein, in alkaloid transport in Coptis japonica. Proc Natl Acad Sci USA 100:751–756

Sidler M, Hassa P, Hasan S, Ringli C, Dudler R (1998) Involvement of an ABC transporter in a developmental pathway regulating hypocotyl cell elongation in the light. Plant Cell 10:1623– 1636

Smith RS, Guyomarch S, Mendel T, Reinhardt D, Kuhlemeier C (2006) A plausible model of phyllotaxis. Proc Natl Acad Sci 103:1301–1306

Stein OL (1955) Rates of leaf initiation in two mutants of Zea mays, dwarf1 and brachytic2. Am J Bot 42:885–892

Stepanova AN, Robertson-Hoyt J, Yun J, Benavente LM, Xie DY, Dolezal K, Schlereth A, Jurgens G, Alonso JM (2008) TAA1-mediated auxin biosynthesis is essential for hormone crosstalk and plant development. Cell 133:177–191

Stoma S, Lucas M, Chopard J, Schaedel M, Traas J, Godin C (2008) Flux-based transport enhancement as a plausible unifying mechanism for auxin transport in meristem development. PLoS Comput Biol 4:e1000207

Sugawara S, Hishiyama S, Jikumaru Y, Hanada A, Nishimura T, Koshiba T, Zhao Y, Kamiya Y, Kasahara H (2009) Biochemical analyses of indole-3-acetaldoxime-dependent auxin biosyn- thesis in Arabidopsis. Proc Natl Acad Sci USA 106:5430–5435

Swarup R, Friml J, Marchant A, Ljung K, Sandberg G, Palme K, Bennett M (2001) Localization of the auxin permease AUX1 suggests two functionally distinct hormone trans- port pathways operate in the Arabidopsis root apex. Genes Dev 15:2648–2653

Swarup K, Benkova E, Swarup R, Casimiro I, Peret B, Yang Y, Parry G, Nielsen E, De Smet I, Vanneste S, Levesque MP, Carrier D, James N, Calvo V, Ljung K, Kramer E, Roberts R, Graham N, Marillonnet S, Patel K, Jones JD, Taylor CG, Schachtman DP, May S, Sandberg G, Benfey P, Friml J, Kerr I, Beeckman T, Laplaze L, Bennett MJ (2008) The auxin influx carrier LAX3 promotes lateral root emergence. Nat Cell Biol 10:946–954

Tanaka K, Fujimura-Kamada K, Yamamoto T (2011) Functions of phospholipid flippases. J Biochem 149:131–143

Tao Y, Ferrer JL, Ljung K, Pojer F, Hong F, Long JA, Li L, Moreno JE, Bowman ME, Ivans LJ, Cheng Y, Lim J, Zhao Y, Ballare CL, Sandberg G, Noel JP, Chory J (2008) Rapid synthesis of auxin via a new tryptophan-dependent pathway is required for shade avoidance in plants. Cell 133:164–176

Tarling EJ, Edwards PA (2011) ATP binding cassette transporter G1 (ABCG1) is an intracellular sterol transporter. Proc Natl Acad Sci USA 108:19719–19724

Teale WD, Paponov IA, Palme K (2006) Auxin in action: signalling, transport and the control of plant growth and development. Nat Rev Mol Cell Biol 7:847–859

Terasaka K, Blakeslee JJ, Titapiwatanakun B, Peer WA, Bandyopadhyay A, Makam SN, Lee OR, Richards EL, Murphy AS, Sato F, Yazaki K (2005) PGP4, an ATP binding cassette P-glycoprotein, catalyzes auxin transport in Arabidopsis thaliana roots. Plant Cell 17:2922– 2939

Theologis A, Huynh TV, Davis RW (1985) Rapid induction of specific mRNAs by auxin in pea epicotyl tissue. J Mol Biol 183:53–68

Titapiwatanakun B, Blakeslee JJ, Bandyopadhyay A, Yang H, Mravec J, Sauer M, Cheng Y, Adamec J, Nagashima A, Geisler M, Sakai T, Friml J, Peer WA, Murphy AS (2009) ABCB19/ PGP19 stabilises PIN1 in membrane microdomains in Arabidopsis. Plant J 57:27–44

Vernoux T, Besnard F, Traas J (2010) Auxin at the shoot apical meristem. Cold Spring Harb Perspect Biol 2:a001487

Verrier PJ, Bird D, Burla B, Dassa E, Forestier C, Geisler M, Klein M, Kolukisaoglu U, Lee Y, Martinoia E, Murphy A, Rea PA, Samuels L, Schulz B, Spalding EJ, Yazaki K, Theodoulou FL (2008) Plant ABC proteins-unified nomenclature and updated inventory. Trends Plant Sci 13:151–159

Vieten A, Vanneste S, Wisniewska J, Benková E, Benjamins R, Beeckman T, Luschnig C, Friml J (2005) Functional redundancy of PIN proteins is accompanied by auxin-dependent cross- regulation of PIN expression. Development 132:4521–4531

Wang B, Bailly A, Zwiewka M, Henrichs S, Azzarello E, Mancuso S, Maeshima M, Friml J, Schulz A, Geisler M (2013) Arabidopsis TWISTED DWARF1 functionally interacts with auxin exporter ABCB1 on the root plasma membrane. Plant Cell 25:202–214

Went FW, Thimann KV (1937) Phytohormones. MacMillan, New YorkWillemsen V, Friml J, Grebe M, van den Toorn A, Palme K, Scheres B (2003) Cell polarity and PIN protein positioning in Arabidopsis require STEROL METHYLTRANSFERASE1 function. Plant Cell 15:612–625

Willige BC, Ahlers S, Zourelidou M, Barbosa ICR, Demarsy E, Trevisan M, Davis PA, Roelfsema MRG, Hangarter R, Fankhauser C, Schwechheimer C (2013) D6PK AGCVIII kinases are required for auxin transport and phototropic hypocotyl bending in Arabidopsis. Plant Cell 25:1674–1688

Wu G, Lewis DR, Spalding EP (2007) Mutations in Arabidopsis multidrug resistance-like ABC transporters separate the roles of acropetal and basipetal auxin transport in lateral root development. Plant Cell 19:1826–1837

Wu G, Otegui MS, Spalding EP (2010) The ER-localized TWD1 immunophilin is necessary for localization of multidrug resistance-like proteins required for polar auxin transport in Arabidopsis roots. Plant Cell 22:3295–3304

Yamada M, Greenham K, Prigge MJ, Jensen PJ, Estelle M (2009) The TRANSPORT INHIBITOR RESPONSE2 gene is required for auxin synthesis and diverse aspects of plant development. Plant Physiol 151:168–179

Yang H, Murphy AS (2009) Functional expression and characterization of Arabidopsis ABCB, AUX 1 and PIN auxin transporters in Schizosaccharomyces pombe. Plant J 59:179–191

Yang Y, Hammes UZ, Taylor CG, Schachtman DP, Nielsen E (2006) High-affinity auxin transport by the AUX1 influx carrier protein. Curr Biol 16:1123–1127

Yang H, Richter GL, Wang X, Młodzinska E, Carraro N, Ma G, Jenness M, Chao D, Peer WA, Murphy AS (2013) Sterols and sphingolipids differentially function in trafficking of the Arabidopsis ABCB19 auxin transporter. Plant J 74:37–47

Zažímalová E, Murphy AS, Yang H, Hoyerová K, Hosek P (2010) Auxin transporters-why so many? Cold Spring Harb Perspect Biol 2:a001552

Zourelidou M, Müller I, Willige BC, Nill C, Jikumaru Y, Li H, Schwechheimer C (2009) The polarly localised D6 PROTEIN KINASE is required for efficient auxin transport in Arabidopsis thaliana. Development 136:627–636

**ABCB11 and 21 regulate rootward auxin transport and leaf expansion in Arabidopsis**

Wiebke Tapken[1][*], Mark K. Jenness[1][*], Haibing Yang[2], Jesica Reemmer[2], Nicola Carraro[2], Yu-Young Kim[2], Jun Zhang[1], Jinshan Lin[4], Joshua J. Blakeslee[4], Wendy Ann Peer[1,3], Angus S. Murphy[1]

[1]Department of Plant Science and Landscape Architecture and [3]Department of Environmental Science and Technology University of Maryland, College Park, MD, 20742, USA. [2]Department of Horticulture, Purdue University, West Lafayette, IN 47907, USA. [4]Department of Horticulture and Crop Science, The Ohio State University, Ohio Agricultural Research and Development Center, 1680 Madison Avenue, Wooster, Ohio 44691, United States
*These authors contributed equally to this work.

**Summary:** Inclusion of the ABCB11 and 21 auxin transporters in combinatorial phenotypic and biochemical analyses shows that ABCB-mediated restriction of flows increases at sub-optimal auxin concentrations.

**Abstract**

Long-distance auxin transport is mediated by ATP-binding cassette transporters of the subclass B (ABCB). ABCBs cluster into four groups according to their sequence homology and four (B1, 4, 19, 21) have been identified as primary auxin transporters. B1 and B19 activity depends on their interaction with FKBP42 (*twd1*), an immunophilin-like protein, at the ER and plasma membrane. In *Arabidopsis thaliana*, simultaneous knock-out of B1 and B19 leads to dwarfism and abaxially curled leaves. *b1b19* resembles the *twd1* mutant, but dwarfism, hypocotyl and root twisting are more pronounced in *twd1-3*. It was hypothesized that the disruption of long-distance rootward auxin transport could be partially responsible for the *twd1* phenotype. Dexamethasone-induced knock-down of each individual ABCB cluster revealed B11 as a primary long distance auxin transporter. GFP expression under the control of the B11 promoter localized it to the root tip, vasculature and epidermal cells. Like B1 and B19, B11 interacts with FKBP42 in a yeast-2-hybrid assay. Together with B21 and B19, B11 also mediates auxin transport in the proliferating leaf. Triple mutants of *b1b19/b11-1/b11-2/b21-1* more closely resemble *twd1* than *b1b19* alone in development, overall plant stature and leaf phenotype. In low light ($\leq 70\ \mu$mol m$^{-2}$ s$^{-1}$) most phenotypes could be further enhanced in *b1b19* and the *abcb* triple mutants, emphasizing the role of light in auxin transport and metabolism.

**Introduction**

   Polarized streams of the phytohormone auxin (indole-3-acetic acid; IAA) regulate major physiological processes such as meristem maintenance, cell elongation and organogenesis in vascular plants (Ljung, 2013; Sassi and Vernoux, 2013). Localized auxin gradients which function in the establishment of the embryonic apical - basal axis and post-embryonic organogenesis are canalized by polarized PIN-FORMED (PIN) carrier proteins (Zažímalová et al., 2010; Robert et al., 2013; De Rybel et al., 2013). Some PIN and PIN-LIKE (PILS) transporters also regulate auxin homeostasis by transporting auxin at the ER membrane to maintain intracellular auxin homeostasis (Mravec et al., 2008; Barbez et al., 2012). Shootward polar auxin fluxes at the root apex and auxin uptake into cortical cells during lateral root emergence are driven primarily by AUXIN1/LIKE-AUX1 (AUX1/LAX) importers (Swarup et al., 2008; Swarup and Péret, 2012; Band et al., 2014). A subclass of ATP-binding cassette transporters, subfamily B (ABCB) transporters is required for the maintenance of long distance polar auxin streams and mobilization of auxin out of the shoot apex. ABCB efflux transporters maintain these streams in the vasculature by continuous exclusion of auxin from cell membranes against the concentration gradient and prevent re-uptake into the cytosol (Noh et al., 2001; Petrášek et al., 2006; Blakeslee et al., 2007). Two ABCB transporters (ABCB4 and 21) contribute to cellular auxin homeostasis by mediating uptake when intracellular auxin concentrations are low, but function as efflux transporters at higher auxin concentrations (Kamimoto et al.; Kubeš et al., 2012). PIN, AUX1/LAX, and ABCB auxin transporters function combinatorially to mobilize long distance auxin streams including those mediating tropic responses to light and gravity (Tsuda et al., 2011; Christie and Murphy, 2013). Function of PIN and ABCB auxin transporters is conserved between monocots and dicots (Hochholdinger et al., 2000; Multani et al., 2003a; Knöller et al., 2010a; Forestan et al., 2012; Gallavotti, 2013).

   The long distance rootward polar auxin transport system was the earliest to be studied, as it plays a fundamental role in seedling growth processes and is more easily studied than micro scale polar streams involved in organogenesis (Went and Thimann, 1937). Although the polarity of the vascular long distance auxin stream is initially canalized by PIN1 and PIN7, it requires the activity of ABCB1 and ABCB19 (hereafter B1 and B19) to be maintained during subsequent growth (Noh et al., 2001; Friml et al., 2003; Zažímalová et al., 2010). PIN1 and ABCB transporters function co-ordinately in long distance transport, and B19 has been shown to stabilize PIN1 at the plasma membrane in cells where PIN1 and B19 are coincident (Titapiwatanakun et al., 2009). PIN1-B19 interactions occur in plasma membrane subdomains

and lead to decreased retrograde cycling of PIN1 (Mravec et al., 2008; Titapiwatanakun et al., 2009; Yang et al., 2013). Inflorescence height is a primary indicator of long distance auxin flows and is partially reduced in *pin1* mutants (Gälweiler et al., 1998), but is much more reduced in the *b1b19* double and *pin1b1b19* triple mutants (Noh et al., 2001a; Multani et al., 2003b; Blakeslee et al., 2007). Consistent with these phenotypes, measured rootward auxin fluxes are reduced 25-30% in *pin1*, and 60-75% in *b1b19* (Blakeslee et al., 2007). Long distance auxin transport in the vasculature also involves PIN3, which is expressed in starch sheath and epidermal cells, as *pin3* mutants exhibit reduced rootward transport (Christie et al., 2011; Ding et al., 2011).

At the subcellular level, multiple PINs are regulated by dynamic subcellular cycling processes and membrane lipid composition (Willemsen et al., 2003; Men et al., 2008; Ischebeck et al., 2013; Yang et al., 2013). PIN transport activity is also activated by the D6 PROTEIN KINASE (D6PK; Zourelidou et al., 2009; Willige et al., 2013). B1 and B19 trafficking is regulated by membrane sterols and sphingolipids, and B19 activity is inhibited by the phototropin1 kinase during phototropic responses (Christie et al., 2011; Yang et al., 2013). However, unlike PIN1 and AUX1, trafficking and activity of B1, B4, and B19 is dependent on FK506-BINDING PROTEIN 42 (FKBP42), also known as TWISTED DWARF1 (TWD1), after the dwarf phenotype of the loss of function mutant in Arabidopsis (Steinmann, 1999; Geisler et al., 2003; Bouchard et al., 2006; Kleine-Vehn et al., 2006; Blakeslee et al., 2007; Wu et al., 2010a; Wang et al., 2013). FKBP42/TWD1 belongs to a multi-domain subclass of immunophilins that forms a complex with calmodulin and high molecular weight heat shock proteins to fold and chaperone large proteins and protein complexes (Eckhoff et al., 2005; Geisler and Bailly, 2007; Gollan et al., 2012). Arabidopsis FKBP42/TWD1 contains an FK506 binding domain that is usually associated with *cis-trans*-peptidylprolyl isomerase (PPIase) activity, a tetracopeptide repeat interaction domain, a calmodulin binding domain, and a C-terminal domain that includes a membrane anchor (Kamphausen et al., 2002). FKBP42 structural organization is similar to that of human FKBP38 that functions in the folding and maturation of the cystic fibrosis transmembrane conductance regulator (CFTR/ABCC7) at the ER (Banasavadi-Siddegowda et al., 2011). However, unlike human FKBP38, FKBP42 exhibits suboptimal PPIase activity (Faure et al., 1998; Kamphausen et al., 2002).

FKBP42 is required for folding and ER exit of B1, B4, and B19 in Arabidopsis and has been shown to directly interact with B1 and B19 *in planta, in vitro,* and in heterologous systems (Geisler et al., 2003; Bailly et al., 2008; Wu et al., 2010a; Wang et al., 2013). In *twd1* mutants,

loss of FKBP42 function results in mislocalization of the transporters and to their subsequent degradation, leaving only residual transporter abundance at the plasma membrane (Geisler et al., 2003; Wu et al., 2010a; Wang et al., 2013; Yang et al., 2013). Notably, when *twd1* mutants are complemented with FKBP42 sans membrane anchor, cell elongation is increased and plants grow distinctly taller (Bailly et al., 2014). This phenotype was directly attributed to an increase in auxin concentration in transformant hypocotyls. FKBP42 interactions appear to be quite selective, as this domain does not interact with the B1/19 homologs B2 and B10 or with PIN1 (Geisler et al., 2003; Bouchard et al., 2006).

The growth phenotypes of Arabidopsis *b1b19* are reminiscent of *twd1*. Like *b1b19*, *twd1* develops epinastic leaves and exhibits short stature, but shows additional pleiotropic non-handed organ twisting (Geisler et al., 2003). Phenotypes of *b1b19* include dwarfism, curly leaves, wavy roots and moderate inflorescence twisting with non-preferential helical orientation (Noh et al., 2001; Bandyopadhyay et al., 2007). Multiple lines of evidence suggests that disruption of ABCB-mediated auxin transport underlies the *twd1* phenotype. Among these are the reduction of rootward auxin transport in *twd1* shoots by ~85%, binding of FKBP42 and B1/19 by the synthetic auxin transport inhibitor 1-naphtylphthalamic acid (NPA) and relatively high specificity and partial reversibility of root twisting after treatment with NPA (Noh et al., 2001; Murphy et al., 2002; Geisler et al., 2003; Bouchard et al., 2006; Wu et al., 2010a). However, the increased severity of *twd1* phenotypes and reductions in rootward auxin transport suggest that FKBP42 activates ABCB auxin transporters in addition to B1/B19 (Wu et al., 2010a).

The Arabidopsis genome encodes 21 full-sized ABCB transporters, which are numbered in order of gene publication, not sequence similarity. Although B1/19 and B4/21 are regarded as relatively specific auxin transporters and cluster in distinct and ancient clades, other ABCBs, particularly *B2/10*, *B11/12*, *B13/14*, and *B15/16/17/18*, occur in clusters that appear to be relatively recent gene duplications (Kamimoto et al.; Noh et al., 2001; Murphy et al., 2002; Multani et al., 2003; Terasaka et al., 2005; Geisler and Murphy, 2006; Verrier et al., 2008; Yang and Murphy, 2009; Knöller et al., 2010). Expression of *B22* has not been detected and *B8* appears to be a pseudogene (Verrier et al., 2008). More recently, transporters in the B13/14 and B15/16/17/18 clusters have been implicated in rootward auxin transport in Arabidopsis inflorescences (Kaneda et al., 2011). One or more of these ABCBs could represent the additional auxin transport activity missing in *twd1*, even if that transport activity is less specific for auxin

than B1/19. In particular, B14 has been shown to mobilize malate and fumarate in guard cells, but also exhibits some activity against other similar organic acids (Lee et al., 2008).

Some *twd1* growth phenotypes may be unrelated to auxin transport, as FKBP42 has been shown to interact with the Arabidopsis tonoplast transporter ABCC1/MRP1 (Geisler et al., 2004), and co-localizes with ABCG36, a promiscuous pleiotropic drug resistance transporter in the root epidermis (McFarlane et al., 2010; Růžička et al., 2010) . Further, detailed analyses of *twd1* phenotypes suggest that the twisting of the inflorescence and roots can be solely explained by the decrease in rootward auxin streams, but that helical organ twisting reflects functional interactions with the cytoskeleton similar to those observed with human FKBP52, which interacts with dynein through its PPIase domain (Silverstein et al., 1999; Weizbauer et al., 2011; Yang et al., 2013; Bailly et al., 2014). However, mutants in microtubule formation show a preference in handedness of cell file orientation (Cnops et al., 2000; Thitamadee et al., 2002; Ishida et al., 2007).

Here we identify additional ABCB transporters involved in rootward auxin transport using RNAi knockdowns followed by analyses of single and double mutants. This approach identified B11 as a missing component of rootward long-range auxin transport. Subsequent mutant crosses demonstrated that *twd1* growth phenotypes can be recapitulated by loss of multiple ABCB transporter function. These efforts also clarify the function of ABCB auxin transporters in Arabidopsis leaf development. Notably, plants homozygous for a new *b21* allele could not be recovered in a *b1b19* background, suggesting that in combination the mutations prevent fertilization or are lethal. We conclude that virtually all of the phenotypes reported for *twd1* can be attributed to impaired long-distance auxin transport. Hypocotyl and silique super-twisting appear to be the exceptions, although a causal connection to loss of ABCB function cannot be ruled out.

**Results**

Phenotypic variation observed between *twd1*/*ucu2* alleles in Wassilewskija (Ws) and Columbia-0 (Col-0) has been primarily attributed to ecotypic differences in rootward auxin transport and total auxin content (Wu et al., 2010a). A rationale for this is the dependence of auxin levels on light intensity and red/far-red light ratios perceived by phytochromes, which are differentially expressed in the two ecotypes (Aukerman et al., 1997; Wu et al., 2010b; Hersch et al., 2014). In both Col-0 and Ws, free IAA levels increase in seedlings and decrease in upper inflorescences with decreased light fluence, but free IAA levels are higher in Ws inflorescences at

130 $\mu$mol m$^{-2}$ s$^{-1}$ than in Col-0 (Fig. 1A). These light-dependent differences are apparently phytochrome dependent, as they are not observed in a *phyA phyB* mutant in the Col-0 background (Fig. 1A).

Phytochrome signaling has been shown to interact genetically with the ABP1 component of the ABP1-TMK auxin receptor, so free IAA levels were examined in ABP1 overexpression lines and in the weak *abp1-5* allele to determine if light-dependent auxin levels were altered (Xu et al., 2010; Effendi et al., 2013; Xu et al., 2014). However, under low light conditions, free IAA levels of the ABP1 overexpressor were comparable to Col-0 and were much higher in all *abp1-5* tissues examined under all light regimes (Fig. 1B). As such, Col-0 was used as the reference wild type and background for all mutants and transformants utilized in the study and all light regimes were rigorously calibrated for all phenotypic analyses. All mutant lines, including *twd1-3*, *pgp1-2 (b1)* and *mdr1-101* (*b19*) were backcrossed into Col-0 at least three times.

An invariant set of "core" phenotypes consistent with previously published reports were observed in *twd1-3* and *b1b19* under all growth conditions (Fig. 2A and C). However, some traits of *b1b19* and *twd1-3* are enhanced by variation of light, temperature, and firmness of the growth medium (Fig. 2B). All *twd1* phenotypes are a superset of those observed in *b1b19*, and the effects of light and temperature on phenotypes of *b1b19* are more pronounced. This is consistent with effects of light intensity, red/ far-red ratios and day-length on the severity of auxin-related phenotypes in Arabidopsis (Jensen, 1998; Geisler et al., 2005; Halliday et al., 2009). The overall plant morphology of Col-0, *b1b19* and *twd1-3* is depicted in Fig. 2D.

**The C-terminus of B11/12 interacts with the PPIase-domain of FKBP42**

We originally reported interactions of FKBP42 with ABCB auxin transporters seen in pull-down, affinity purification, and yeast two-hybrid assays between FKBP42 with a deletion of its C-terminal membrane anchor region and C-terminal soluble domains of Arabidopsis ABCB transporters (Murphy et al., 2002; Geisler et al., 2003). B4 interaction with FKBP42 was subsequently suggested when B4 was observed to be mislocalized in the *twd1* background (Wu et al., 2010a). However, in previously published pull-down experiments, some identities of the tryptic fragments were shared by multiple ABCBs, and not all Arabidopsis ABCB C-termini were analyzed (Geisler et al., 2003).

Repetition of the yeast two-hybrid experiments utilizing ABCB C-terminal domains (last predicted cytosolic entry to the C-terminus; $BXX_{CT}\Delta pAS2$) were analyzed for interaction with FKBP42 (PPIase domain, binding-domain; $FKBP_{CT}\Delta pACT2$). Previously assayed transporter fragments (interactors: B1, B19; non-interactors: B2, B10, B14; and the putative interactor: B4) were revisited with results similar to the published report, although the B2 interaction was slightly stronger than previously observed (Fig. 2E; Geisler et al., 2003). New B3, B4 and B21 pAS2 constructs were generated. As the very high degree of sequence similarity between B11 and B12 does not allow for generation of distinct yeast two hybrid fragments, the construct was designated B11/12. The C-terminus of B11/12 bound more strongly to the PPIase domain of FKBP42 than B4, but to a lesser extent than B1 and B19 (Fig. 2E). B3 and B21 exhibited weak interaction with FKBP42. Comparable results were obtained in HIS-auxotrophy assays for all tested interaction partners. Minor auto-activation was observed only with B4. These results suggested that B11/12 were appropriate candidates for further analysis as putative auxin transporters.

**Using RNAi to identify ABCBs associated with *twd1* phenotypes**

With the duplications observed in the Arabidopsis *ABCB* gene family, it is not surprising that an initial screen of single *abcb* mutations available from the Salk and GABI-Kat T-DNA insertion collections revealed some conditional phenotypic variability, but no clear phenotypes reminiscent of *twd1* or *b1b19*. Four sets of inducible RNAi lines targeting cluster-specific regions within open reading frames encoding ABCB transmembrane domains were implemented to knock-down a total of 12 *ABCB* transporters (hereafter designated *B2/10RNAi*, *B3/5/11/12RNAi*, *B13/14RNAi* and *B15/16/17/18RNAi*; Supplemental Fig. S1). Three independent homozygous lines for each cluster were generated and subsequently examined for auxin-related phenotypes after induction with dexamethasone. Successful knock-down of individual transporters was confirmed through qRT-PCR (Supplemental Fig. S2).

**Selection of B21 and B11/12 as candidate rootward auxin transporters**

*Selection of B21*

An *RNAi* line designed to knock down *B21* had been shown to exhibit the increased lateral/adventitious root formation phenotype previously reported for *b4* mutants (Santelia et al., 2005; Kamimoto et al., 2012). That report also showed that *B21* is expressed in leaves, shoot apices, and the vascular cylinder and regulates rootward auxin transport from the root-shoot transition zone (Kamimoto et al., 2012). B21 was also shown to function as a concentration-

dependent uptake/efflux transporter similar to B4 in *Saccharomyces cerevisiae* expression assays. Although our own analysis (qRT-PCR) indicated a ~ 60% decrease in *B4* expression in the reported knock-down line, the evidence for B21 function in rootward auxin transport was compelling and B21 was advanced as a primary candidate for further analysis.

*Selection of B11/12*

A highly reproducible phenotype of *b19* and *twd1* is cotyledon epinasty in 4-6 d seedlings (Noh et al., 2001; Geisler et al., 2003). Roots of *B2/10RNAi* and *B3/5/11/12RNAi* lines exhibited strong waviness and left-handed skewing and cotyledons were epinastic in both lines at 5 d, but resembled the wild-type after 7 d (Fig. 3 A, B). Non-handed twisting similar to what was previously reported for *b1b19* double mutants was increased (Fig. 3C; Wu et al., 2010a). Rootward $^3$H-IAA transport in the hypocotyl was reduced in both *B2/10RNAi* and *B3/5/11/12RNAi* (Fig. 3D, E). In crosses of both lines, reduced DR5rev$_{Pro}$:GFP signals were observed in the root tip (Fig. 3D, E insets). These results suggest that at least one member of each cluster is a functional long-distance auxin transporter.

A *b2/10* double mutant exhibited growth phenotypes and rootward $^3$H-IAA transport that were more variable, but not different from Col-0 (not shown). Expression of B2 in *Schizosaccharomyces pombe* did not result in altered net auxin uptake or efflux (Yang and Murphy, 2009), and *b2-1* and *b10-1* single mutants did not show any auxin related phenotypes (Supplemental Fig. S3). As such, further analyses of B2 and B10 was deferred. Single mutants in the *B3/5/11/12* cluster resembled Col-0, but *b11* alleles showed a greater extent of phenotypic plasticity in leaf size and root growth when light conditions were varied. Further, a previously published report implicated B11 in rootward auxin transport in inflorescences, although *b11* mutants utilized in that study appear to contain insertion in *b12* instead (Kaneda et al., 2011). Taken together, these results prioritized B11/12 and not B2/10 for further analysis.

*Lower priority for B7/9, B6/20, B13/14, B15/16/17/18*

The B7/9 and B6/20 clusters exhibit the least amount of sequence similarity with B19. As a reliable knockdown strategy could not be implemented for the *B7/9* and *B6/20* pairs, *b7b9* and *b6b20* double knockout mutants were constructed. No auxin-related phenotypes were observed, and rootward $^3$H-IAA transport in the hypocotyl was not different from Col-0 (not shown). As such, these transporters were assigned low priority. However, B13 and B14 exhibit some sequence similarity to B1 and B19 (Knöller et al., 2010; Carraro et al., 2013). B14 is localized to

guard cells and the vascular cylinder, has been shown to transport non-aromatic organic acids, and knockout mutants show reduced rootward auxin conductance in inflorescence stems (Kaneda et al., 2011). However, rootward $^3$H-IAA transport in hypocotyls was not different from Col-0 in *B13/14RNAi* and only slightly reduced in *b14* (Fig. 4A; Supplemental Fig. S4B). Further, co-application of $^3$H-IAA with malate (5:1 molar ratio) in hypocotyl transport assays reduced rootward transport in Col-0, *b1*, *b19*, but not *b14*, suggesting that B14 preferentially transports malate over auxin *in vivo* (Fig. 4A). Lateral root number, a good indicator of reduced rootward transport, was also unaffected in *B13/14RNAi* and *b14* compared to wild type (not shown). These observations decreased the priority of further analyses of the B13/14 cluster.

*B15/16/17/18RNAi* exhibited epinastic cotyledons and wavy, but not skewed roots, with no apparent gravitropic defects (Supplemental Fig. S5A,B). *B19* expression levels were also slightly affected in *B15/16/17/18RNAi* compared to WT plants (Supplemental Fig. S2). Root waving was more frequent than in *B2/10RNAi* and *B3/5/11/12RNAi*. Consistent with expression of this cluster in both hypocotyls and roots, rootward $^3$H-IAA transport in the hypocotyl was reduced by about 40% compared to Col-0 (Genevestigator; Supplemental Fig. S5C). Expression of this cluster in the seed coat suggests additional function (Genvestigator). As this cluster exhibits a very high degree of sequence identity, loss of function analysis would require generation of quadruple-sextuple mutant lines. For this reason, the B15/16/17/18 cluster was given a lower priority.

**Phenotypic and molecular characterization of *b21* and *b11***

*Characterization of B21*

A previously described *b21-1* allele forms a partial transcript, which encodes two full transmembrane domains, the first nucleotide binding domain (NBD), and a partial second NBD to form a partially functional transporter (Kamimoto et al., 2012). A second allele (*b21-2*) was identified from the GABI-Kat collection with a large T-DNA insertion that would interrupt transcription of the second NBD (Fig. 4C, top). Like *b21-1*, *b21-2* still formed partial transcripts, albeit at lower abundance compared to Col-0 (Fig. 4C, bottom). When grown on soil, *b21-2* was phenotypically indistinguishable from Col-0. Primary root-length of 5 d *b21-2* seedlings were comparable to wild-type, but lateral root length was quantitatively more variable. Rootward $^3$H-IAA transport from the root-shoot transition zone (RSTZ) to the root apex was significantly reduced in *b21-1*, and even more reduced in *b21-2* (Fig. 4D; Supplemental Fig. S6A). B21 was subsequently expressed in *S. pombe* and exhibited a concentration-dependent directional auxin

transport activity (Supplemental Fig. S6B) analogous to B4 and consistent with a previous report (Yang and Murphy, 2009; Kamimoto et al., 2012).

*Characterization of B11*

Two homozygous *b11* T-DNA insertion lines (exon 1, *b11-1*, and 5'-end of exon 6, *b11-2*) were obtained from the SALK collection (Fig. 4B, top). *B11* transcript is absent in both *b11* mutants (Fig. 4B, bottom). As is the case with *b1* and *b19* mutants, *b11-1* and *b11-2* exhibited a growth phenotype that was dependent on light intensity. In low light ($\leq 70\ \mu$mol m$^{-2}$ s$^{-1}$), plants were shorter and developed larger leaves compared to Col-0 (Fig. 5A, B).

In 5 d seedlings, *B11* expression was low and about equal in shoots and roots (Fig. 4B, bottom). Visualization of *B11* with B11$_{Pro}$:GFP revealed an expression domain overlapped with *B1* at the root apex and *B19* in the central vasculature of the mature root (Fig. 5C; Geisler et al., 2005; Wu et al., 2007). However, *B11* expression decreased near the root-shoot transition zone and was exclusive to epidermal cell layers at the root-hair zone.

Rootward transport of $^3$H-IAA was reduced in *b11-1* hypocotyls to the same extent as in *b14* mutants, but was not reduced by malate competition, suggesting greater affinity of B11 for auxin (Fig. 4A). Expression of B11 in *S. pombe* resulted in increased net efflux (18% and 27% greater than empty vector controls at four and six minutes, respectively) equivalent to expression of B19 positive controls (Fig. 5D). However, B11 exhibited less specificity for $^3$H-IAA than B19 in these assays, as more net efflux of a $^3$H-benzoic acid substrate specificity control (Yang and Murphy, 2009) was observed in cells expressing B11 than in cells expressing B19 (Fig. 5E).

*Comparison of B11 and B21 activity in the leaf*

Despite low levels of *B11* expression in mature leaves, both *b11* mutants showed clear auxin-related leaf phenotypes (Fig. 5A, B). In contrast, *B21* is strongly expressed in the tip of the cotyledons and mature leaves (Kamimoto et al., 2012). In order to understand the role of B11 and B21 in leaf auxin transport, we measured basipetal (leaf tip to petiole) and centrolateral (center of leaf mid-vein to the margins) auxin movement in *b1, b11, b19* and *b21* mutants. Auxin transport was significantly reduced from the leaf tip to the petiole in *b11-1* and *b19,* but not *b1* and *b21-2* (Fig. 6A). In centrolateral assays, only *b21-2* had a significant decrease in auxin transport (Fig. 6B). Consistent with these results, free IAA levels in both *b11* and *b21* were significantly decreased at the center of young leaves (Fig. 6C). Together, these data indicate that B11 functions

coordinately with B19 and PIN1 to maintain basipetal (rootward) auxin streams in leaves, hypocotyls and inflorescences. In addition to a role in rootward auxin movement in hypocotyls and roots, B21 functions in auxin distribution within the leaf.

### *b1b19b11* and *b1b19b21* triple mutants mimic most *twd1-3* phenotypes

*Phenotypes during pre-flowering vegetative growth*

Both alleles of *b11* and *b21* were crossed with *b1b19* (henceforth referred to as $^Tb11\text{-}1$, $^Tb11\text{-}2$, $^Tb21\text{-}1$ and $^Tb21\text{-}2$). We generated $^Tb11\text{-}1$, $^Tb11\text{-}2$ and $^Tb21\text{-}1$ homozygous triple mutants, while $^Tb21\text{-}2$ lines homozygous for *b21-2* could not be recovered. Homozygous quadruple mutants were also not obtained when either *b21* allele was crossed with *b1b11b19*. As selfing of the $^Tb21\text{-}2$ line heterozygous for *b21-2* requires hand pollination and all seeds recovered from incompletely filled siliques failed to germinate, it appears that loss of *B1, B19,* and *B21* function prevents fertilization or is embryo lethal.

One of the core seedling phenotypes in *twd1-3* is the twisting of root cell files and resultant root skewing without root waving (Fig. 2C; Pérez-Pérez et al., 2004; Bailly et al., 2006; Wu et al., 2010a). When grown at ≤70 $\mu$mol m$^{-2}$ s$^{-1}$, cell files of *twd1-3* twisted more tightly than *b1b19*, $^Tb11\text{-}1$, $^Tb11\text{-}2$ or $^Tb21\text{-}1$ (Fig. 7A). Root twisting was invariant and continuous along the root axis in *twd1-3* above the elongation-differentiation zone boundary and involved both cortical and epidermal cells. In contrast, twisting in *b1b19*, $^Tb11\text{-}1$, $^Tb11\text{-}2$ and $^Tb21\text{-}1$ strongly coincided with root wave maxima and was most pronounced in the cortex (Fig. 7A). Root waving was most pronounced in $^Tb21\text{-}1$ (Fig. 7B) and was similar among $^Tb11\text{-}1$, $^Tb11\text{-}2$, and *b1b19*. Skewing was not observed in any of the *abcb* mutants if directional light was eliminated. Under low light, *twd1-3*, *b1b19,* and all triple *abcb* mutants exhibited short, wavy hypocotyls.

Subsequently, *b1b19* and all *abcb* triple mutants were indistinguishable from *twd1-3* in later vegetative developmental stages. *b1b19* and all *abcb* triple mutants developed strong abaxially curled leaves and small compact rosettes (Fig. 7C; Noh et al., 2001; Geisler et al., 2003; Pérez-Pérez et al., 2004). Rosettes of $^Tb11\text{-}1$ and $^Tb11\text{-}2$ were initially smaller than *b1b19* and *twd1-3*. However, by 45 d, $^Tb11\text{-}1$ and $^Tb11\text{-}2$ rosettes phenocopied *twd1-3*.

In *twd1-3*, older leaves bulged and frequently curled towards the adaxial side at the leaf tip and exhibit a spoon-like shape with a reduced mid-vein (Pérez-Pérez et al., 2004). The spoon-like shape and reduced mid-vein were observed in *b1b19* and all triple *abcb* mutants, but bulging

occurred with reduced frequency (Fig. 8C). Unrolling of the mature leaves of the triple mutants often resulted in their tearing due to movement restrictions by the mid-vein (Fig. 8C, $^{T}b11$-2), whereas older leaves of *twd1-3* were often not folded.

*Floral and post-flowering phenotypes*

Under all conditions, *twd1*, *b1b19*, and triple *abcb* mutant flowers exhibited the short anther filaments and occasional floral asymmetry that are characteristic of *b1b19* (Noh et al., 2001b). Under low light *twd1-3*, *b1b19*, $^{T}b11$-1, $^{T}b11$-2 and $^{T}b21$-1 exhibited reductions in inflorescence height compared to Col-0, as well as waving inflorescences and epinastic, incompletely filled siliques (Fig. 2D, Fig. 8A, D). In *b1b19*, $^{T}b11$-1, and $^{T}b11$-2, pedicel number often increased (Fig. 8D, top). The waving of the inflorescence was greatly increased in *abcb* triple mutants grown at 30 $\mu$mol m$^{-2}$ s$^{-1}$ in a 16/8 h photoperiod (Fig. 8A). Waving of the inflorescence increased in all *abcb* mutants when light was obstructed by green tissues (Fig. 8B).

The axillary buds of *twd1-3*, *b1b19*, and *abcb* triple mutants deviated from the "golden angle" of 137.5º resulting in more distichous phyllotactic patterning (Fig. 8D, top). This patterning was more distinct in $^{T}b11$-1, $^{T}b11$-2 and $^{T}b21$-1 compared to *b1b19*. The junction of the inflorescence and the base of the axillary buds were swollen at the basal side of the pedicel, contributing to the aberrations in the angle of the silique-inflorescence junction in *b1b19* and the triple mutants (Fig. 8D, bottom). This phenotype was also observed in *twd1-3*.

**Discussion**

Auxin homeostasis in vascular plants can only be sustained through the careful interplay between local synthesis coupled with short- and long-distance transport. Although auxin can be synthesized in multiple cell types, long-distance rootward auxin streams are essential for maintenance of the inflorescence and the root meristem. The coordinated activities of PIN1, B1, and B19 mediate the majority of rootward auxin transport in all monocot and dicot species (Figure 9; Noh et al., 2001b; Multani et al., 2003c; Knöller et al., 2010). The results show that B11, perhaps in concert with B12, and B21 are responsible for the bulk of residual fluxes in the basipetal streams, and participate in leaf shape and size. Virtual loss of B1, B19 and B4 activity in *twd1*, and the associated loss of long-distance auxin transport, was hypothesized to contribute to the organ twisting phenotype. This report shows that FKBP42/TWD1 interacts with at least five auxin-transporting ABCBs and confirms FKBP42 as an integral part of auxin homeostasis.

**The function of ABCB transporters in the leaf**

Plants maximize light acquisition by developing a planar leaf surface. Recent reports have demonstrated antagonism mediated by phototropins (leaf flattening) and phytochrome B (leaf curling) in light responsive growth (de Carbonnel et al., 2010; Kozuka et al., 2013). Auxin pools change with the developmental stage of the plant as well as incident light intensity and quality. Low red/far-red light ratios trigger leaf expansion through phyB, phyE and phyD-mediated shade avoidance response that increases auxin levels via the TAA1 auxin biosynthetic pathway (Devlin, 1999; Tao et al., 2008; Hersch et al., 2014). In contrast, high light can reduce active auxin pools through photo-oxidation (Ray and Curry, 1958; Stasinopoulos and Hangarter, 1990; Liu et al., 2011). In addition to auxin homeostasis, small RNAs mediate expression of transcription factors involved in auxin-responsive gene regulation (Li et al., 2007; Rodriguez et al., 2014). Therefore, the challenge during leaf development is to maintain malleability, while preserving the planar leaf structure.

It has been difficult to discern the relative contributions of auxin homeostasis and auxin transport to leaf growth (Scarpella et al., 2010). Amongst the auxin biosynthetic mutants with these leaf curling phenotypes are *iamt1-D*; *arf3, 4 and 7*, and the triple and quadruple mutants of YUCCA: *yuc1yuc2yuc4*, *yuc1yuc4yuc6 and yuc1yuc2yuc4yuc6* (Watahiki, 1997; Qin et al., 2005; Cheng et al., 2006; Yifhar et al., 2012). When constitutively expressed in Arabidopsis, wheat TaWRKY71-1, of the yield-associated family of WRKY transcription factors, increased the abundance of IAMT1, which resulted in hypernastic leaf formation (Qin et al., 2013). In addition to auxin metabolism, the auxin efflux proteins PIN1, 3, 4 and 7 create localized auxin fluxes that promote cotyledon formation in embryos and leaf initiation during vegetative growth (Okada et al., 1991; Gälweiler, 1998b; Benková et al., 2003). In seedlings, PIN3 mediates the shade-avoidance response in the hypocotyl (Keuskamp et al., 2010). However, *pin* mutants do not develop curled leaves, whereas *b1b19* and $^Tb11$-*1*, $^Tb11$-*2* and $^Tb21$-*1* do.

Disruption of auxin transport appears to mainly affect cells on the abaxial side, as these are smaller in *b1b19*, $^Tb11$-*1*, $^Tb11$-*2* and $^Tb21$-*1* and *twd1-3* compared to the wild-type (Supplemental Fig. S8). This mechanically forces the leaves to curl downward toward the petiole during expansion and low light enhances this effect (Fig. 1A; Fig. 7C; Fig. 8B). We show that B11, B19 and B21 are active in the leaf and coordinate transport from the leaf tip to the petiole (B11 and B19) and from the center to the margins (B21) respectively (Fig. 6A, B). Hyponastic leaf curling is not observed in *b11* and *b21* single mutants. In contrast to *b19*, leaves of *b11* are

larger in low light compared to the wild-type, suggesting the existence of a compensatory mechanism. The results dismiss a role of B19 in this process, as transcriptional levels were only increased in *b1* and not *b11* (Supplemental Fig. S7).

**Conclusion**

Consistent with data suggesting the presence of additional ABCB auxin transporters (Wu et al., 2010a; Wang et al., 2013; Kaneda et al., 2011), the experimental evidence presented herein demonstrates that B11 functions as a long-distance rootward auxin transporter in Arabidopsis. Further, with the additional results presented here, B1, B4, B11, B19 and B21 can all be described as transporters that are regulated to a greater or lesser extent by FKBP42/TWD1 and exhibit an apparent preference for auxin over other substrates. The triple mutants $^{T}b11$-1, $^{T}b11$-2 and $^{T}b21$-1 resemble *twd1-3* more than the *b1b19* double, especially in lower light, suggesting that impaired auxin transport resulting from loss of ABCB function is the underlying reason for the majority of phenotypes observed in *twd1-3*. However, as the extreme twisting of siliques and mature roots observed in *twd1-3* are not observed in microtubule orientation or triple *abcb* mutants, it is quite possible that FKBP42 has inherent activities that are independent of auxin and microtubule function (Wang et al., 2013).

However, it is important to note that homozygous quadruple *b1b11b19b21* mutants could not be recovered and that some residual B1, B4, and B19 is found at the plasma membrane in *twd1* (Wang et al., 2013). As such, *twd1* phenotypes could still reflect less than complete loss of function of multiple ABCBs. It is also important to resolve the function of the expanded cluster of *B15/16/17/18*, but clear positive evidence of additional FKBP42 function would be the best means of resolving this question.

Perhaps the most important outcome of the experiments presented herein is the evidence that ABCB prevention of auxin reuptake in apical and starch sheath cells makes the greatest contribution to rootward long distance auxin transport at sub-par auxin levels. PIN3 may function cooperatively with B1 and B19 in a manner similar to what is observed with PIN1 (Blakeslee et al., 2007; Titapiwatanakun et al., 2009) to maintain the integrity of the rootward stream. Overall, these results indicate that preventing diversion and trapping of auxin in cells adjoining vascular transport streams appears to be worth considerable energetic expenditure and genetic redundancy on the part of the plant.

**Materials and Methods**

**Plant Material and growth conditions**

All Arabidopsis plants were in the Columbia-0 (Col-0) background, including *b1* (Noh et al., 2001; AT2G36910), *b2-1* (SALK_025155; AT4G25960), *b10-1* (SALK_021744; AT1G10680), *b19 (mdr1-101*; Lin and Wang, 2005; AT3G28860), *b1b19* and *twd1-3* (Geisler et al., 2003; AT3G21640), *b11-1*, *b11-2*, *b14-1* (Lee et al., 2008; AT1G02520, AT1G28010, respectively), *b21-1* (Kamimoto et al., 2012; AT3G62150) and *b21-2*. Both *b11* (*b11-1*, SALK_057628; *b11-2*, SALK_037942) T-DNA insertion lines were obtained from the Arabidopsis Biological Resource Center (ABRC, www.arabidopsis.org). *b21-1* (WiscDsLox1C2) was obtained from the Nottingham Arabidopsis Stock Centre (NASC, www.arabidopsis.info) and *b21-2* (Gabi_954H06) from GABI-Kat (www.gabi-kat.de). Seedlings were grown on 0.8% (w/v) agar, containing quarter-strength Murashige and Skoog (MS) basal salts with 0.5 % (w/v) sucrose at pH 5.5, if not otherwise specified. Seeds were stratified for 2 days at 4 ºC before transfer to a growth chamber: 21 °C with a 12/12 hr photoperiod at 70 $\mu$mol m$^{-2}$s$^{-1}$. *ABCB*-RNAi plants on soil were grown in the greenhouse under natural light conditions. In the winter, the day length was extended to 14/10 hr photoperiod with high-intensity discharge (HID) lights at 150 $\mu$mol m$^{-2}$ s$^{-1}$. When *b1b19*, $^{T}$*b11-1*, $^{T}$*b11-2*, $^{T}$*b21-1* and *twd1-3* were grown on soil, they were placed in a temperature and humidity-controlled growth chamber under conditions specified for each experiment.

**Construction of ABCB-RNAi lines**

In order to knock down multiple *ABCB* genes with one RNAi construct, a fragment of at least 25 bp in length was designed to target a unique region within the transmembrane domain of all target genes within a given cluster (Zamore et al., 2000; Supplemental Fig. S1). RNAi fragments were obtained through reverse transcription PCR and then cloned into pENTR D-TOPO (Invitrogen). RNAi fragments were then transferred into the inducible pOpOff Gateway-compatible system (Wielopolska et al., 2005) by LR reaction (Invitrogen). All four *ABCB*-RNAi constructs were transformed into Col-0 wild-type plants via floral dip and transformants backcrossed three times into Col-0. More than 5 independent homozygous lines for each RNAi line were recovered. At least three transformed lines for each cluster were analyzed and representative data reported. For phenotypic analysis, plants were grown for 7 d on quarter-strength MS basal salts containing 10 $\mu$M dexamethasone. All kits and enzymes were used according to manufacturer's instructions. Primers are listed in Supplemental Table S1.

**RNA isolation and Quantitative real-time PCR (qRT-PCR)**

For the *ABCB*-RNAi lines, total RNA was isolated from 7 d seedlings grown on quarter-strength MS basal salts containing 10 $\mu$M dexamethasone using the RNeasy Mini Kit (Qiagen). Three $\mu$g total RNA was reverse transcribed using the BioScript RNase H Minus reverse transcription kit (Bioline). qRT-PCR was performed on an iCycler (Bio-Rad Laboratories) using the EvaGreen qPCR master mix (Biotium) with two biological and three technical replicates. Relative expression levels were calculated as $\Delta\Delta C_T$. For qRT-PCR of *B11* mutants, plants were grown on quarter-strength MS basal salts for 5 d under continuous light at 100 $\mu$mol m$^{-2}$ s$^{-1}$. Roots and shoots were separated and total RNA extracted using ZR Plant RNA Mini Prep kit (Zymo Research) followed by treatment with DNasel (New England Biolabs). Integrity of the RNA was analyzed on a 1% (w/v) agarose gel. RNA (1.5 $\mu$g) was reversed transcribed using SuperScript lll reverse transcriptase (Invitrogen). qRT-PCR was performed on a CFX Connect (Bio-Rad Laboratories) using the EvaGreen qPCR master mix (Biotium). Transcript levels were normalized against the two control genes *PP2A* and *18S*. Samples without template served as negative controls. *B11* transcript abundance in roots and shoots was analyzed in biological triplicates and technical duplicates. Comparable results were obtained using either reference gene. qRT-PCR results were analyzed with the Bio-Rad CFX Manager software. Primers are listed in Supplemental Table S1.

**Cytological studies**

Cytological studies were conducted on an LSM 710 laser spectral scanning confocal microscope with a laser intensity of 5 %, and images analyzed using the Zeiss ZEN software (Carl Zeiss). Plasma membranes were visualized by staining with 5 $\mu$M FM4-64 (Invitrogen, Molecular Probes) for 5-10 min, followed by a rinse with water. The following settings were used for fluorescence acquisition: GFP, 488 nm excitation and 493–598 nm emission; FM4-64, 594 nm excitation and 599–647 nm emission. For expression analysis of *B11* the native promoter (-1650 bp) was cloned into the Gateway-ready vector pGWB4 (GFP fusion) (Nakagawa et al., 2007). Primers are listed in Supplemental Table S1.

**Auxin transport assays and quantification**

Transport assays in seedlings were conducted as previously described (Blakeslee et al., 2007). $^3$H-IAA and $^3$H-benzoic acid efflux in *S. pombe* were performed as described (Yang and Murphy, 2009). The ABCB constructs for the yeast assay of B1 and B19 are described in Yang and Murphy, 2009. The *B11* construct was created by ligating an Ncol-*B11*-Xmal fragment into

an Ncol-pREP42-Xmal digested vector. Primers are listed in Supplemental Table S1. $^3$H-IAA movement within leaves of 4 week-old plants was conducted on leaves of equal size. An agarose bead containing 1 $\mu$M $^3$H-IAA was placed on the leaf tip or leaf center and allowed to incubate for 3 hours and 2 hours, respectively, under dim yellow light. Then petioles or 1 mm tissue punches from both leaf margins were collected and $^3$H-IAA was measured by scintillation counting. Free IAA quantification was conducted as described in Novák et al., 2012.

**Yeast 2-Hybrid assay**

Yeast 2-Hybrid assays were performed according to Geisler et al., 2003.

**Statistical analysis**

Statistical analyses were performed using the software Sigmastat (Jandel Scientific Software).

**Acknowledgements**
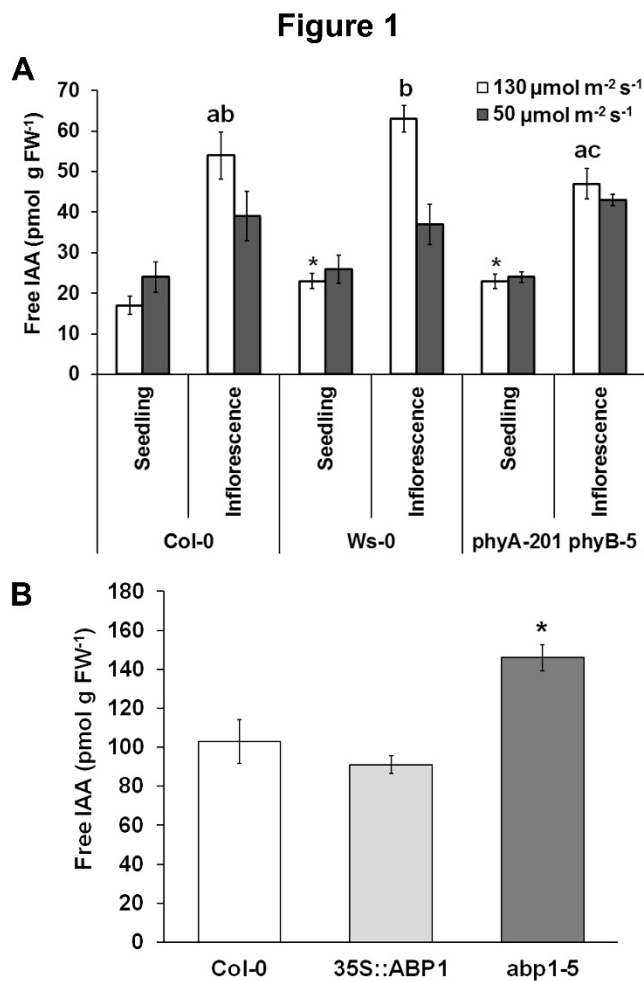
**Figure 1. Quantification of free auxin levels.** A, Auxin levels in Col-0, Ws-0 and *phyA-201phyB-5* double mutant in relation to light intensity. Plants were grown at 130 $\mu$mol m$^{-2}$ s$^{-1}$. Significant differences between free auxin levels in 6 d seedlings was determined using ANOVA followed by Tukey's *post-hoc* analysis, 10 plants per replicate, $n = 3$, *$P \leq 0.05$. Values are means ± SD. Significance of free auxin levels in the inflorescence is indicated by lower case letters and was determined by ANOVA using the Newman-Keuls *post-hoc* analysis, $n = 3$. Measurements were taken at the inflorescence apex (1 cm) one day after bolting. B, Free IAA levels in seedlings of 35S::ABP1-GFP and *abp1-5* (Xu et al., 2010; Robert et al., 2010). Values are means ± SD, $n = 2$. Significance was determined by ANOVA, *$P = 0.012$.

# Figure 2
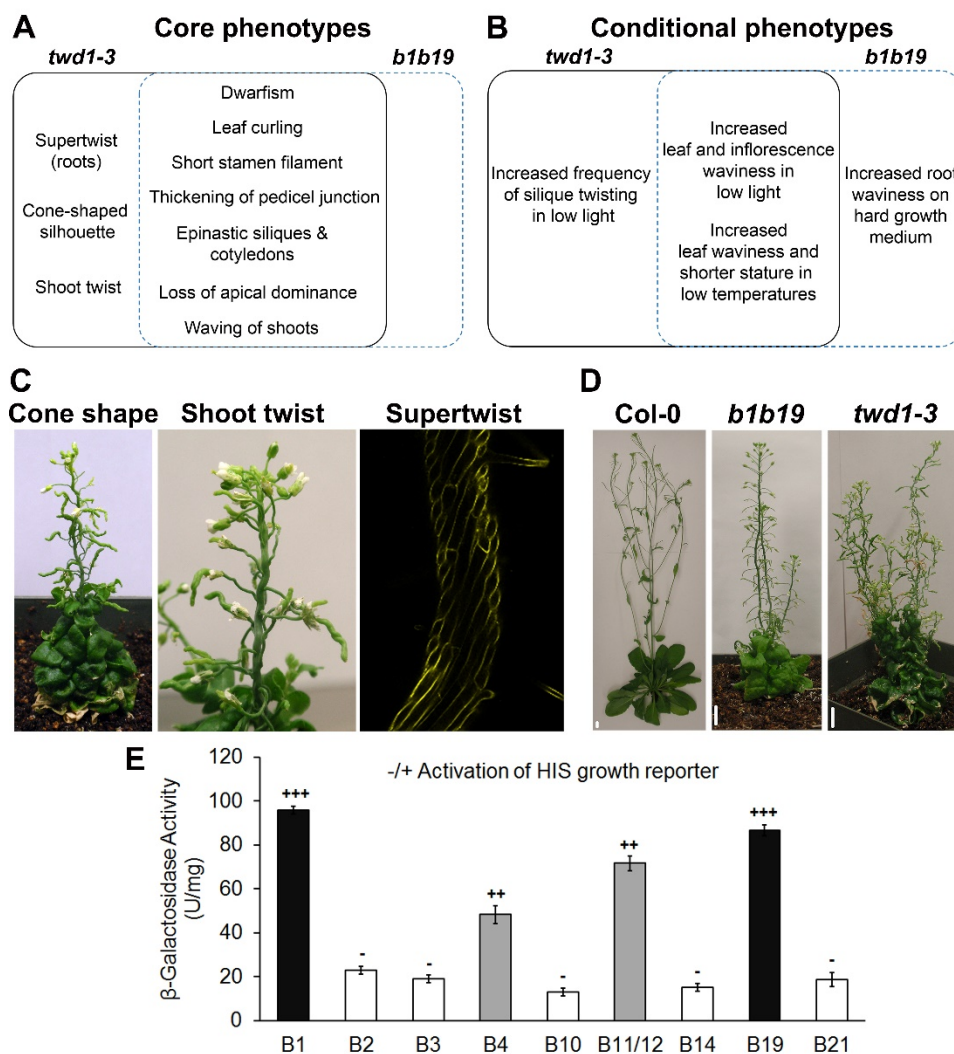


**Figure 2. Relationship between ABCB transporters and FKBP42.** A and B, Venn diagrams illustrating the core phenotypes of *twd1-3* and *b1b19* and the plasticity of phenotypes in response to light, temperature and media firmness. A, *b1b19* and *twd1-3* share numerous invariant core phenotypes. *b1b19* shares all its core phenotypes with *twd1-3*, whereas some are exclusive to *twd1-3*. B, Certain core phenotypes can be altered by temperature and particularly light intensity. C, *twd1-3* exclusive core phenotypes, root twist (left), cone-shaped silhouette (center), shoot twist (right). D, Comparison of the overall plant stature of Col-0 (left), *b1b19* (center) and *twd1-3* (right). White bar = 1 cm. E, Yeast 2-hybrid assay of the C-terminus of multiple ABCB transporters with the PPIase domain of FKBP42. + and - symbolize activation of the HIS growth reporter on medium without HIS.

**Figure 3**
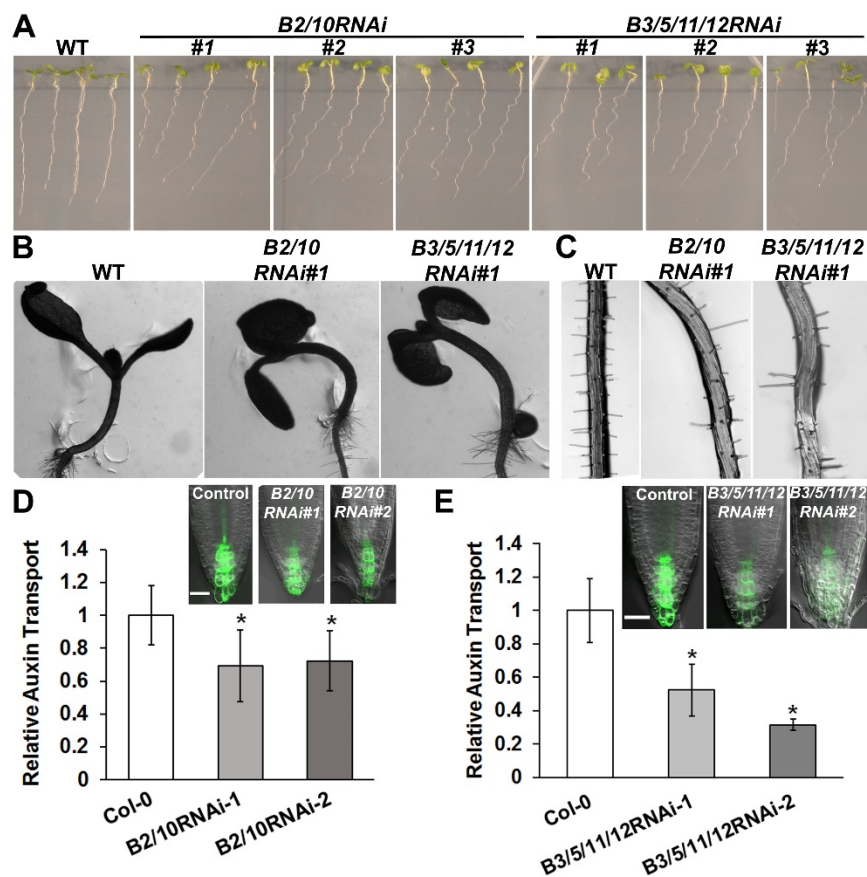


**Figure 3. RNAi-mediated knock down of *ABCB* clusters reveal transporters involved in long distance transport.** A, All three individual transgenic lines of *B2/10RNAi* and *B3/5/11/12RNAi* exhibited left-handed root skewing, B, delayed opening of cotyledons and C, root twisting. D and E, Relative auxin transport was measured by applying $^3$H-IAA to the shoot apex of 4-5 d seedlings and radioactivity measured at the root tip (D) and RSTZ (E), respectively. Values are mean of 10 seedlings, $n = 3$, error bars = SD. Significance determined by Student's *t-test*, *$P \leq$ 0.05. Insets, Expression of DR5rev$_{Pro}$::GFP in the root tip of 5 d seedlings in the background of *B2/10RNAi* and *B3/5/11/12RNAi*. White bar = 50 $\mu$m.

**Figure 4**
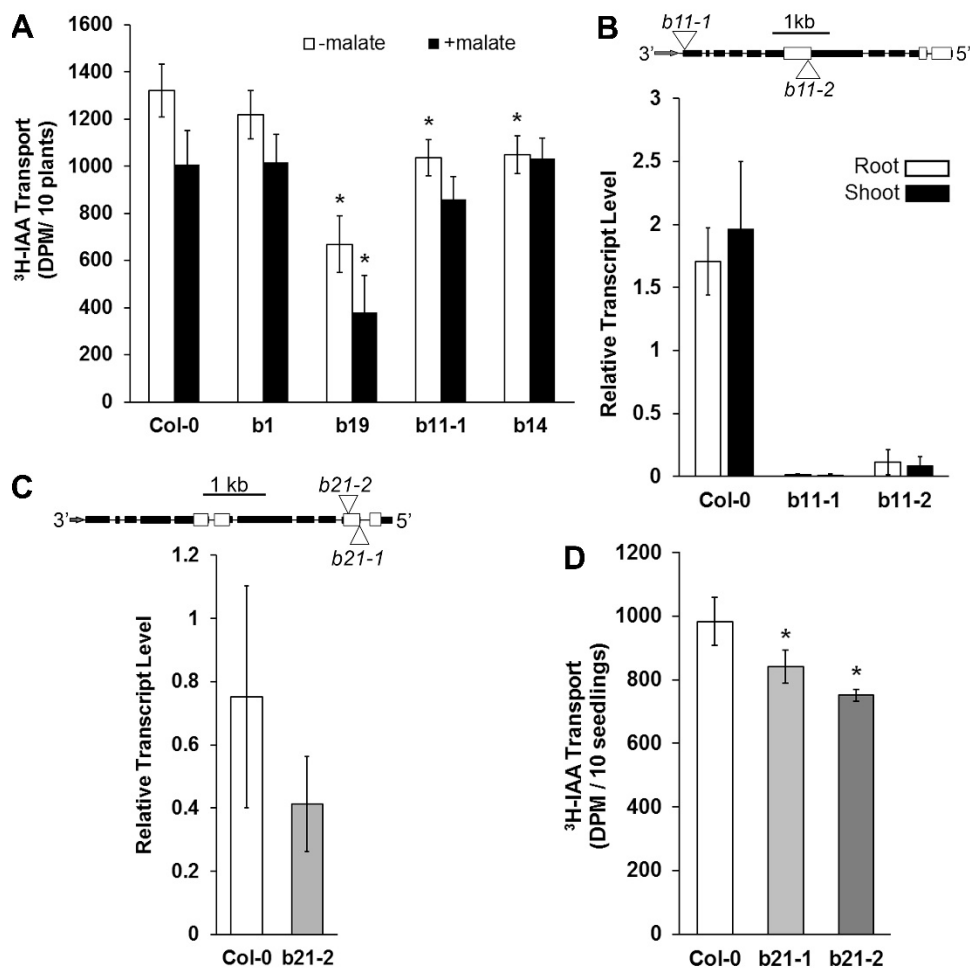


**Figure 4. Qualification of ABCBs for further analysis.** A, ³H-IAA transport in *abcb* single mutants in absence and presence of excess malate. Values represent averages of 10 seedlings with $n = 3$. Significant differences were determined by ANOVA, followed by Dunnett's *post-hoc* analysis with *$P \leq 0.05$. Error bars = ±SD. B, (Top) Schematic representation of the genomic sequence encoding B11. Exons are black boxes, introns black lines and the coding region for the NBD (nucleotide-binding domain) is a white box. T-DNA insertion sites are marked by triangles. (Bottom) Expression level of *B11* in wild-type (Col-0), *b11-1* and *b11-2* shoots (white) and roots (black), quantified by qRT-PCR, with $n = 3$. C, (Top) schematic representation of the genomic sequence encoding for *B21*. Both alleles disrupt the region encoding for the second NBD. (Bottom) mRNA levels of *B21* in leaves of 5 week-old soil-grown wild-type (Col-0) and *b21-2*. Error bars = ±SD. D, ³H-IAA transport from RSTZ to root tip in 5 d seedlings of wild-type, *b21-1* and *b21-2*. Values are average of 10 seedlings with $n = 3 \pm$ SD. Significant differences (*$P \leq$ 0.05) were determined by ANOVA followed by Dunnett's *post-hoc* analysis.

# Figure 5
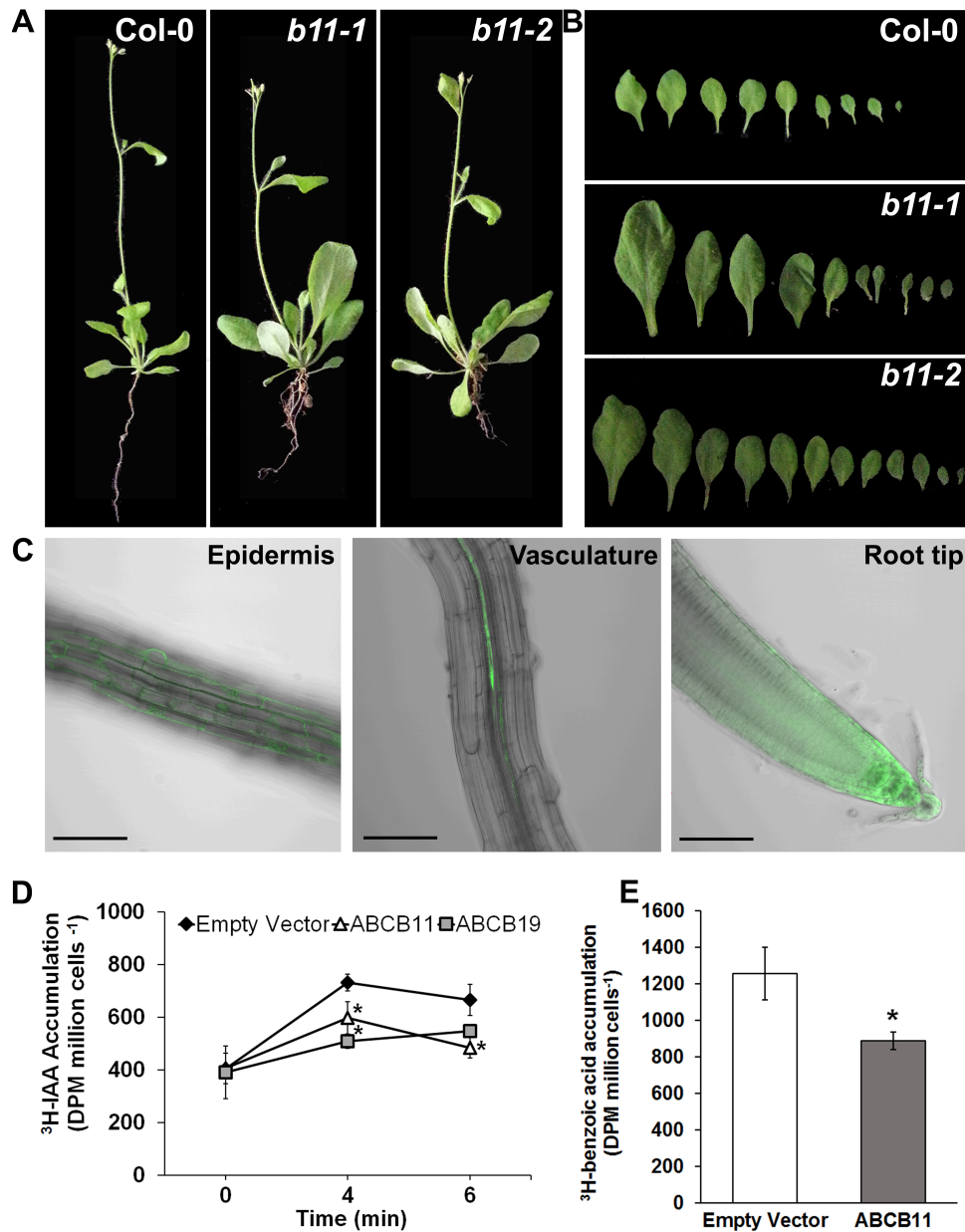


**Figure 5. Phenotypic characterization of *b11* alleles.** A and B, Morphology and leaf-size phenotype of *b11-1* and *b11-2* grown in short day conditions (12/12h light/dark cycle, 80 $\mu$mol m$^{-2}$ s$^{-1}$). C, *B11* expression in roots of 5 d B11$_{Pro}$::GFP seedlings at different locations at the root. Images were digitally enhanced to the same extent after the pictures were taken using the level's tool of the Adobe Photoshop software. Black bar = 100 $\mu$m. D, $^3$H-IAA transport assay in *S. pombe* transformed with either the empty vector, *B11* or *B19*. A reduction in $^3$H-IAA accumulation indicates export activity. Values are given as mean, *n = 3*, error bars = SD. Statistical analysis was performed by Student's *t-test*, *\*P ≤ 0.05*. E, $^3$H-benzoic acid accumulation in *S. pombe* expressing *B11* after 8 min of incubation. Values are mean ± SD, *n = 3*. Statistical analysis was performed by Student's *t-test*, *\*P ≤ 0.05*.

**Figure 6**
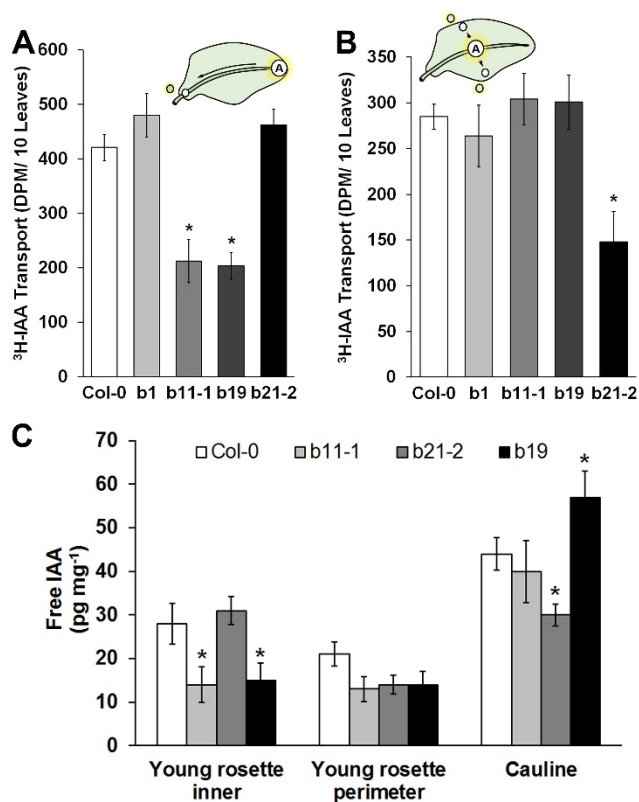


**Figure 6. Auxin levels and auxin transport in *abcb* mutants.** A, $^3$H-IAA movement from the leaf tip to the petiole in 4 week old plants. B, Centrolateral movement of $^3$H-IAA in 4 week old plants. C, Quantification of free IAA in different parts of the rosette of 6 week old *abcb* mutants. All values are mean ±SD of 10 plants, $n = 3$. Significances were determined by ANOVA followed by Dunnett's *post-hoc* analysis, *$P \le 0.05$.

# Figure 7
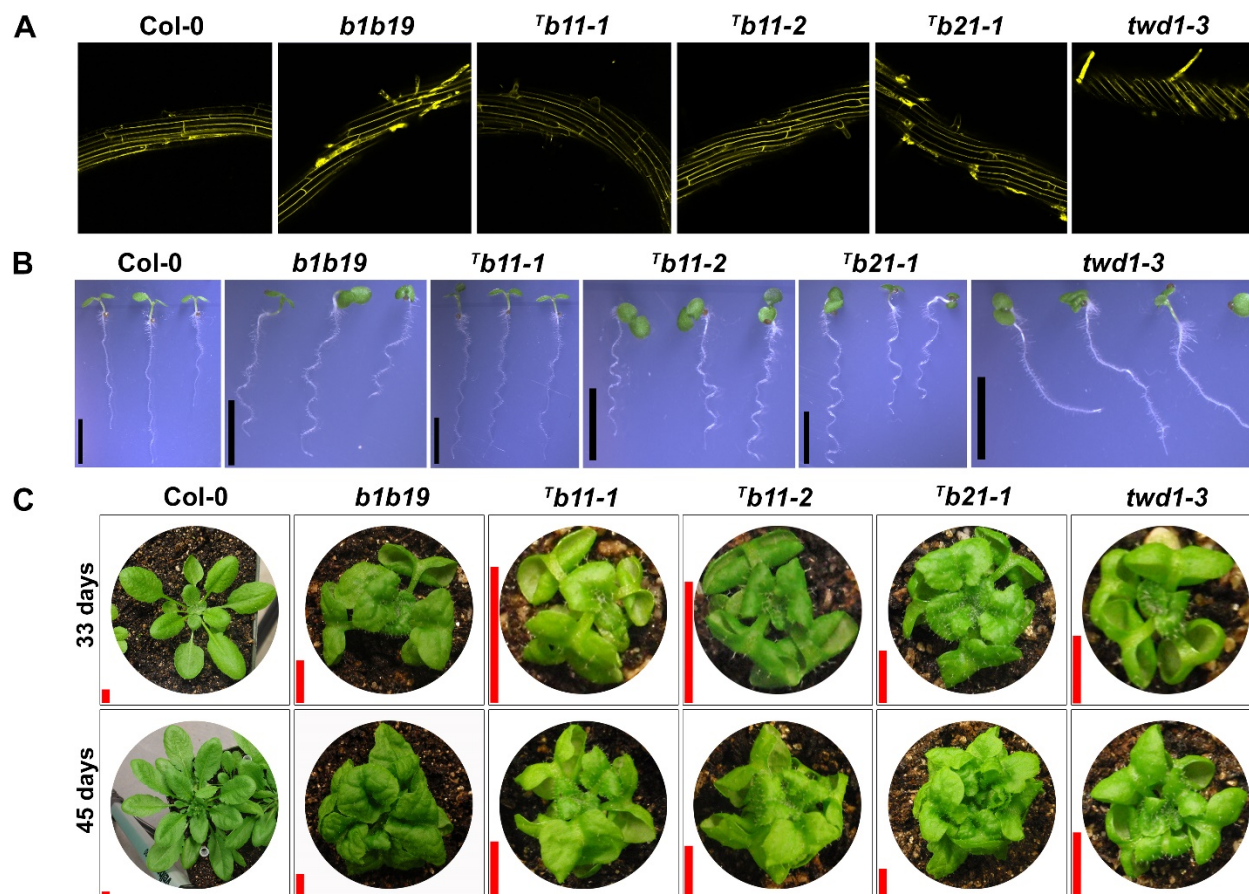


**Figure 7. Phenotypes of *b1b19*, *twd1-3* and *abcb* triple mutants during pre-flowering stages.** A, Root twisting phenotype of 5 d roots stained with 5 $\mu$M FM4-64. B, Root waving phenotype of 5 d seedlings. C, Rosette phenotype of adult pre-flowering plants on day 33 and 45 after sowing. Red bar = 0.5 cm.

# Figure 8
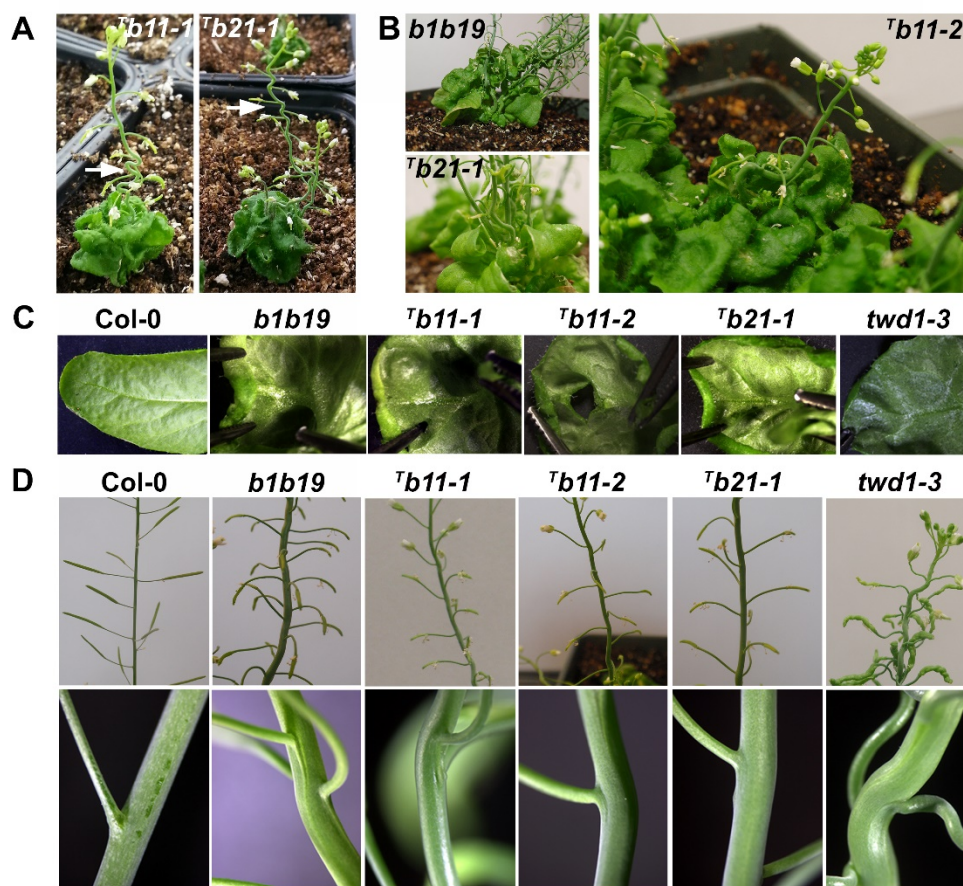


**Figure 8. Inflorescence phenotypes of *b1b19*, *twd1-3* and *abcb* triple mutants.** A, Exaggerated inflorescence waviness of $^{T}b11-1$ and $^{T}b21-1$ in low light conditions (16/8 hr photoperiod, 30 $\mu$mol m$^{-2}$ s$^{-1}$). B, Close-ups of the rosette-proximal segment of the inflorescence. C, Mid-vein phenotype. Shown is the abaxial side of mature leaves. D, (Top) Close-up of the inflorescence of mature plants grown at a 12/12 hr photoperiod at 70 $\mu$mol m$^{-2}$ s$^{-1}$ (Col-0, *b1b19*, $^{T}b11-1$, $^{T}b11-2$ and $^{T}b21-1$) and 16/8 hr photoperiod at 60 $\mu$mol m$^{-2}$ s$^{-1}$ (*twd1-3*). (Bottom), Close-up of the inflorescence-pedicel junction.

**Figure 9**
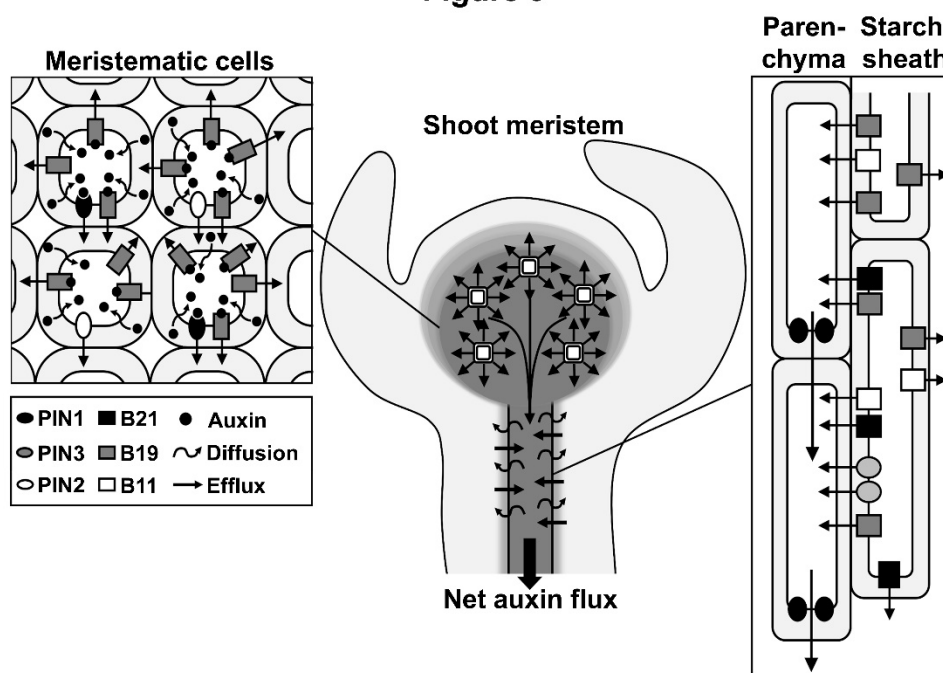


**Figure 9. ABCBs facilitate shoot-to-root auxin movement in two distinct ways.** Center, Auxin fluxes from the meristematic cells towards the root in light-grown seedlings. Auxin biosynthesis is high in the shoot apical meristem (grey background). Left, Auxin export is facilitated by polar-localized PINs and non-polar ABCBs in the meristem. Around 20% of apoplastic auxin is protonated and as such can re-enter the cell via diffusion. In the cytosol it quickly dissociates, trapping it inside. PIN1, PIN2 and especially the ATP-driven activity of B19 shifts the net auxin movement toward efflux. Due to the small size of the meristematic cells, auxin should be equally accessible to PINs and ABCBs, resulting in non-directional fluxes of auxin. Center, The increase in apoplastic auxin within the meristem then initiates the basipetal flux, analogous to the principle of gel chromatography. Right, In the larger vascular cells, auxin concentrates mainly at the apical and basal regions of the cell where PIN1 (rootward) and PIN3 (lateral) facilitate directional efflux. Along the way, auxin has to be continuously re-introduced into the main auxin stream. B19, B11 and B21 are highly expressed in the adjoining cell layers, such as the starch sheaths. The contribution of B21 appears to be more significant in the root than in the shoot, possibly due to compensatory action of PIN3 in the shoot. Loss of multiple ABCBs disrupts the basipetal stream, leading to the inflorescence and root waving phenotypes in *b1b19*, the *abcb* triple mutants and *twd1-3*.

## Supplemental Figure S1
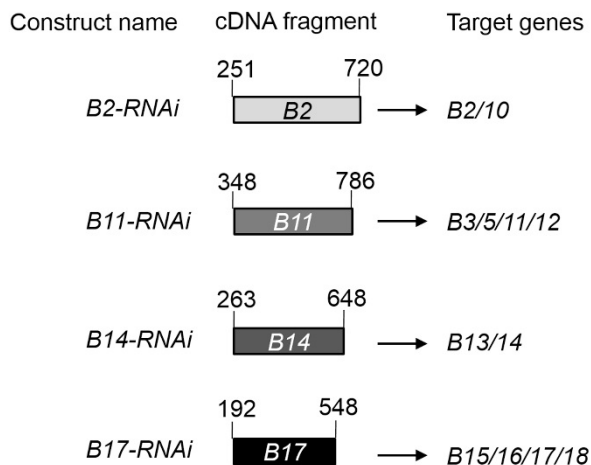


Supplemental Figure S1. RNAi constructs targeting paralogous *ABCB* genes. Depicted are the cDNA fragments used to target the paralogous genes. For example, a 469 bp fragment of *B2* cDNA (nt 251-720) was RT-PCR amplified and cloned into the pDONR Gateway entry vector. The fragment was then transferred to a pOpOff Gateway-compatible RNAi vector, which was designed to contain two Gateway cloning sites in opposite direction (Wielopolska et al., 2005). The construct allowed for a dexamethasone-inducible expression of the RNAi fragments.

## Supplemental Figure S2
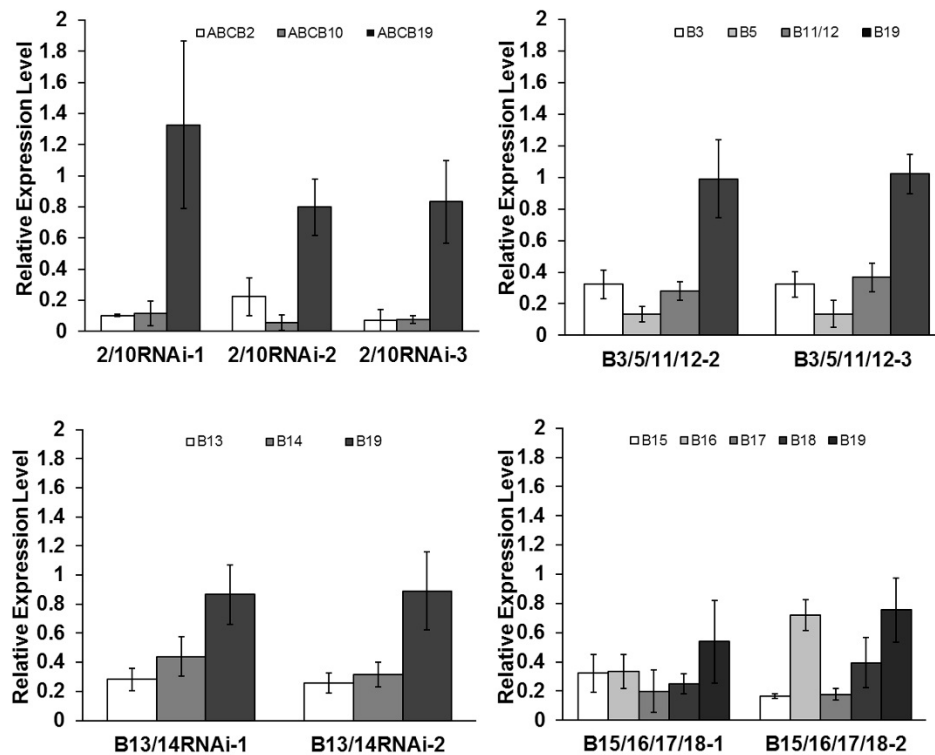


**Supplemental Figure S2. Quantification of targeted genes in the RNAi transgenic lines. Expression levels of targeted and non-targeted (*B19*) genes was verified by qRT-PCR after induction with 10 $\mu$M dexamethasone.**

## Supplemental Figure S3
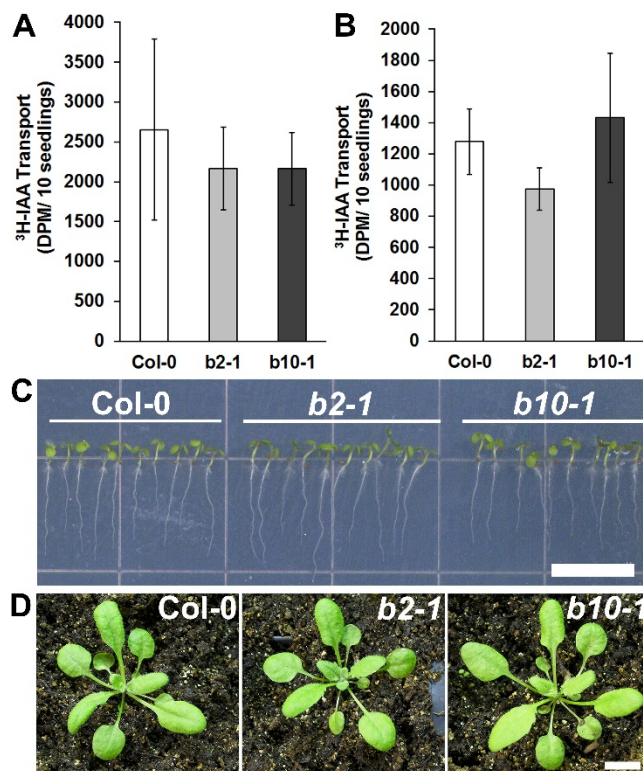


**Supplemental Figure S3. Phenotypic and functional characterization of *b2-1* and *b10-1* single mutants. A,** IAA transport from the shoot apex to RSTZ is not significantly affected in *b2-1* and *b10-1*. **B,** IAA transport from RSTZ to the root tip is only slightly affected in *b2-1* and resembles wild-type levels in *b10-1*. **C,** Root phenotype of *b2-1* and *b10-1*. White bar = 1 cm. **D,** Phenotype of 25 d plants grown on soil. White bar = 1 cm.

**Supplemental Figure S4**
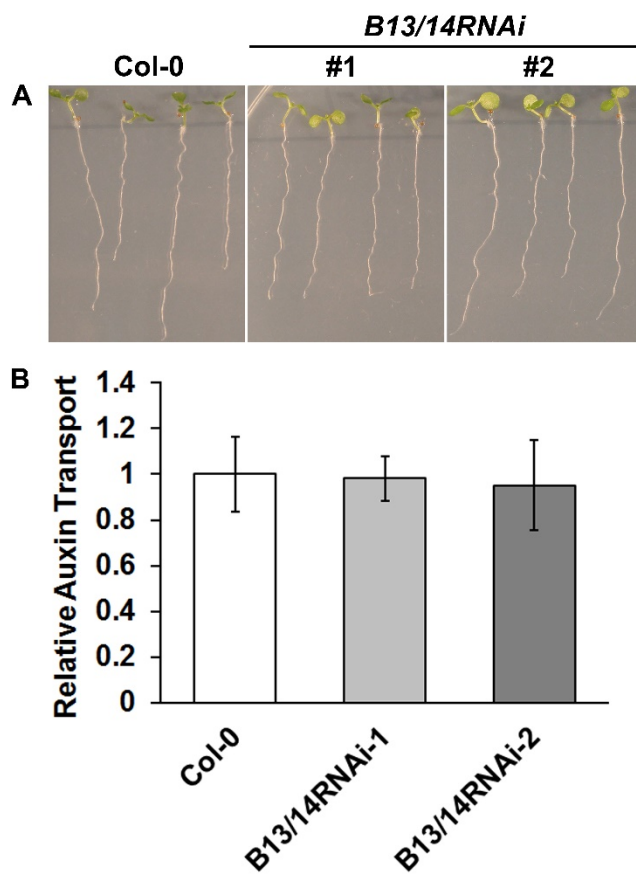


**Supplemental Figure S4. Characterization of *B13/14RNAi*. A, *B13/14RNAi* does not show any root phenotype after induction with 10 *μ*M dexamethasone. B, Auxin transport from the shoot apex to the root tip is not affected in *B13/14RNAi*. Values are an average of 10 seedlings with *n* = 3. Error bars = sd.**

## Supplemental Figure S5
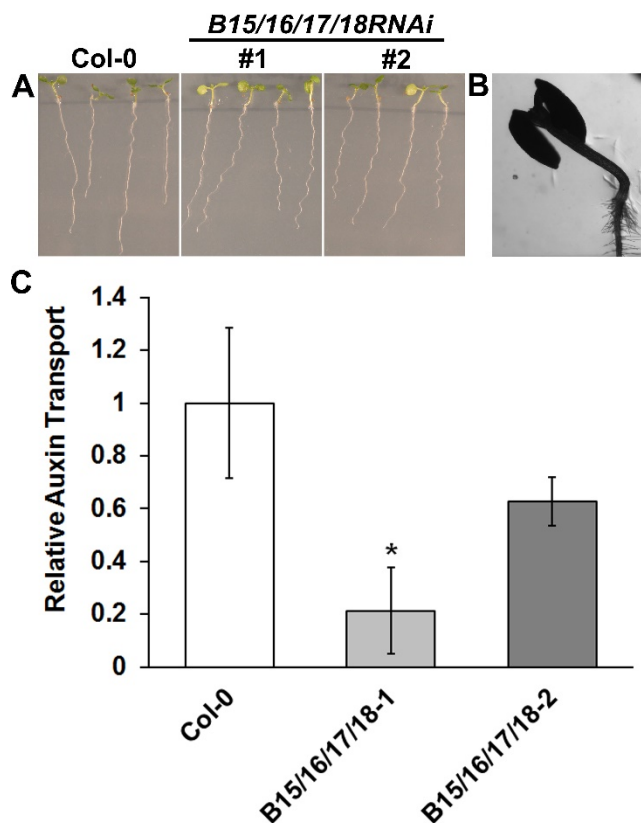


**Supplemental Figure S5. Characterization of *B15/16/17/18RNAi*. A,** *B15/16/17/18RNAi*
shows wavy, but not skewed, roots after induction with 10 $\mu$M dexamethasone. **B,** In the
presence of 10 $\mu$M dexamethasone *B15/16/17/18RNAi* develops epinastic cotyledons. **C,**
Auxin transport from the shoot apex to the RSTZ is significantly reduced in one transgenic
line and slightly reduced in another. Significant differences were determined (*$P \leq 0.05$)
using Student's *t-test* with $n = 3$, and 10 seedlings per replicate. Error bars = sd.

## Supplemental Figure S6
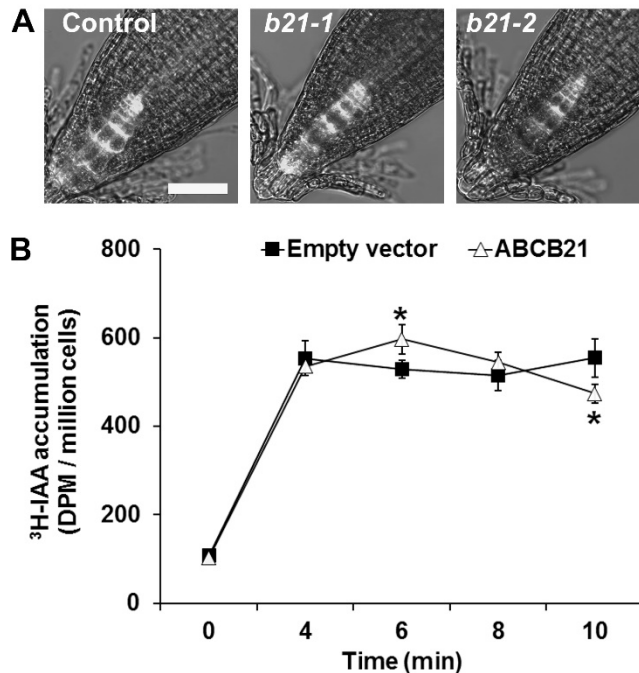


**Supplemental Figure S6. B21 is a concentration-dependent rootward auxin transporter. A,** *b21-1* **and** *b21-2* **were crossed into DR5rev$_{Pro}$:GFP. Auxin abundance at the root tip of 5 d seedlings is reduced in both** *b21-1* **and** *b21-2* **compared to the wild-type, with** *b21-2* **the most strongly affected. White bar = 50 $\mu$m. B, B21 functions as a facultative auxin transporter in** *S. pombe***. At lower auxin concentrations (< 6 min) cells expressing B21 contain more auxin compared to the empty vector control. With increasing auxin concentrations (> 6 min) B21 exports auxin out of the cells. Significant differences were determined (\*$P \le 0.05$) using Student's** *t-test* **with** *n* **= 3. Error bars = sd.**

**Supplemental Figure S7**
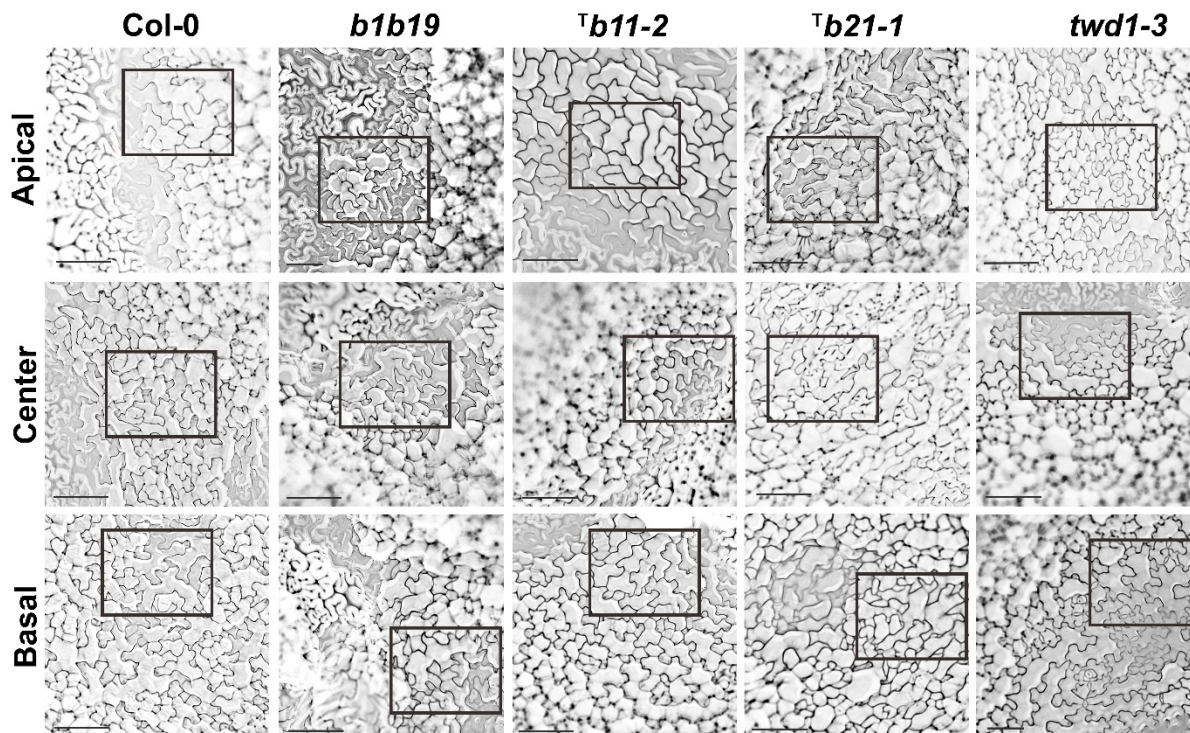


**Supplemental Figure S7. Epidermal cells are smaller in *abcb* double/triple mutants and *twd1-3*. Leaf imprints of the abaxial epidermal cells at three different locations of adult leaves: Basal = margin close to the petiole, center = margin in the center of the leaf, apical = margin at the leaf tip. Imprints were taken according to Schmid and Billich, 1996. Black line = 200 *µ*m.**

**Supplemental Figure S8**
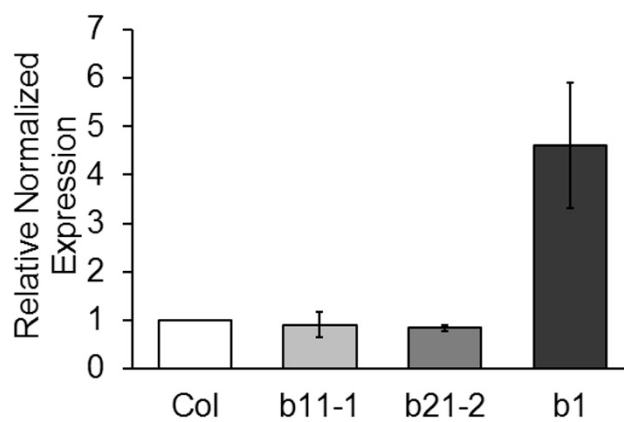


**Supplemental Figure S8. Expression profile of *B19* in the roots of *abcb* mutants. The expression of *B19* in the Col-0 background was set to 1. *B19* expression in *b1* is about 4.5-fold higher than in the wild-type, *b11-1* and *b21-1*. qRT-PCR was performed on 5 d seedlings with biological replicates *n* = 2, technical replicates *n* = 2. Expression levels were normalized to the housekeeping gene *18S*.**

**Supplemental Table S1. List of primers used in this manuscript.**

**qRT-PCR Primers**

| AGI | Gene | Sequence (5' to 3') | Sense |
|---|---|---|---|
| At4g25960 | *ABCB2* | TTCGTCGCCATCGGACTTATTGCT | Forward |
| | | TTGTACGGTCCTCACATTCCCGAT | Reverse |
| At4g01820 | *ABCB3* | GCCTATCGAGCGAGTGTTAAGCAA | Forward |
| | | AGACATCGAACTTGCGACCACAGT | Reverse |
| At4g01830 | *ABCB5* | GCTTTGGGTACATGGTTTGGTGGT | Forward |
| | | ACAAGGTGATGCTTGCCCTAAAGC | Reverse |
| At1g10680 | *ABCB10* | ATCGCAGAAGAGGTGATCGGGAAT | Forward |
| | | AATGCAACGAACCAAGCCCTAGTC | Reverse |
| At1g02520 | *ABCB11* | CGCAGCTCATTCGATTACAAG | Forward |
| | | ACGAAGTTCCCTCCATTGAC | Reverse |
| At1g27940 | *ABCB13* | TCTCATTGCGGCTTCACTTACCGA | Forward |
| | | GACAAAGGCATTCTTGGTGGGCTT | Reverse |
| At1g28010 | *ABCB14* | CTGCTAAAGCAGCCAACGCAGATT | Forward |
| | | TGCCCTCCTGAAAGTTGAGTTCCT | Reverse |
| At3g28345 | *ABCB15* | TCGTTAGTGGGTGATCGAATGGCA | Forward |
| | | ACCCGACGAGTGTAGAAGCAAACA | Reverse |
| At3g28360 | *ABCB16* | TTGGACAGCCAATCAGAGCGTGTA | Forward |
| | | TCGTGCTAAGCCTATGTGCGATCA | Reverse |
| At3g28380 | *ABCB17* | AAGCGGATCGGGTAAATCGACAGT | Forward |
| | | TGCGACCTCAACCAATTCACTTGC | Reverse |
| At3g28390 | *ABCB18* | AAGCTTGGGTTGAGACAAGGGCTA | Forward |
| | | ACCGAAGGTGACGCAAACAATGAC | Reverse |
| At3g28860 | *ABCB19* | AGGATTGACCCGGATGATGCTGAT | Forward |
| | | TCGGGTCTTGAAGGGTAAGCGAAA | Reverse |
| At3g62150 | *ABCB21* | TCGCTCATACGTCTACAAGAAGATAC TAAACAG | Forward |
| | | CGAAAGAGACTTTCTTTTCTTTGATC GG | Reverse |
| At3g18780 | *ACT2* | ACACTGTGCCAATCTACGAGGGTT | Forward |
| | | ACAATTTCCCGCTCTGCTGTTGTG | Reverse |
| At1g10430 | *PP2A* | TCGTGGTGCAGGCTACACTTTC | Forward |
| | | TCAGAGAGAGTCCATTGGTGTGG | Reverse |
| | 18S | AAGCAAGCCTACGCTCTGGA | Forward |
| | | AGGCCAACACAATAGGATCGA | Reverse |

**Continuation of Supplemental Table S1.**

**RNAi constructs**

| Construct | Sequence (5' to 3') | Sense |
|---|---|---|
| *B2/10RNAi* | CACCCAGAGTCGCCAAGTACTCGT | Forward |
| | GTACGGTCCTCACATTCCCGA | Reverse |
| *B3/5/11/12RNAi* | CACCCGCGAGGATAAGAAGTACATATC | Forward |
| | GATGTTATGAACTTCTTGTAGCTGTTAATG | Reverse |
| *B13/14RNAi* | CACCCTCGCGTTTCACAGAATGCT | Forward |
| | CATGACTATAGCATACCCTCCTC | Reverse |
| *B15/16/17/18RNAi* | CACCCACTTCCTCTTCCAATAATAAA | Forward |
| | CTCCACATCAAGATGAAACTC | Reverse |

**Cloning**

| Construct | Transformed | Sequence (5' to 3') | Sense |
|---|---|---|---|
| B11<sub>Pro</sub>::GFP | *A. thaliana* | CACCTGGACCCTCATGTTTTTCCTT | Forward |
| | | ATTTCGGCGCTGACAAAAATCAG | Reverse |
| B1 | *S. pombe* | See Yang and Murphy, 2009 | Forward |
| | | | Reverse |
| B11 | *S. pombe* | atcatatgATGAACGGTGACGGCGCCAGAGAAG | Forward |
| | | atcccgggTCAATTAGAAGCAGTCATGTGAAGCTG | Reverse |
| B19 | *S. pombe* | See Yang and Murphy, 2009 | Forward |
| | | | Reverse |

**Mutant verification**

| T-DNA line | Gene | Sequence (5' to 3') | Sense |
|---|---|---|---|
| SALK_057628 | *b11-1* | TGGCATCTTGAATAAGAACCG | Forward |
| | | ATTTTACGGGCAAGCAAAAG | Reverse |
| SALK_037942 | *b11-2* | AACATCTCCATGTGTAACCGC | Forward |
| | | TCGGGTGAGTGATACTTTTGG | Reverse |
| WiscDsLox1C2 | *b21-1* | AATCGACAGTGATTGCGTTG | LP |
| | | TTAACCATAACCCGGTCCAA | RP |
| Gabi_954H06 | *b21-2* | TTCTCCACGATGACTCCATTC | LP |
| | | TCATTGTCTCCTGATTCCAGC | RP |
| T-DNA (SALK) | LBb1.3 | ATTTTGCCGATTTCGGAAC | N/A |
| T-DNA (Wisc) | p745 | AACGTCCGCAATGTGTTATTAAGTTGTC | N/A |
| T-DNA (GABI) | o8409 | ATATTGACCATCATACTCATTGC | N/A |

BIBLIOGRAPHY

BIBLIOGRAPHY

**Aukerman MJ, Hirschfeld M, Wester L, Weaver M, Clack T, Amasino RM, Sharrock RA** (1997) A deletion in the PHYD gene of the Arabidopsis Wassilewskija ecotype defines a role for phytochrome D in red/far-red light sensing. Plant Cell **9**: 1317–26

**Bailly A, Sovero V, Geisler M** (2006) The TWISTED DWARF's ABC: How Immunophilins Regulate Auxin Transport. Plant Signal Behav **1**: 277–280

**Bailly A, Sovero V, Vincenzetti V, Santelia D, Bartnik D, Koenig BW, Mancuso S, Martinoia E, Geisler M** (2008) Modulation of P-glycoproteins by auxin transport inhibitors is mediated by interaction with immunophilins. J Biol Chem **283**: 21817–26

**Bailly A, Wang B, Zwiewka M, Pollmann S, Schenck D, Lüthen H, Schulz A, Friml J, Geisler M** (2014) Expression of TWISTED DWARF1 lacking its in-plane membrane anchor leads to increased cell elongation and hypermorphic growth. Plant J (1) **77**: 108-118

**Banasavadi-Siddegowda YK, Mai J, Fan Y, Bhattacharya S, Giovannucci DR, Sanchez ER, Fischer G, Wang X** (2011) FKBP38 peptidylprolyl isomerase promotes the folding of cystic fibrosis transmembrane conductance regulator in the endoplasmic reticulum. J Biol Chem **286**: 43071–80

**Band LR, Wells DM, Fozard JA, Ghetiu T, French AP, Pound MP, Wilson MH, Yu L, Li W, Hijazi HI, et al** (2014) Systems analysis of auxin transport in the Arabidopsis root apex. Plant Cell **26**: 862–75

**Bandyopadhyay A, Blakeslee JJ, Lee OR, Mravec J, Sauer M, Titapiwatanakun B, Makam SN, Bouchard R, Geisler M, Martinoia E, et al** (2007) Interactions of PIN and PGP auxin transport mechanisms. Biochem Soc Trans **35**: 137–41

**Barbez E, Kubeš M, Rolčík J, Béziat C, Pěnčík A, Wang B, Rosquete MR, Zhu J, Dobrev PI, Lee Y, et al** (2012) A novel putative auxin carrier family regulates intracellular auxin homeostasis in plants. Nature **485**: 119–22

**Benková E, Michniewicz M, Sauer M, Teichmann T, Seifertová D, Jürgens G, Friml J** (2003) Local, Efflux-Dependent Auxin Gradients as a Common Module for Plant Organ Formation. Cell **115**: 591–602

**Blakeslee JJ, Bandyopadhyay A, Lee OR, Mravec J, Titapiwatanakun B, Sauer M, Makam SN, Cheng Y, Bouchard R, Adamec J, et al** (2007) Interactions among PIN-FORMED and P-glycoprotein auxin transporters in Arabidopsis. Plant Cell **19**: 131–47

**Bouchard R, Bailly A, Blakeslee JJ, Oehring SC, Vincenzetti V, Lee OR, Paponov I, Palme K, Mancuso S, Murphy AS, et al** (2006) Immunophilin-like TWISTED DWARF1 modulates auxin efflux activities of Arabidopsis P-glycoproteins. J Biol Chem **281**: 30603–30612

**De Carbonnel M, Davis P, Roelfsema MRG, Inoue S-I, Schepens I, Lariguet P, Geisler M, Shimazaki K-I, Hangarter R, Fankhauser C** (2010) The Arabidopsis PHYTOCHROME KINASE SUBSTRATE2 protein is a phototropin signaling element that regulates leaf flattening and leaf positioning. Plant Physiol **152**: 1391–405

**Carraro N, Tisdale-Orr TE, Clouse RM, Knöller AS, Spicer R** (2012) Diversification and expression of the PIN, AUX/LAX, and ABCB families of putative auxin transporters in *Populus*. Front Plant Sci (3) **17**

**Cheng Y, Dai X, Zhao Y** (2006) Auxin biosynthesis by the YUCCA flavin monooxygenases controls the formation of floral organs and vascular tissues in Arabidopsis. Genes Dev **20**: 1790–9

**Christie JM, Murphy AS** (2013) Shoot phototropism in higher plants: new light through old concepts. Am J Bot **100**: 35–46

**Christie JM, Yang H, Richter GL, Sullivan S, Thomson CE, Lin J, Titapiwatanakun B, Ennis M, Kaiserli E, Lee OR, et al** (2011) phot1 inhibition of ABCB19 primes lateral auxin fluxes in the shoot apex required for phototropism. PLoS Biol **9**: e1001076

**Cnops G, Wang X, Linstead P, Van Montagu M, Van Lijsebettens M, Dolan L** (2000) Tornado1 and tornado2 are required for the specification of radial and circumferential pattern in the Arabidopsis root. Development **127**: 3385–3394

**Devlin PF** (1999) Phytochrome D Acts in the Shade-Avoidance Syndrome in Arabidopsis by Controlling Elongation Growth and Flowering Time. PLANT Physiol **119**: 909–916

**Ding Z, Galván-Ampudia CS, Demarsy E, Łangowski Ł, Kleine-Vehn J, Fan Y, Morita MT, Tasaka M, Fankhauser C, Friml J** (2011) Light-mediated polarization of the PIN3 auxin transporter for the phototropic response in Arabidopsis. Nat Cell Biol **13**: 447–52

**Eckhoff A, Granzin J, Kamphausen T, Büldt G, Schulz B, Weiergräber OH** (2005) Crystallization and preliminary X-ray analysis of immunophilin-like FKBP42 from Arabidopsis thaliana. Acta Crystallogr Sect F Struct Biol Cryst Commun **61**: 363–5

**Effendi Y, Jones AM, Scherer GFE** (2013) AUXIN-BINDING-PROTEIN1 (ABP1) in phytochrome-B-controlled responses. J Exp Bot **64**: 5065–74

**Faure J, Vittorioso P, Santoni V, Fraisier V, Prinsen E, Barlier I, Van Onckelen H, Caboche M, Bellini C** (1998) The PASTICCINO genes of Arabidopsis thaliana are involved in the control of cell division and differentiation. Development **125**: 909–918

**Forestan C, Farinati S, Varotto S** (2012) The Maize PIN Gene Family of Auxin Transporters. Front Plant Sci **3**: 16

**Friml J, Vieten A, Sauer M, Weijers D, Schwarz H, Hamann T, Offringa R, Jürgens G** (2003) Efflux-dependent auxin gradients establish the apical-basal axis of Arabidopsis. Nature **426**: 147–53

**Gallavotti A** (2013) The role of auxin in shaping shoot architecture. J Exp Bot **64**: 2593–608

**Gälweiler L** (1998) Regulation of Polar Auxin Transport by AtPIN1 in Arabidopsis Vascular Tissue. Science (80) **282**: 2226–2230

**Gao X, Yuan H-M, Hu Y-Q, Li J, Lu Y-T** (2014) Mutation of Arabidopsis CATALASE2 results in hyponastic leaves by changes of auxin levels. Plant Cell Environ **37**: 175–88

**Geisler M, Bailly A** (2007) Tête-à-tête: the function of FKBPs in plant development. Trends Plant Sci **12**: 465–73

**Geisler M, Blakeslee JJ, Bouchard R, Lee OR, Vincenzetti V, Bandyopadhyay A, Titapiwatanakun B, Peer WA, Bailly A, Richards EL, et al** (2005) Cellular efflux of auxin catalyzed by the Arabidopsis MDR/PGP transporter AtPGP1. Plant J **44**: 179–94

**Geisler M, Girin M, Brandt S, Vincenzetti V, Plaza S, Paris N, Kobae Y, Maeshima M, Billion K, Kolukisaoglu UH, et al** (2004) Arabidopsis immunophilin-like TWD1 functionally interacts with vacuolar ABC transporters. Mol Biol Cell **15**: 3393–405

**Geisler M, Kolukisaoglu HU, Bouchard R, Billion K, Berger J, Saal B, Frangne N, Koncz-Kalman Z, Koncz C, Dudler R, et al** (2003) TWISTED DWARF1, a unique plasma membrane-anchored immunophilin-like protein, interacts with Arabidopsis multidrug resistance-like transporters AtPGP1 and AtPGP19. Mol Biol Cell **14**: 4238–4249

**Geisler M, Murphy AS** (2006) The ABC of auxin transport: the role of p-glycoproteins in plant development. FEBS Lett **580**: 1094–102

**Gollan PJ, Bhave M, Aro E-M** (2012) The FKBP families of higher plants: Exploring the structures and functions of protein interaction specialists. FEBS Lett **586**: 3539–47

**Halliday KJ, Martínez-García JF, Josse E-M** (2009) Integration of light and auxin signaling. Cold Spring Harb Perspect Biol **1**: a001586

**Hersch M, Lorrain S, de Wit M, Trevisan M, Ljung K, Bergmann S, Fankhauser C** (2014) Light intensity modulates the regulatory network of the shade avoidance response in Arabidopsis. Proc Natl Acad Sci U S A **111**: 6515–6520

**Hochholdinger F, Wulff D, Reuter K, Park WJ, Feix G** (2000) Tissue-specific expression of AUX1 in maize roots. J Plant Physiol **157**: 315–319

**Ischebeck T, Werner S, Krishnamoorthy P, Lerche J, Meijón M, Stenzel I, Löfke C, Wiessner T, Im YJ, Perera IY, et al** (2013) Phosphatidylinositol 4,5-bisphosphate influences PIN polarization by controlling clathrin-mediated membrane trafficking in Arabidopsis. Plant Cell **25**: 4894–911

**Ishida T, Kaneko Y, Iwano M, Hashimoto T** (2007) Helical microtubule arrays in a collection of twisting tubulin mutants of Arabidopsis thaliana. Proc Natl Acad Sci USA **104**: 8544–9

**Jensen PJ** (1998) Auxin Transport Is Required for Hypocotyl Elongation in Light-Grown but Not Dark-Grown Arabidopsis. Plant Physiol **116**: 455–462

**Kamimoto Y, Terasaka K, Hamamoto M, Takanashi K, Fukuda S, Shitan N, Sugiyama A, Suzuki H, Shibata D, Wang B, et al** Arabidopsis ABCB21 is a Facultative Auxin Importer/Exporter Regulated by Cytoplasmic Auxin Concentration. Plant Cell Physiol **53**: 2090–2100

**Kamphausen T, Fanghänel J, Neumann D, Schulz B, Rahfeld J-U** (2002) Characterization of Arabidopsis thaliana At FKBP42 that is membrane-bound and interacts with Hsp90. Plant J **32**: 263–276

**Kaneda M, Schuetz M, Lin BSP, Chanis C, Hamberger B, Western TL, Ehlting J, Samuels AL** (2011) ABC transporters coordinately expressed during lignification of Arabidopsis stems include a set of ABCBs associated with auxin transport. J Exp Bot **62**: 2063–77

**Keuskamp DH, Pollmann S, Voesenek LACJ, Peeters AJM, Pierik R** (2010) Auxin transport through PIN-FORMED 3 (PIN3) controls shade avoidance and fitness during competition. Proc Natl Acad Sci USA **107**: 22740–4

**Kleine-Vehn J, Dhonukshe P, Swarup R, Bennett M, Friml J** (2006) Subcellular trafficking of the Arabidopsis auxin influx carrier AUX1 uses a novel pathway distinct from PIN1. Plant Cell **18**: 3171–81

**Knöller AS, Blakeslee JJ, Richards EL, Peer WA, Murphy AS** (2010) Brachytic2/ZmABCB1 functions in IAA export from intercalary meristems. J Exp Bot **61**: 3689–96

**Kozuka T, Suetsugu N, Wada M, Nagatani A** (2013) Antagonistic regulation of leaf flattening by phytochrome B and phototropin in Arabidopsis thaliana. Plant Cell Physiol **54**: 69–79

**Kubeš M, Yang H, Richter GL, Cheng Y, Młodzińska E, Wang X, Blakeslee JJ, Carraro N, Petrášek J, Zažímalová E, et al** (2012) The Arabidopsis concentration-dependent influx/efflux transporter ABCB4 regulates cellular auxin levels in the root epidermis. Plant J **69**: 640–54

**Lee M, Choi Y, Burla B, Kim Y-Y, Jeon B, Maeshima M, Yoo J-Y, Martinoia E, Lee Y** (2008) The ABC transporter AtABCB14 is a malate importer and modulates stomatal response to $CO_2$. Nat Cell Biol **10**: 1217–23

**Li L-C, Kang D-M, Chen Z-L, Qu L-J** (2007) Hormonal Regulation of Leaf Morphogenesis in Arabidopsis. J Integr Plant Biol **49**: 75–80

**Lin R, Wang H** (2005) Two homologous ATP-binding cassette transporter proteins, AtMDR1 and AtPGP1, regulate Arabidopsis photomorphogenesis and root development by mediating polar auxin transport. Plant Physiol **138**: 949–64

**Liu X, Cohen JD, Gardner G** (2011) Low-fluence red light increases the transport and biosynthesis of auxin. Plant Physiol **157**: 891–904

**Ljung K** (2013) Auxin metabolism and homeostasis during plant development. Development **140**: 943–50

**McFarlane HE, Shin JJH, Bird DA, Samuels AL** (2010) Arabidopsis ABCG transporters, which are required for export of diverse cuticular lipids, dimerize in different combinations. Plant Cell **22**: 3066–75

**Men S, Boutté Y, Ikeda Y, Li X, Palme K, Stierhof Y-D, Hartmann M-A, Moritz T, Grebe M** (2008) Sterol-dependent endocytosis mediates post-cytokinetic acquisition of PIN2 auxin efflux carrier polarity. Nat Cell Biol **10**: 237–44

**Mravec J, Kubeš M, Bielach A, Gaykova V, Petrásek J, Skůpa P, Chand S, Benková E, Zažímalová E, Friml J** (2008) Interaction of PIN and PGP transport mechanisms in auxin distribution-dependent development. Development **135**: 3345–54

**Multani DS, Briggs SP, Chamberlin MA, Blakeslee JJ, Murphy AS, Johal GS** (2003) Loss of an MDR transporter in compact stalks of maize br2 and sorghum dw3 mutants. Science **302**: 81–4

**Murphy AS, Hoogner KR, Peer WA, Taiz L** (2002) Identification, purification, and molecular cloning of N-1-naphthylphthalmic acid-binding plasma membrane-associated aminopeptidases from Arabidopsis. Plant Physiol **128**: 935–50

Nakagawa T, Kurose T, Hino T, Tanaka K, Kawamukai M, Niwa Y, Toyooka K, Matsuoka K, Jinbo T, Kimura T (2007) Development of series of gateway binary vectors, pGWBs, for realizing efficient construction of fusion genes for plant transformation. J Biosci Bioeng **104**: 34–41

Noh B, Murphy AS, Spalding EP (2001) Multidrug Resistance-like Genes of Arabidopsis Required for Auxin Transport and Auxin-Mediated Development. Plant Cell **13**: 2441–2454

Novák O, Hényková E, Sairanen I, Kowalczyk M, Posíšil T, Ljung K (2012) Tissue-specific profiling of the Arabidopsis thaliana auxin metabolome. Plant J (3) **72**: 523 - 536

Okada K, Ueda J, Komaki MK, Bell CJ, Shimura Y (1991) Requirement of the Auxin Polar Transport System in Early Stages of Arabidopsis Floral Bud Formation. Plant Cell **3**: 677–684

Pérez-Pérez JM, Ponce MR, Micol JL (2004) The ULTRACURVATA2 gene of Arabidopsis encodes an FK506-binding protein involved in auxin and brassinosteroid signaling. Plant Physiol **134**: 101–17

Petrášek J, Mravec J, Bouchard R, Blakeslee JJ, Abas M, Seifertová D, Wisniewska J, Tadele Z, Kubeš M, Covanová M, et al (2006) PIN proteins perform a rate-limiting function in cellular auxin efflux. Science **312**: 914–8

Qin G, Gu H, Zhao Y, Ma Z, Shi G, Yang Y, Pichersky E, Chen H, Liu M, Chen Z, et al (2005) An indole-3-acetic acid carboxyl methyltransferase regulates Arabidopsis leaf development. Plant Cell **17**: 2693–704

Qin Z, Lv H, Zhu X, Meng C, Quan T, Wang M, Xia G (2013) Ectopic expression of a wheat WRKY transcription factor gene TaWRKY71-1 results in hyponastic leaves in Arabidopsis thaliana. PLoS One **8**: e63033

Ray PM, Curry GM (1958) Intermediates and Competing Reactions in the Photodestruction of Indoleacetic Acid. Nature **181**: 895–896

Robert HS, Grones P, Stepanova AN, Robles LM, Lokerse AS, Alonso JM, Weijers D, Friml J (2013) Local auxin sources orient the apical-basal axis in Arabidopsis embryos. Curr Biol **23**: 2506–12

Rodriguez RE, Debernardi JM, Palatnik JF (2014) Morphogenesis of simple leaves: regulation of leaf size and shape. Wiley Interdiscip Rev Dev Biol **3**: 41–57

**Růžička K, Strader LC, Bailly A, Yang H, Blakeslee J, Langowski L, Nejedlá E, Fujita H, Itoh H, Syono K, et al** (2010) Arabidopsis PIS1 encodes the ABCG37 transporter of auxinic compounds including the auxin precursor indole-3-butyric acid. Proc Natl Acad Sci USA **107**: 10749–53

**De Rybel B, Breda AS, Weijers D** (2013) Prenatal plumbing-vascular tissue formation in the plant embryo. Physiol Plant **151**: 126–33

**Santelia D, Vincenzetti V, Azzarello E, Bovet L, Fukao Y, Düchtig P, Mancuso S, Martinoia E, Geisler M** (2005) MDR-like ABC transporter AtPGP4 is involved in auxin-mediated lateral root and root hair development. FEBS Lett **579**: 5399–5406

**Sassi M, Vernoux T** (2013) Auxin and self-organization at the shoot apical meristem. J Exp Bot **64**: 2579–92

**Scarpella E, Barkoulas M, Tsiantis M** (2010) Control of Leaf and Vein Devolment by Auxin. Cold Spring Harb Perspect Biol **2**: a001511

**Schmid JA and Billich A** (1996) Method of preparation of epidermal imprints using agarose. Interactions **69**: 2451- 2461

**Silverstein AM, Galigniana MD, Kanelakis KC, Radanyi C, Renoir J-M, Pratt WB** (1999) Different Regions of the Immunophilin FKBP52 Determine Its Association with the Glucocorticoid Receptor, hsp90, and Cytoplasmic Dynein. J Biol Chem **274**: 36980–36986

**Stasinopoulos TC, Hangarter RP** (1990) Preventing Photochemistry in Culture Media by Long-Pass Light Filters Alters Growth of Cultured Tissues. Plant Physiol **93**: 1365–1369

**Steinmann T** (1999) Coordinated Polar Localization of Auxin Efflux Carrier PIN1 by GNOM ARF GEF. Science (80) **286**: 316–318

**Swarup K, Benková E, Swarup R, Casimiro I, Péret B, Yang Y, Parry G, Nielsen E, De Smet I, Vanneste S, et al** (2008) The auxin influx carrier LAX3 promotes lateral root emergence. Nat Cell Biol **10**: 946–54

**Swarup R, Péret B** (2012) AUX/LAX family of auxin influx carriers-an overview. Front Plant Sci **3**: 225

**Tao Y, Ferrer J-L, Ljung K, Pojer F, Hong F, Long JA, Li L, Moreno JE, Bowman ME, Ivans LJ, et al** (2008) Rapid synthesis of auxin via a new tryptophan-dependent pathway is required for shade avoidance in plants. Cell **133**: 164–76

**Terasaka K, Blakeslee JJ, Titapiwatanakun B, Peer WA, Bandyopadhyay A, Makam SN, Lee OR, Richards EL, Murphy AS, Sato F, et al** (2005) PGP4, an ATP binding cassette P-glycoprotein, catalyzes auxin transport in Arabidopsis thaliana roots. Plant Cell **17**: 2922–39

**Thitamadee S, Tuchihara K, Hashimoto T** (2002) Microtubule basis for left-handed helical growth in Arabidopsis. Nature **417**: 193–6

**Titapiwatanakun B, Blakeslee JJ, Bandyopadhyay A, Yang H, Mravec J, Sauer M, Cheng Y, Adamec J, Nagashima A, Geisler M, et al** (2009) ABCB19/PGP19 stabilises PIN1 in membrane microdomains in Arabidopsis. Plant J **57**: 27–44

**Tsuda E, Yang H, Nishimura T, Uehara Y, Sakai T, Furutani M, Koshiba T, Hirose M, Nozaki H, Murphy AS, et al** (2011) Alkoxy-auxins are selective inhibitors of auxin transport mediated by PIN, ABCB, and AUX1 transporters. J Biol Chem **286**: 2354–64

**Verrier PJ, Bird D, Burla B, Dassa E, Forestier C, Geisler M, Klein M, Kolukisaoglu Ü, Lee Y, Martinoia E, et al** (2008) Plant ABC proteins – a unified nomenclature and updated inventory. Trends Plant Sci **13**: 151–159

**Wang B, Bailly A, Zwiewka M, Henrichs S, Azzarello E, Mancuso S, Maeshima M, Friml J, Schulz A, Geisler M** (2013) Arabidopsis TWISTED DWARF1 functionally interacts with auxin exporter ABCB1 on the root plasma membrane. Plant Cell **25**: 202–14

**Watahiki M** (1997) The massugu1 mutation of Arabidopsis identified with failure of auxin-induced growth curvature of hypocotyl confers auxin insensitivity to hypocotyl and leaf. Plant Physiol **115**: 419–426

**Weizbauer R, Peters WS, Schulz B** (2011) Geometric constraints and the anatomical interpretation of twisted plant organ phenotypes. Front Plant Sci **2**: 62

**Went FW, Thimann K V.** (1937) Phytohormones.

**Wielopolska A, Townley H, Moore I, Waterhouse P, Helliwell C** (2005) A high-throughput inducible RNAi vector for plants. Plant Biotechnol J **3**: 583–90

**Willemsen V** (2003) Cell Polarity and PIN Protein Positioning in Arabidopsis Require STEROL METHYLTRANSFERASE1 Function. Plant Cell Online **15**: 612–625

**Willige BC, Ahlers S, Zourelidou M, Barbosa ICR, Demarsy E, Trevisan M, Davis PA, Roelfsema MRG, Hangarter R, Fankhauser C, et al** (2013) D6PK AGCVIII kinases are required for auxin transport and phototropic hypocotyl bending in Arabidopsis. Plant Cell **25**: 1674–88

**Wu G, Cameron JN, Ljung K, Spalding EP** (2010b) A role for ABCB19-mediated polar auxin transport in seedling photomorphogenesis mediated by cryptochrome 1 and phytochrome B. Plant J **62**: 179–91

**Wu G, Lewis DR, Spalding EP** (2007) Mutations in Arabidopsis multidrug resistance-like ABC transporters separate the roles of acropetal and basipetal auxin transport in lateral root development. Plant Cell **19**: 1826–37

**Wu G, Otegui MS, Spalding EP** (2010a) The ER-localized TWD1 immunophilin is necessary for localization of multidrug resistance-like proteins required for polar auxin transport in Arabidopsis roots. Plant Cell **22**: 3295–304

**Xu T, Dai N, Chen J, Nagawa S, Cao M, Li H, Zhou Z, Chen X, De Rycke R, Rakusová H, et al** (2014) Cell surface ABP1-TMK auxin-sensing complex activates ROP GTPase signaling. Science **343**: 1025–8

**Xu T, Wen M, Nagawa S, Fu Y, Chen J-G, Wu M-J, Perrot-Rechenmann C, Friml J, Jones AM, Yang Z** (2010) Cell surface- and rho GTPase-based auxin signaling controls cellular interdigitation in Arabidopsis. Cell **143**: 99–110

**Yang H, Murphy AS** (2009) Functional expression and characterization of Arabidopsis ABCB, AUX 1 and PIN auxin transporters in Schizosaccharomyces pombe. Plant J **59**: 179–91

**Yang H, Richter GL, Wang X, Młodzińska E, Carraro N, Ma G, Jenness M, Chao D, Peer WA, Murphy AS** (2013) Sterols and sphingolipids differentially function in trafficking of the Arabidopsis ABCB19 auxin transporter. Plant J **74**: 37–47

**Yifhar T, Pekker I, Peled D, Friedlander G, Pistunov A, Sabban M, Wachsman G, Alvarez JP, Amsellem Z, Eshed Y** (2012) Failure of the tomato trans-acting short interfering RNA program to regulate AUXIN RESPONSE FACTOR3 and ARF4 underlies the wiry leaf syndrome. Plant Cell **24**: 3575–89

**Zamore PD, Tuschl T, Sharp PA, Bartel DP** (2000) RNAi: double-stranded RNA directs the ATP-dependent cleavage of mRNA at 21 to 23 nucleotide intervals. Cell **101**: 25–33

**Zažímalová E, Murphy AS, Yang H, Hoyerová K, Hosek P** (2010) Auxin transporters--why so many? Cold Spring Harb Perspect Biol **2**: a001552

**Zourelidou M, Müller I, Willige BC, Nill C, Jikumaru Y, Li H, Schwechheimer C** (2009) The polarly localized D6 PROTEIN KINASE is required for efficient auxin transport in Arabidopsis thaliana. Development **136**: 627–36

APPENDICES

Appendix A

# *AUX/LAX* Genes Encode a Family of Auxin Influx Transporters That Perform Distinct Functions during *Arabidopsis* Development[C][W]

Benjamin Péret,[a,1] Kamal Swarup,[a] Alison Ferguson,[a] Malvika Seth,[a] Yaodong Yang,[b] Stijn Dhondt,[c,d]
Nicholas James,[a] Ilda Casimiro,[e] Paula Perry,[a] Adnan Syed,[b] Haibing Yang,[f] Jesica Reemmer,[f] Edward Venison,[a]
Caroline Howells,[a] Miguel A. Perez-Amador,[g,2] Jeonga Yun,[g] Jose Alonso,[g] Gerrit T.S. Beemster,[h] Laurent Laplaze,[i]
Angus Murphy,[f] Malcolm J. Bennett,[a] Erik Nielsen,[b] and Ranjan Swarup[a,3]

[a] School of Biosciences and Centre for Plant Integrative Biology, University of Nottingham, LE12 5RD Nottingham, United Kingdom
[b] Department of Molecular, Cellular, and Developmental Biology, University of Michigan, Ann Arbor, Michigan 48109
[c] Department of Plant Systems Biology, Flanders Institute for Biotechnology, 9052 Ghent, Belgium
[d] Department of Plant Biotechnology and Bioinformatics, Ghent University, 9052 Ghent, Belgium
[e] Universidad de Extremadura, Facultad de Ciencias, 06071 Badajoz, Spain
[f] Department of Horticulture and Landscape Architecture, Purdue University, West Lafayette, Indiana 47906
[g] Department of Genetics, North Carolina State University, Raleigh, North Carolina 27695
[h] Laboratory for Molecular Plant Physiology and Biotechnology, University of Antwerpen, B-2020 Antwerp, Belgium
[i] Institut de Recherche pour le Développement, Unité Mixte de Recherche Diversité Adaptation et Développement des Plantes (Institut de Recherche pour le Développement/Université Montpellier 2), 34394 Montpellier, France

**Auxin transport, which is mediated by specialized influx and efflux carriers, plays a major role in many aspects of plant growth and development. *AUXIN1* (*AUX1*) has been demonstrated to encode a high-affinity auxin influx carrier. In *Arabidopsis thaliana*, *AUX1* belongs to a small multigene family comprising four highly conserved genes (i.e., *AUX1* and *LIKE AUX1* [*LAX*] genes *LAX1*, *LAX2*, and *LAX3*). We report that all four members of this AUX/LAX family display auxin uptake functions. Despite the conservation of their biochemical function, *AUX1*, *LAX1*, and *LAX3* have been described to regulate distinct auxin-dependent developmental processes. Here, we report that *LAX2* regulates vascular patterning in cotyledons. We also describe how regulatory and coding sequences of *AUX/LAX* genes have undergone subfunctionalization based on their distinct patterns of spatial expression and the inability of LAX sequences to rescue *aux1* mutant phenotypes, respectively. Despite their high sequence similarity at the protein level, transgenic studies reveal that LAX proteins are not correctly targeted in the AUX1 expression domain. Domain swapping studies suggest that the N-terminal half of AUX1 is essential for correct LAX localization. We conclude that *Arabidopsis* AUX/LAX genes encode a family of auxin influx transporters that perform distinct developmental functions and have evolved distinct regulatory mechanisms.**

## INTRODUCTION

The phytohormone auxin indole-3-acetic acid (IAA) is a versatile trigger for plant development (Vanneste and Friml, 2009). Auxin regulates embryogenesis, organogenesis, vascular tissue formation,

and tropic responses in plants (Vieten et al., 2007; Petrásek and Friml, 2009). The polar transport of auxin from cell to cell is achieved through the coordinated process of efflux and influx transporters, encoded by *PIN-FORMED* (*PIN*) and *P-GLYCOPROTEIN* (*PGP*), respectively (Geisler et al., 2005; Petrásek et al., 2006; Cho et al., 2007) and *AUXIN1/LIKE AUX1* (*AUX/LAX*) genes (Bennett et al., 1996; Swarup et al., 2008). The PIN efflux transporters have a polar plasma membrane (PM) localization that regulates the direction of auxin flow (Wisniewska et al., 2006). Their mode of action during plant development shows strong redundancy and auxin-dependent cross-regulation of their expression (Vieten et al., 2005). Localization of AUX1 has been described to be cell type–dependent and, together with PIN efflux transporters, it provides directionality of intercellular auxin flow (Swarup et al., 2001; Kleine-Vehn et al., 2006).

In *Arabidopsis thaliana*, the *AUX/LAX* family is represented by four highly conserved genes called *AUX1*, *LAX1*, *LAX2*, and *LAX3* (see Supplemental Figure 1A and Supplemental Data Set 1 online), which encode multimembrane-spanning transmembrane proteins and share similarities with amino acid transporters. This

protein family forms a plant-specific subclass within the amino acid/auxin permease super family (Young et al., 1999). Mutations in *AUX1* or *LAX3* result in auxin-related developmental defects. For example, *aux1* mutants are agravitropic and have a decreased number of lateral roots. By comparison, a loss-of-function mutation in *LAX3* results in delayed lateral root emergence, and together, *LAX3* and AUX1 act concomitantly to regulate lateral root development by regulating the emergence (Swarup et al., 2008) and initiation (Marchant et al., 2002) steps, respectively. Auxin uptake experiments in heterologous expression systems have confirmed that AUX1 and LAX3 are high-affinity auxin transporters (Yang et al., 2006; Carrier et al., 2008; Swarup et al., 2008).

In contrast with *AUX1* and *LAX3*, the functional roles of the other two members of the *AUX/LAX* family are not well understood. Experimental observations suggest that both may also function as auxin influx carriers (Bainbridge et al., 2008), because mutating multiple members of the *AUX/LAX* family affects phyllotactic patterning—a process that is known to be regulated by auxin. This is supported by the fact that AUX1 shares 82, 78, and 76% identity with LAX1, LAX2, and LAX3, respectively (see Supplemental Figure 1B online). Examination of their gene structure revealed well-conserved exon/intron boundaries for most of the sequence (see Supplemental Figure 1C online), indicating that all four members of the family have originated from a common ancestor through gene duplication. In this study, using a combination of genetic, molecular, and biochemical approaches, we provide experimental evidence that all members of the *AUX/LAX* family have auxin influx activity. Despite the conservation of biochemical function, we demonstrate that their regulatory and coding sequences have undergone subfunctionalization. We also show that the N-terminal domain of AUX1 provides information for correct localization of LAX proteins in the *AUX1* expression domain.

## RESULTS

### AUX/LAX Genes Exhibit Nonredundant and Complementary Expression Patterns in Roots

To provide insight into the roles of *AUX/LAX* family members in plant growth and development, their expression was analyzed in detail using in situ immunolocalization and/or promoter:β-*glucuronidase* (*GUS*) fusions and genomic yellow fluorescent protein (YFP)/VENUS translational fusions. These studies revealed that the expression patterns of *AUX/LAX* genes are mostly nonredundant and complementary in the primary root apex. Previous studies have shown that *AUX1* is expressed in the columella, lateral root cap (LRC), epidermis, and stele tissues (Figure 1A; see Supplemental Figure 2A online) (Swarup et al., 2001; Swarup et al., 2005), whereas *LAX3* is expressed in the columella and stele (Figure 1D; see Supplemental Figure 2D online) (Swarup et al., 2008).

As part of this investigation, using two different approaches (promoter:*GUS* and genomic YFP/VENUS translational fusions), we report that *LAX1* is expressed in the mature regions of primary root vascular tissues (Figures 1E to 1I; see Supplemental Figures 2E to 2I online). Weak *LAX1* expression was also detected in the vascular tissues in the primary root apex in

*ProLAX1:LAX1-VENUS* lines (see Supplemental Figure 2B online) but was not detectable in the *ProLAX1:GUS* lines (Figure 1B) even after prolonged GUS staining. This discrepancy is likely to be caused by the much larger genomic region used in *ProLAX1-LAX1-VENUS* lines.

*LAX2* expression is detected in young vascular tissues, the quiescent center, and columella cells (Figures 1C, 6A, and 6B; see Supplemental Figure 2C online). *LAX2* signal in the columella cells is most pronounced in the *ProLAX2:GUS* lines (Figure 1C), but is almost absent or very weak in the *ProLAX2:LAX2-VENUS* lines (see Supplemental Figure 2C online). Localization of LAX2 by in situ immunolocalization using anti-LAX2 antibody also showed a relatively weak expression of LAX2 in the columella cells (Figures 6A and 6B), suggesting that the stronger signal of LAX2 in *ProLAX2:GUS* lines is likely to be caused by the more stable nature of the GUS reporter.

The divergence in spatial expression patterns of *AUX/LAX* members is also clearly illustrated during lateral root development. As previously described, *LAX3* is expressed outside the emerging lateral root primordia (Swarup et al., 2008), whereas *AUX1* is localized within the lateral root primordia during all stages of development (Marchant et al., 2002). In comparison, *LAX1* expression is first detected in stage I primordia and then mainly persists at the primordium base throughout lateral root formation (Figures 1E to 1I; see Supplemental Figures 2E to 2I online). By contrast, *LAX2* expression is only detected in the central region of lateral root primordia (Figures 1J to 1N; see Supplemental Figures 2J to 2N online).

As previously reported, *LAX3* expression is auxin inducible (Swarup et al., 2008) (Figures 2G and 2H; see Supplemental Figure 4G and 4H online). We then tested whether the expression of other *AUX/LAX* genes can be regulated by auxin. A bioinformatic search for auxin-related transcription factor binding sites and the presence of canonical auxin response elements in a 2-kb upstream sequence from ATG of the *AUX/LAX* promoters revealed that *LAX3* and *LAX1* have the highest number of transcription factor binding sites (see Supplemental Figure 3 online). To test this directly, 7-d-old seedlings were treated for 16 h with 100 nM 2,4 dichlorophenoxyacetic acid (2,4-D). Under these conditions, both *LAX3-GUS* (Figures 2G and 2H) and *LAX3-YFP* (see Supplemental Figures 4G and 4H online) expression was strongly induced by auxin. Our results also revealed that *LAX1* transcript abundance was upregulated by auxin (Figures 2C and 2D; see Supplemental Figures 4C and 4D online). *LAX1* expression seems stronger in the presence of auxin and is detected much closer to the root apex compared with untreated controls (arrow in Figure 2D). However, unlike *LAX3*, *LAX1* is not induced in outer root tissues (compare Figure 2D with Figure 2H and Supplemental Figure 4D with Supplemental Figure 4H online). In contrast with *LAX3* and *LAX1*, neither *AUX1* (Figures 2A and 2B; see Supplemental Figures 4A and 4B online) nor *LAX2* (Figures 2E and 2F; see Supplemental Figures 4E and 4F online) expression seem to be altered in the presence of auxin.

These results indicate that the regulation of *AUX/LAX* gene expression has diverged during the course of evolution, suggesting that they have acquired distinct roles in different developmental/physiological processes, an evolutionary mechanism described as subfunctionalization.
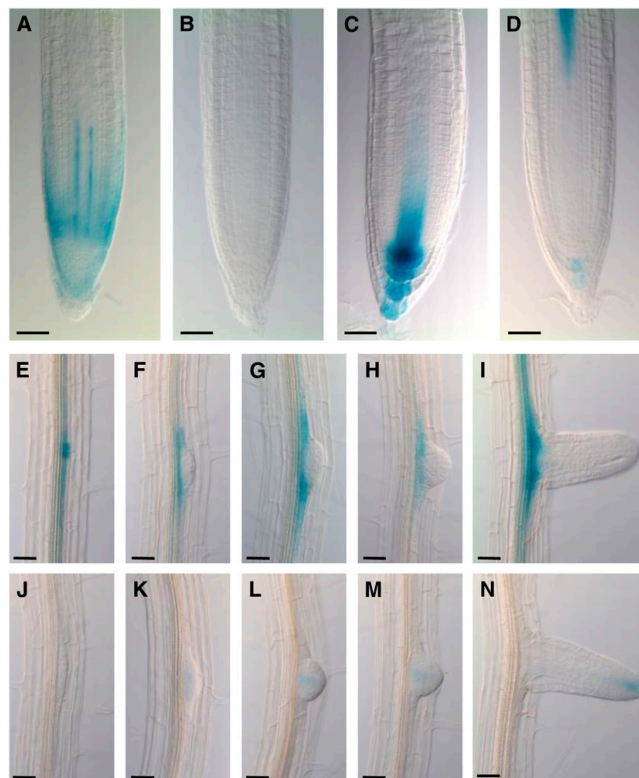
**Figure 1.** *Promoter:GUS* Studies Show That *AUX/LAX* Genes Exhibit Complementary Expression Patterns.

**(A)** to **(D)** Expression profile of *AUX1* **(A)**, *LAX1* **(B)**, *LAX2* **(C)**, and *LAX3* **(D)** in the primary root apex.
**(E)** to **(H)** Expression profile of *LAX1* (**[E]** to **[I]**) and *LAX2* (**[J]** to **[N]**) during lateral root primordium development.
Bars in **(A)** to **(D)** = 35 μm; bars in **(E)** to **(N)** = 40 μm.

## Members of the AUX/LAX Family Facilitate Distinct Auxin-Regulated Developmental Programs

To probe whether the AUX/LAX family of proteins exhibit subfunctionalization, a genetic approach was used to test the roles of these genes during *Arabidopsis* growth and development. AUX1 has previously been reported to play an important role during the root gravitropic response (Swarup et al., 2001; Swarup et al., 2004; Swarup et al., 2005) as well as lateral root initiation (Marchant et al., 2002), whereas LAX3 has recently been shown to be involved in lateral root emergence (Swarup et al., 2008). As part of this study, *lax1* and *lax2* mutants were analyzed for auxin-regulated developmental phenotypes. No root growth–related defects were obvious in either *lax1* or *lax2* mutants (see Supplemental Figures 5 to 7 online). Unlike *aux1*, mutations in *lax1* or *lax2* did not affect their root gravitropic responses (see Supplemental Figures 5A and 5B online) or sensitivity to synthetic auxin 2,4-D (see Supplemental Figure 6 online). Similarly, unlike *aux1* and *lax3*, no lateral root–related

defects were observed for either *lax1* or *lax2* mutant alleles (see Supplemental Figure 7 online).

To test the possibility of genetic redundancy between *AUX1*, *LAX1*, and *LAX2*, growth responses to synthetic auxin 2,4-D and lateral root development were investigated in double and triple mutants. The growth responses of double and triple mutant combinations to synthetic auxin 2,4-D were similar to *aux1*, suggesting that loss of *lax1* and/or *lax2* did not enhance the *aux1* phenotype (see Supplemental Figure 8A online). Similarly, the lateral root phenotypes of *aux1 lax1* and *aux1 lax2* double mutants or *aux1 lax1 lax2* triple mutants were not significantly different from single *aux1* mutants (see Supplemental Figures 8B and 8C online). Under the same conditions, the *aux1 lax3* double mutant showed a severe reduction in emerged lateral roots, in agreement with Swarup et al. (2008).

These results suggest that during the course of evolution, at least two members of the *AUX/LAX* family, *AUX1* and *LAX3*, have subfunctionalized, whereas *LAX1* and *LAX2* gene products do not
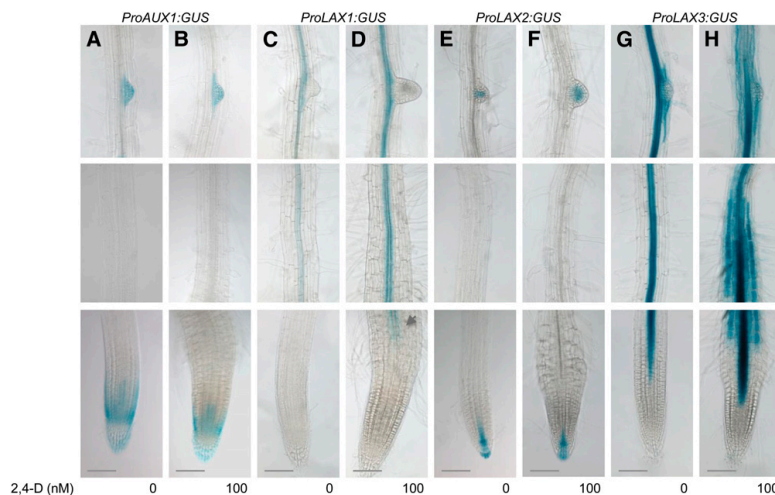
**Figure 2.** *LAX1* and *LAX3* Genes Are Induced by Auxin.

Expression profile of *AUX1* (**[A]** and **[B]**), *LAX1* (**[C]** and **[D]**), *LAX2* (**[E]** and **[F]**), and *LAX3* (**[G]** and **[H]**) in absence and presence of 100 nM 2,4-D. Note *LAX1* expression in the presence of auxin is detected much closer to the root apex (arrow in **[D]**).

Bars = 50 μm.

seem to influence root system architecture. However, it cannot be ruled out that LAX1 and LAX2 perform more subtle patterning functions, and specific conditions are required to uncover a root-related mutant defect. Alternatively, these genes may have acquired novel functions (neofunctionalization—no longer auxin influx carriers) or new roles (subfunctionalization—still auxin influx carriers) in other plant organs. The latter view is supported by the discovery that mutating all four members of the *AUX/LAX* family affects phyllotactic patterning (Bainbridge et al., 2008), and both *AUX1* and *LAX3* have also been implicated in apical hook development (Vandenbussche et al., 2010), processes that are known to be regulated by auxin.

Auxin is also known to regulate vascular development, and many auxin transport and response mutants have defects in vascular development (Reinhardt, 2003; Petrásek and Friml, 2009). *LAX2* promoter:*GUS* studies show that *ProLAX2*:*GUS* expression is associated with procambial and vascular tissues during embryogenesis (Figures 3A to 3C). In developing leaves, *ProLAX2*:*GUS* expression is detected very early at the sites of initiating veins, and starting from day 5, *LAX2* is expressed along the secondary loops, starting with the first loop followed by the second, third, and fourth (Figures 3D to 3I). By days 7 to 8, *LAX2* expression is also detected near the position of tertiary veins. Interestingly, *LAX2* is not expressed along the midvein (Figures 3D to 3I).

To assess the role of *LAX2* during vascular development, two different alleles of *LAX2* were analyzed (Figure 3J). The *lax2-1* allele represents an En element inserted into intron 2 (position 452 from ATG), whereas *lax2-2* has a T-DNA insertion in exon 6 (position 1239 from ATG). Both these alleles seem to be null alleles, because no *LAX2* cDNA is detected by RT-PCR (Figures

3K and 3L). Examination of vascular development in *lax2-1* and *lax2-2* cotyledons revealed that both alleles exhibit a significantly higher propensity of discontinuity in vascular strands, with almost 64% of *lax2-1* and 77% of *lax2-2* seedlings showing vascular breaks in their cotyledons (Figures 3M to 3Q) compared with only 20% of control seedlings. In contrast with cotyledons, no defect in vascular patterning was apparent in *lax2* leaves. This auxin-related developmental phenotype for *lax2* provides indirect evidence for a role for LAX2 in facilitating auxin transport.

### *AUX1*, *LAX1*, and *LAX3* Encode Functional Auxin Influx Carriers

To directly test whether every AUX/LAX protein has auxin transport activity, experiments were performed in heterologous expression systems. Using an oocyte expression system, both AUX1 (Yang et al., 2006) and LAX3 (Swarup et al., 2008) were previously shown to be high-affinity auxin transporters. Similar experiments were performed for LAX1 and LAX2. These experiments revealed that LAX1 exhibited auxin uptake activity in oocytes (Figure 4A). Competition experiments with cold 2,4-D or IAA significantly reduced the uptake of radiolabeled IAA by oocytes injected with *LAX1* complementary RNA (cRNA), suggesting a carrier-mediated uptake (Figure 4B). By contrast, there was only a small reduction in tritium-labeled IAA ([³H]IAA) uptake in the presence of the lipophilic auxin analog 1-naphthalene acetic acid or indole butyric acid (Figure 4B). Surprisingly, no auxin uptake activity was seen in *LAX2*-expressing oocytes (Figure 4A). Immunoblot experiments using specific anti-LAX2 antibodies revealed that the protein was correctly expressed in these oocytes (Figure 4C, lane 1), thus ruling out defects in its translation. To test
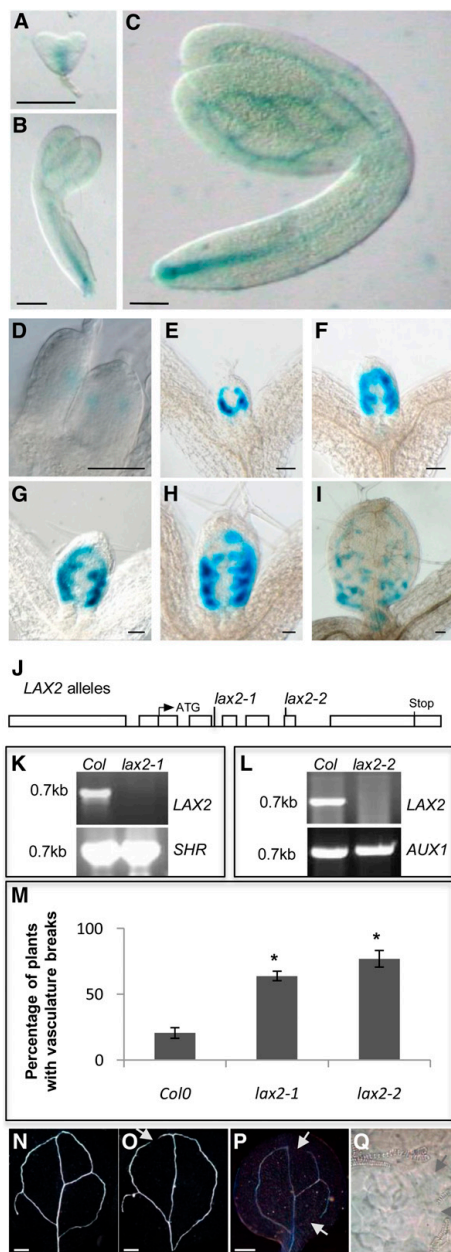
whether LAX2 is correctly targeted to the PM in oocytes, a YFP-tagged version of *LAX2* (*LAX2-YFP*) was expressed. Immunodetection again showed that *LAX2-YFP* was correctly expressed in these oocytes and was detected in the membrane and not the cytosolic fractions (Figure 4C, lanes 2 and 3). However, confocal analysis revealed no detectable LAX2-YFP on the PM (Figure 4D, panel III). In comparison, YFP fluorescence was clearly seen on the PM of oocytes expressing *AUX1-YFP* (Figure 4D, panel II). These results show that LAX2-YFP, unlike AUX1-YFP, is not properly targeted to the PM in *Xenopus laevis* oocytes and may suggest a requirement for some plant-specific accessory proteins/factors for its correct targeting that are lacking in *X. laevis*. As an alternative approach, LAX2 transport activity was also assayed using a yeast-based heterologous expression system (Yang and Murphy, 2009) to determine the role of LAX2 in IAA uptake. In this system, *LAX2*-expressing yeast cells displayed a weak but consistent IAA uptake activity compared with control cells (Figures 4E and 4F).

To further probe whether *LAX2* encodes an auxin influx transporter, we also used a genetic assay. We reasoned that if *LAX2* encodes a functional auxin transporter, an *AUX1* promoter-driven *LAX2* sequence would be expected to complement *aux1* mutants. The *aux1* mutant shows reduced sensitivity to auxins 2,4-D and IAA and has a strong agravitropic root phenotype (Bennett et al., 1996; Swarup et al., 2001, 2005) and a defect in lateral root initiation (Marchant et al., 2002). To test the ability of *LAX2* to complement the *aux1* mutant, a *ProAUX1:LAX2* construct was created to express *LAX2* under the control of the 1.7-kb *AUX1* promoter and was then introduced into an *aux1* mutant allele, *aux1-22* (Figure 5A). Homozygous T3 seedlings were then tested for the restoration of the *aux1* mutant phenotype (root gravitropic response and sensitivity to 2,4-D). As expected, *ProAUX1:AUX1* lines (*AUX1* promoter driving *AUX1* that was used as a positive control) fully rescued the 2,4-D–resistant root growth and agravitropic phenotypes of *aux1* seedlings (Figures 5B and 5C). By contrast, *ProAUX1:LAX2* lines failed to rescue the root agravitropic phenotypes of *aux1*

**Figure 3.** The *lax2* Mutant Exhibits Vascular Patterning Defects in the Cotyledons.

**(A)** to **(C)** *Promoter:GUS* analysis of *LAX2* expression in heart stage **(A)**, torpedo **(B)**, and mature **(C)** embryos.

**(D)** to **(I)** *Promoter:GUS* analysis of expression of *LAX2* in developing leaf primordia.

**(J)** Structure of the *LAX2* with the positions of the *lax2* mutant alleles indicated. Boxes represent promoter, 5′, and 3′ untranslated regions and exons; lines represent introns.

**(K)** and **(L)** RT-PCR analysis of *lax2-1* **(K)** and *lax2-2* **(L)** alleles showing that *LAX2* cDNA is detectable in the wild type (Col-0) but not in *lax2-1* **(K)** and *lax2-2* **(L)**. Positive controls *SHR* **(K)** and *AUX1* **(L)** are detected both in wild-type (Col-0) and *lax2* alleles (*n* = 2).

**(M)** Graph showing the frequency of vascular breaks in cotyledons of *lax2* mutant alleles compared with the wild type (Col-0). Error bars represent se. * indicates statistically significant difference compared with the wild type (Col-0); *n* = 30; Student's *t* test, P < 0.01.

**(N)** to **(P)** Differential interference contrast images of wild-type **(N)**, *lax2-1* **(O)**, and *lax2-2* **(P)** cotyledons showing the vascular defect in *lax2*.

**(Q)** High-magnification differential interference contrast image pinpointing vascular break in a *lax2* cotyledon.

Bars in **(A)** to **(C)** = 40 μm; bars in **(D)** to **(I)** = 100 μm; bars in **(N)** to **(P)** = 200 μm.

seedlings (Figure 5B) as well as 2,4-D–resistant root growth (Figure 5C).

### LAX2 Is Mistargeted in AUX1-Expressing Cells

To determine why *LAX2* did not rescue the *aux1* phenotypes, a quantitative RT-PCR experiment was initially used to measure transgene expression levels of *ProAUX1:AUX1*, *ProAUX1:LAX2*, and *ProAUX1:N-terminal HA epitope–tagged AUX1* (*NHA-AUX1*) (Swarup et al., 2001) lines compared with wild-type *AUX1* levels (see Methods). Quantitative RT-PCR revealed that *LAX2* transgene was consistently expressed at equivalent levels to those of *ProAUX1:AUX1* and *ProAUX1:NHA-AUX1* (see Supplemental Figure 9 online). Hence, transgene expression was not the basis for the lack of rescue of the *aux1* phenotypes. Next, we tested whether LAX2 was either incorrectly translated or trafficked in *AUX1*-expressing cells in these lines by in situ immunolocalization using anti-LAX2 antibodies. Because of the high similarity between all AUX/LAX family members, the specificity of the antipeptide antibody was tested. In wild-type seedling roots, a strong signal was seen in vascular tissues, the S1 columella layer, and the quiescent center (Figures 6A and 6B), but no signal was detected in equivalent tissues of *lax2* seedlings (Figure 6C), confirming the high specificity of this antibody for LAX2. Furthermore, immunolocalization of LAX2 exhibited a broadly similar spatial expression pattern to that obtained using *ProLAX2:GUS* (Figure 1C) and *ProLAX2:LAX2-VENUS* lines (see Supplemental Figure 2C online), suggesting the absence of posttranscriptional control of *LAX2* in *LAX2*-expressing cells (Figures 1C, 6A, and 6B; see Supplemental Figure 2C online). Slight differences in expression of *ProLAX2:GUS*, particularly in the columella cells, may be caused by differences in stability of GUS and LAX2 proteins.

We then tested the localization of LAX2 in *ProAUX1:LAX2* lines. As reported previously (Swarup et al., 2001; Swarup et al., 2005), *AUX1* is expressed in columella, LRC, epidermis, and protophloem cells (Figure 6D). In *ProAUX1:LAX2* lines, as expected, a strong LAX2 signal was seen in *LAX2*-expressing cells (endogenous LAX2; Figures 6E and 6F); however, in cells that normally also express AUX1, the transgene-derived LAX2 signal was either weak (LRC and columella; Figures 6F and 6G) or absent (epidermis; Figure 6H). Surprisingly, the LAX2 signal in columella and LRC cells accumulated inside the cell and was only occasionally found

**Figure 4.** AUX/LAX Proteins Are Functional Auxin Influx Transporters.

**(A)** Uptake of [³H]IAA into *X. laevis* oocytes injected with water or *AUX1*, *LAX1*, *LAX2*, and *LAX3* cRNAs at pH 6.4. Oocytes injected with *AUX1*, *LAX1*, and *LAX3* cRNAs showed increased [³H]IAA uptake when compared with the water-injected control (*n* = 8).

**(B)** Uptake of [³H]IAA into oocytes injected with *LAX1* cRNA was examined in the presence of excess unlabeled IAA, the auxin analogs 2,4-D and 1-naphthalene acetic acid (NAA), and the naturally occurring auxin form indole butyric acid (IBA) (*n* = 5).

**(C)** Immunoblot analysis of oocytes injected with *LAX2* (lane 1) or *LAX2-YFP* (lanes 2 and 3) cRNAs. Total oocyte extract expressing *LAX2* (lane 1) or *LAX2-YFP* (cytosolic fraction, lane 2; microsomal fraction, lane 3) were separated by SDS-PAGE and immunodetected using anti-LAX2 antibodies

(dilution 1/1000). Note the size difference between native LAX2 (42 kD) and LAX2-YFP (68 kD).

**(D)** Laser scanning confocal images of oocytes injected with water (I), *AUX1-YFP* cRNA (II), or *LAX2-YFP* cRNA (III).

**(E)** Immunoblot analysis of empty vector control or *LAX2* expressing *S. pombe* cells. Proteins were separated by SDS-PAGE and immunodetected using anti-LAX2 antibodies (dilution 1/1000).

**(F)** Uptake of [³H]IAA into empty vector control (dashed line) versus LAX2-expressing (solid line) *S. pombe* cells compared with zero time point.

Error bars represent SD. * indicates statistically significant difference. Student's *t* test P < 0.05.

Bar in **(D)** = 100 μm.

[See online article for color version of this figure.]

**A**

*ProAUX1:AUX1*



*ProAUX1:LAX2*

**B**



**C**
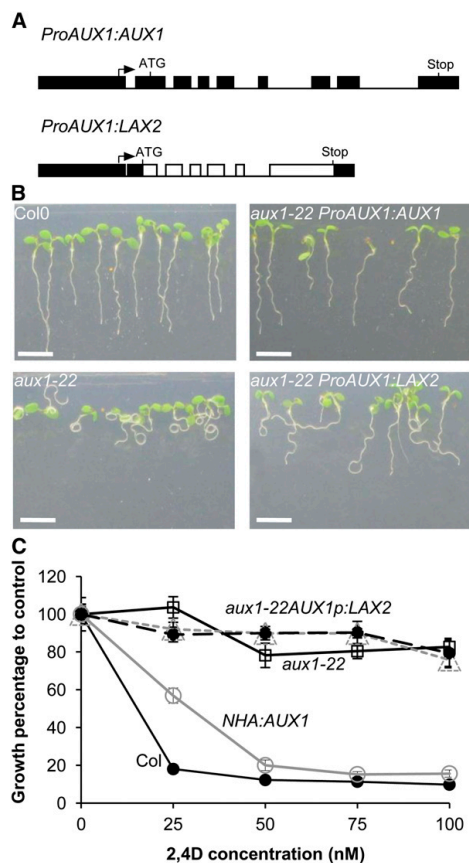


**Figure 5.** *AUX/LAX* Genes Are Not Fully Functionally Interchangeable.

**(A)** Gene constructs used for genetic complementation assays. *AUX1* (control) or *LAX2* genomic sequences were cloned between the *AUX1* promoter and terminator to create *ProAUX1:AUX1* and *ProAUX1:LAX2* (boxes represent promoter, 5′, and 3′ untranslated regions and exons; lines represent introns).

**(B)** Root gravitropic phenotypes of the wild type (Col-0), *aux1-22*, and *aux1-22* complemented by either *ProAUX1:AUX1* (control) or *ProAUX1:LAX2* transgenes (*n* = 40).

**(C)** Growth responses of the wild type (Col-0), *aux1-22*, and *aux1-22* complemented by either *ProAUX1:AUX1* (control) or *ProAUX1:LAX2* transgenes grown at various concentrations of 2,4-D and root growth expressed as percentage of zero control (*n* = 40). Error bars represent SE. Bar in **(B)** = 5 cm.

[See online article for color version of this figure.]

at the PM (Figures 6G and 6H, compare with inset in Figure 6D). Altogether, our data demonstrate that misexpressing *LAX2* in *AUX1*-expressing cells results in targeting defects for the protein in these tissues. This was further supported by an analysis of *Pro35S:LAX2-YFP* lines. In these lines, YFP signal was clearly seen in

*AUX1*-expressing cells, including the epidermis, but most of the signal is localized inside the cell. By contrast, LAX2-YFP seems to be correctly localized to the PM in the *LAX2*-expressing cells (Figures 6I and 6J). These results suggest that the subcellular distribution of LAX2 is distinct in different plant cells and tissues. To investigate whether other members of the family are also subject to such regulation, we expressed *LAX3* under the control of the *AUX1* promoter. The *AUX1* promoter-driven *LAX3* lines also failed to rescue *aux1* mutant phenotypes. In situ immunolocalization revealed reduced LAX3 protein abundance and targeting defects that were similar in nature to those observed for *ProAUX1:LAX2* lines (Figures 6K and 6L). We conclude that although AUX1/LAX family members may share auxin transport characteristics, these transport activities seem to be dependent on their unique cell- or tissue-type expression patterns.

### The AUX1 N Terminus Is Required for Correct Localization in the AUX1 Expression Domain

To further investigate the inability of LAX2 to correctly localize in the AUX1 expression domain, domain swap experiments were designed where either the N-terminal half of *LAX2* was fused to the C-terminal half of *AUX1* (*DS1*) or the N-terminal half of *AUX1* was fused to the C-terminal half of *LAX2* (*DS2*) to create chimeric genes driven by the *AUX1* promoter (Figure 7A). These constructs were then introduced into an *aux1* mutant allele, *aux1-22*. Homozygous T3 seedlings were then tested for the rescue of the *aux1* mutant phenotype (root gravitropic response and sensitivity to 2,4-D). The results revealed that, like *ProAUX1:LAX2* (Figures 7B, panels III and IV, and 7C), DS1 lines also failed to rescue root agravitropic phenotypes of *aux1* seedlings (Figure 7B, panels V and VI) as well as 2,4-D–resistant root growth (Figure 7C). By contrast, DS2 lines rescued both the 2,4-D–resistant root growth (Figure 7C) and agravitropic phenotypes of *aux1* seedlings (Figure 7B, panels VII and VIII).

To probe the molecular basis of rescue, in situ immunolocalization experiments were done using either anti-HA antibody (for DS1) or anti-LAX2 antibody (for DS2). As shown in Figures 7F and 7G, DS2 lines show strong signal in *AUX1* expression domains in the LRC and epidermal cells besides endogenous LAX2 signal in the vascular tissues. By contrast, DS1 lines show almost no signal in the LRC and the epidermal cell (Figures 7D and 7E), but a surprisingly strong signal is seen in the vascular tissues (Figure 7D). On the basis of these results, we conclude that the N-terminal half of AUX1 is required for correct localization in the AUX1 expression domain.

### DISCUSSION

During evolution, gene family members acquire mutations that alter one or more subfunctions of the single gene progenitor. The fate of duplicated genes can encompass pseudogenization (loss of function), subfunctionalization, and neofunctionalization (Moore and Purugganan, 2005). This study shows that *AUX/LAX* family members in *Arabidopsis* have not undergone pseudogenization or neofunctionalization but have experienced subfunctionalization.
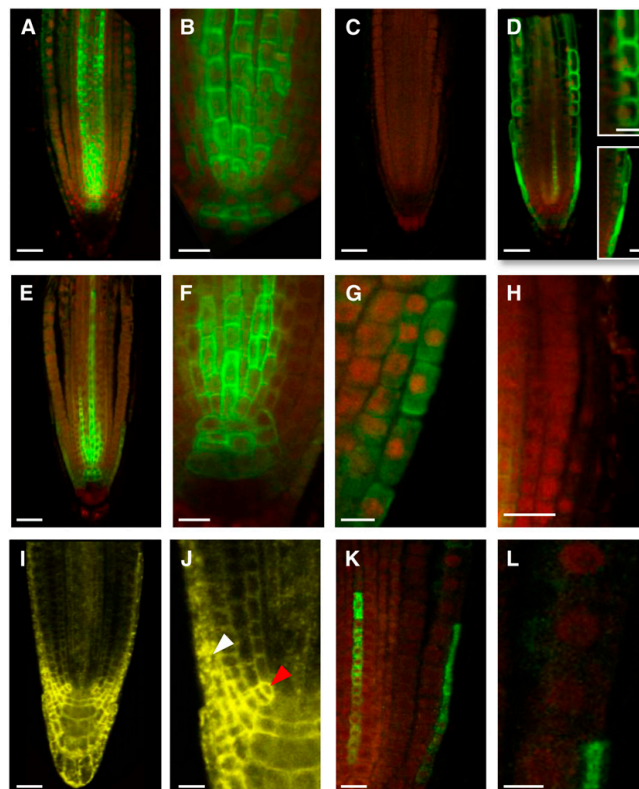
**Figure 6.** LAX2 and LAX3 Cannot Be Correctly Targeted in *AUX1*-Expressing Cells.

**(A)** to **(C)** In situ immunodetection of LAX2 (green) in the wild type (**[A]** to **[B]**) or *lax2* **(C)** primary roots counter stained with propidium iodide (red).
**(D)** In situ immunodetection of NHA-AUX1 in root apex. Inset: Close-up of epidermal (Top) and LRC (Bottom) cells.
**(E)** to **(H)** In situ immunodetection of LAX2 in *aux1-22 ProAUX1:LAX2* roots showing targeting defect of LAX2 in *AUX1*-expressing cells, including LRC **(G)** and epidermal cells **(H)**.
**(I)** and **(J)** Confocal imaging of seedlings expressing *LAX2-YFP* under the control of *CaMV35S* promoter showing correct targeting of LAX2 in *LAX2*-expressing cells (red arrowhead) but not in *AUX1*-expressing cells (white arrowhead).
**(K)** and **(L)** In situ immunodetection of LAX3-FLAG in *aux1-22 ProAUX1>>LAX3* (Methods) roots, showing targeting defects of LAX3 in *AUX1* expression domains including LRC and epidermal cells **(L)**.
Bars in **(A)**, **(C)** to **(E)**, and **(I)** = 25 μm; bars in **(B)**, **(F)** to **(H)**, **(J)**, and **(K)** = 10 μm; bars in **(L)** and insets = 5 μm.

Genetic evidence presented in this and other articles demonstrates that each *AUX/LAX* family member regulates an auxin-dependent development process. For example, several studies support a role for AUX1 in auxin-mediated developmental programs, including root gravitropism (Swarup et al., 2001; Swarup et al., 2005; Dharmasiri et al., 2006), root hair development (Grebe et al., 2002; Jones et al., 2009), and leaf phyllotaxy (Reinhardt et al., 2003; Bainbridge et al., 2008), whereas both AUX1 and LAX3 are required for lateral root development (Swarup et al., 2008) and apical hook formation (Vandenbussche et al., 2010). Although a role for LAX1 and LAX2 in auxin-regulated root development is limited, evidence is growing that they are both required for *Arabidopsis* aerial development. In our study, we have

provided evidence that LAX2 regulates vascular development, whereas LAX1 and LAX2 are required for leaf phyllotactic patterning (Bainbridge et al., 2008).

There is also no evidence to support neofunctionalization of *AUX/LAX* genes. Instead, all four AUX/LAX proteins retain an auxin influx carrier function. Using either heterologous oocyte or yeast expression systems or complementation of *aux1* mutant root phenotypes, we demonstrated that *AUX1* (Yang et al., 2006), *LAX3* (Swarup et al., 2008), and *LAX1* and *LAX2* (this study) encode a family of auxin uptake transporters.

Our study provides clear evidence for subfunctionalization of *AUX/LAX* sequences. As a result of divergence to their regulatory sequences, we observed that *AUX/LAX* spatial expressions

**A**

AUX1, LAX2, DS1, DS2 — gene constructs

**B**

I Col
II aux1-22
III aux1-22/ProAUX1:LAX2-2
IV aux1-22/ProAUX1:LAX2-11
V aux1-22/DS1-2
VI aux1-22/DS1-4
VII aux1-22/DS2-3
VIII aux1-22/DS2-4

**C**

Growth (% to zero 2,4D) vs 2,4D concentration (nM)

Legend: Col, aux1-22, CHA, AUX1LAX2, DS1-2, DS1-4, DS2-3, DS2-4, DS2-6

**D** DS1
**E**
**F** DS2
**G**
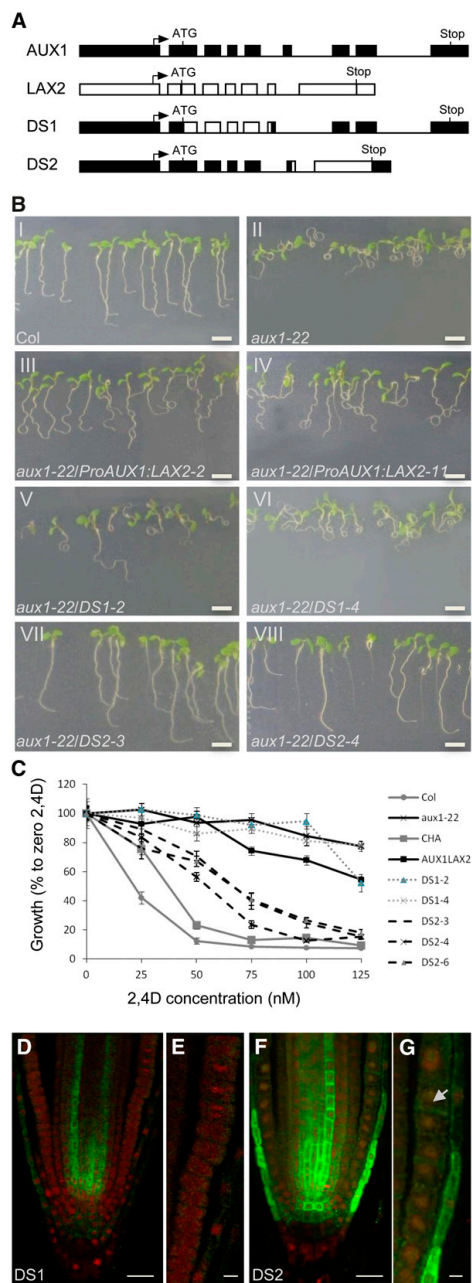
**Figure 7.** N-Terminal Half of AUX1 Is Required for Correct Localization in the *AUX1* Expression Domain.

differ considerably within and between plant tissues (Figure 1; see Supplemental Figure 2 online) (Bainbridge et al., 2008; Swarup et al., 2008; Jones et al., 2009). We also report subfunctionalization of *AUX/LAX* coding sequences that regulate intracellular trafficking. When ectopically expressed, in situ immunolocalization revealed that LAX2 and LAX3 proteins were unable to be correctly targeted to the PMs of *AUX1*-expressing root cells. In wild-type roots, AUX1 is localized in cells that are involved in gravity perception (columella), signal transmission (LRC), and gravity response (epidermis) (Swarup et al., 2001; Swarup et al., 2005). The PM targeting defect of LAX2 and LAX3 is particularly severe in epidermal cells, where almost no LAX2 or LAX3 could be detected (Figures 6E to 6L). The simplest explanation for the observed tissue-specific intracellular targeting defect is the requirement of LAX2 and LAX3 for additional trafficking factors that are coexpressed in stele cells but absent in outer root tissues.

Domain swap experiments designed to test this support this notion and suggest that intramolecular trafficking signals are located in the N-terminal half of AUX1. Besides, the ability of DS2 to rescue the *aux1* mutant phenotype clearly suggests that the C-terminal half of LAX2 in the chimeric DS2 protein must play a key role in its overall function as auxin influx carrier, because several missense loss-of-function *aux1* alleles are located in the C-terminal half of AUX1 (Swarup et al., 2004).

All DS2 (ProAUX1:$^N$AUX1-$^C$LAX2 chimeric protein fusion) lines can rescue the root agravitropic defect and 2,4-D–resistant root growth of *aux1* seedlings plus show correct localization of chimeric DS2 protein in LRC and epidermal cells when probed using anti-LAX2 antibodies (Figure 7). By contrast, none of the DS1 (ProAUX1:$^N$LAX2-$^C$HA-AUX1 chimeric protein fusion) lines rescued *aux1* mutant phenotypes or showed much signal in LRC and epidermal cells (Figure 7). It has been previously shown that these expression domains of AUX1 are crucial for its function (Swarup et al., 2005), and the inability of DS1 but not DS2 to correctly localize in these expression domains provides strong

**(A)** Gene constructs used for domain swap experiments (boxes represent promoter, 5′, and 3′ untranslated regions and exons; lines represent introns).

**(B)** Root gravitropic responses of the wild type (Col-0), *aux1-22*, and *aux1-22* complemented by *ProAUX1:LAX2*, *DS1*, or *DS2* transgenes (*n* = 40).

**(C)** Growth responses of the wild type (Col-0), *CHA-AUX1* (*CHA*), and *aux1-22* complemented by *ProAUX1:LAX2*, *DS1*, or *DS2* transgenes grown at various concentrations of 2,4-D (*n* = 40). Error bars represent SE.

**(D)** In situ immunodetection of chimeric DS1 protein (green) by anti-HA antibody in primary roots counter stained with propidium iodide (red).

**(E)** Close-up of LRC and epidermal cells in DS1 roots.

**(F)** In situ immunodetection of chimeric DS2 protein (green) by anti-LAX2 antibody in primary roots counter stained with propidium iodide (red).

**(G)** Close up of LRC and epidermal cells in DS2 roots showing localization of DS2 protein (green) in epidermal (arrow) and LRC cells.

**(E)** to **(H)** Expression profile of *ProLAX1:LAX1-VENUS* [**(E)** to **(I)**] and *ProLAX2:LAX2-VENUS* [**(J)** to **(N)**] during lateral root primordium development.

Bar in **(B)** = 5 cm; bars in **(D)** and **(F)** = 20 μm; bar in **(G)** = 5 μm.

evidence that the N-terminal half of AUX1 is required for correct localization in these expression domains. Surprisingly, when probed using anti-HA antibodies, although almost no signal was detected in the LRC and epidermal cells, strong DS1 signal was detected in the vascular cells. As mentioned above, the DS1 protein is a translational fusion between the N-terminal half of LAX2 and C-terminal half of AUX1 (Figure 7A), and vascular tissues are the natural/endogenous expression domain of LAX2. Although we do not currently understand the molecular basis for this differential localization of DS1 protein, it is tempting to speculate that, because the N-terminal half of AUX1 is required for correct localization in the AUX1 expression domain, the N-terminal half of LAX2 contains molecular signals that are recognized by trafficking factors in those tissues. However, compared with endogenous LAX2, DS1 chimeric protein does not seem to be correctly targeted to the PM, suggesting that, in contrast with AUX1, in the case of LAX2, the N-terminal part is still not sufficient for proper membrane targeting. AUX1 intracellular targeting is known to be regulated by AXR4, which encodes a putative endoplasmic reticulum (ER) chaperone that has been proposed to facilitate the correct folding of AUX1 and its export from ER to golgi (Dharmasiri et al., 2006). Hence, the failure of LAX2 and LAX3 to be properly targeted in *AUX1*-expressing cells may simply reflect a need for their own specific ER chaperones. Future identification of such trafficking factors and of intramolecular trafficking signals within *AUX/LAX* coding sequences will help reveal how and why they have undergone subfunctionalization during evolution.

## METHODS

### Plant Materials and Growth Conditions

The *aux1-22* allele was used throughout this study (Swarup et al., 2004). *lax1*, *lax2*, and *lax3* insertion lines have been described previously (Bainbridge et al., 2008; Swarup et al., 2008). Plants were grown on vertical Murashige and Skoog plates at 23°C under continuous light at 150 μmol m$^{-2}$ s$^{-1}$. Gravitropic assays were performed as previously described (Swarup et al., 2005). Lateral root numbers were determined on 6-d-old plants using a stereomicroscope. Primary root length was measured using the NeuronJ plugin of ImageJ software.

### Isolation of the LAX dSpm Insertion Lines and RT-PCR Analysis

Insertion lines for the *Arabidopsis thaliana LAX1*, *LAX2*, *and LAX3* were identified in the Sainsbury Laboratory *Arabidopsis thaliana* population as described previously (Swarup et al. 2008). *LAX2* RT-PCR analysis on RNA isolated from the wild type (ecotype Columbia [Col-0]) and dSpm *lax2-1* allele was performed using primers Lax2F2 (5′-GAGAACGGTGAGA-AAGCAGC-3′) and Lax2R4 (5′-CGCAGAAGGCAGCGTTAGCG-3′).

### Isolation of *LAX2* GABI-Kat Allele (*lax2-2*) and RT-PCR Analysis

The *lax2-2* allele (line ID GK_345D11; Nottingham Arabidopsis Stock Centre ID N433071) of *LAX2* was identified from the GABI-Kat T-DNA insertional population (Kleinboelting et al., 2012). T-DNA insertion was confirmed by PCR using primer pairs 0849 (left border primer 5′-ATATTGACCATCA-TACTCATTGC-3′) and Lx2-25 (gene-specific primer 5′-CACAAAGTA-GAGTGGCGTG-3′). The homozygous line was confirmed by the absence of a *LAX2*-specific band using primers Lx2-19 (5′-GGCACAAGTGCTGTTGAC-3′) and Lx2-28 (5′-CAGACGCAGAAGGCAGCG-3′). *LAX2* RT-PCR analysis of RNA isolated from the wild type (Col-0) and GABI-kat *lax2-2* allele was

performed using primers Lx2-19 (5′-GGCACAAGTGCTGTTGAC-3′) and Lx2-28.

### Generation of Transgenic Lines

The promoter GUS lines *ProAUX1:GUS* (Marchant et al., 2002), *ProLAX1*:*GUS*, *ProLAX2:GUS* (Bainbridge et al., 2008), and *ProLAX3:GUS* (Swarup et al., 2008) have been described before. Similarly, N- or C-terminal HA-AUX1 (NHA-AUX1 or CHA-AUX1) have been described before (Swarup et al., 2001). For genetic complementation of *aux1*, *AUX1* and *LAX2* genomic sequences were PCR amplified and fused with the *Arabidopsis AUX1* promoter (1.7 kb) and terminator (0.3 kb) in a pMOG402 binary vector (MOGEN International) as previously described (Péret et al., 2007). For creation of domain swap constructs (DS1 and DS2), CHA-AUX1 (Swarup et al., 2001) and LAX2 genomic sequences were cloned into Gateway entry vector pENTR11 (Invitrogen). Both these vectors were then cut with *Sph*I (internal unique site at identical position in both CHA-AUX1 and LAX2) and *Xho*I (in the vector), and the resulting inserts were swapped to create DS1 and DS2. The resulting chimeric constructs DS1 and DS2 were cut out with *Bam*HI and *Xho*I and fused with the *Arabidopsis AUX1* promoter (1.7 kb) and terminator (0.3 kb) in a pMOG402 binary vector (MOGEN International) as previously described (Péret et al., 2007). The LAX3-FLAG line was created by fusing the 2× FLAG epitope tag (MDYKDHDIDYKDDDDK) to the C-terminal of LAX3. The upstream activating sequence was then fused upstream of *LAX3-FLAG*. This *UAS:LAX3-FLAG* line was then crossed to the *ProAUX1:GAL4* line (Swarup et al., 2005) to transactivate *LAX3-FLAG* in *AUX1*-expressing cells. The VENUS fluorescent protein (Tursun et al., 2009) fusions of *LAX1 and LAX2* were generated by a recombineering approach (Zhou et al., 2011). VENUS was fused in frame after the codon 122 for *ProLAX1:LAX1-VENUS* and codon 110 for *ProLAX2:LAX2-VENUS*. Transformation of *Agrobacterium* (C58) and *Arabidopsis* was done as described before (Péret et al., 2007). Transgene-specific cDNA sequences of these lines were PCR-amplified and sequenced to ensure against rearrangements of the transgenes. All complementation experiments were performed on two independent homozygous T3 lines.

### Histochemical GUS Staining

GUS staining was done as described previously (Péret et al., 2007). Plants were cleared for 24 h in 1 M chloral hydrate and 33% glycerol. Seedlings were mounted in 50% glycerol and observed with a Leica DMRB microscope.

### Quantitative RT-PCR

Total RNA was extracted from roots using the Qiagen RNeasy Plant Mini Kit with on-column DNase treatment (RNase free DNase set, Qiagen). Poly (dT) cDNA was prepared from 3 μg total RNA using the Transcriptor First Strand cDNA Synthesis Kit (Roche). Quantitative PCR was performed using SYBR Green Sensimix (Quantace) on a Stratagene Mx3005P apparatus. PCR was performed in 96-well optical reaction plates heated for 5 min to 95°C, followed by 40 cycles of denaturation for 10 s at 95°C and annealing-extension for 30 s at 60°C. Target quantifications were performed with the following specific primer pairs: AtAUX1F 5′-tgctctgatcaaagtcttctcct-3′ and AtAUX1R 5′-gaagagaagaacccagaaatgtg-3′. Expression levels were normalized to UBA using the following primers: UBAforward 5′-agtgga-gaggctgcagaaga-3′ and UBAreverse 5′-ctcgggtagcacgagcttta-3′. All quantitative RT-PCR experiments were performed in triplicate, and the values presented represent means ± SE.

### Production of LAX2 Antibody

For generation of LAX2 antibody, a peptide containing the C-terminal 15 amino acids of LAX2 (PPPISHPHFNHTHGL) plus an added Cys (for

attachment to carrier protein KLH) was conjugated to KLH and was injected to rabbits in complete Freunds adjuvant. Boosters were given on days 14, 28, 42, 56, and 70. Immune serum was collected on days 49, 63, and 77. Affinity purification of the antiserum was done against the LAX2 peptide that was coupled to Pierce SulfoLink resin as per manufacturer's instruction. The column was washed twice with 10 mM Tris-Cl buffer (pH 7.5) containing 0.5 M NaCl, once with 100 mM Gly (pH 2.5), and finally with two more washes with 10 mM Tris-Cl buffer (pH 7.5). Crude LAX2 antiserum (10 mL) buffered in 100 μL 1 M Tris-Cl (pH 7.5) was then applied on the column and rotated at 4°C overnight. Flow-through was passed twice on the column at room temperature followed by a wash each with 10 mM Tris-Cl buffer (pH 7.5) and 10 mM Tris-Cl buffer (pH 7.5) containing 0.5 M NaCl. Purified antibodies were eluted in 250-μL fractions with 100 mM Gly (pH 2.5) and neutralized with 50 μL of Tris-Cl buffer (pH 8.0).

### Immunolocalization

Four-d-old seedlings were fixed, and immunolocalization experiments were performed as described previously (Swarup et al., 2005) using various primary and secondary antibodies. Localization was visualized using confocal microscopy. Primary antibodies anti-HA (Roche) and anti-FLAG (Sigma-Aldrich) were used at a dilution of 1:200, whereas anti-LAX2 was used at a dilution of 1:100. Oregon Green or Alexa Fluor–coupled secondary anti-rat, anti-mouse, or anti-rabbit antibodies (Invitrogen) were used at a dilution of 1:200. Background staining was performed with propidium iodide (Sigma-Aldrich).

### Auxin Transport Assays

Auxin transport assays in oocytes were performed as previously described (Swarup et al., 2008). For uptake experiments in *Schizosaccharomyces pombe*, the *LAX2* cDNA was amplified from pOO2-LAX2 using primers ccacLAX5 (CACCATGGAGAACGGTGAGAA) and LAX2nonstop3 (AAGGCCGTGAGTGTGATTGA), cloned into Gateway cloning vector pENTR/TOPO (Invitrogen), and confirmed by sequencing. *LAX2* cDNA was subsequently cloned into the *S. pombe* expression vector pREP41GWHA (Yang and Murphy, 2009). *LAX2* expression in *S. pombe* vat3 cells (Yang and Murphy, 2009) was confirmed by immunoblot using anti-HA primary antibody (1:500 dilution; Santa Cruz Biotechnology).

### Accession Numbers

Atg nomenclature gene accession numbers of The Arabidopsis Information Resource database (http://www.Arabidopsis.org) are: At2g38120 (*AUX1*), At5g01240 (*LAX1*), At2g21050 (*LAX2*), At1g77690 (*LAX3*), and UBA (At1g04850).

### Supplemental Data

The following materials are available in the online version of this article.

**Supplemental Figure 1.** The *AUX/LAX* Genes Represent a Highly Conserved Family of Auxin Influx Transporters.

**Supplemental Figure 2.** *AUX/LAX* Genes Exhibit Complementary Expression Patterns.

**Supplemental Figure 3.** Promoter Analysis of *AUX/LAX* Genes.

**Supplemental Figure 4.** *LAX1* and *LAX3* Genes Are Induced by Auxin.

**Supplemental Figure 5.** *lax1*, *lax2*, and *lax3* Mutants Exhibit Normal Gravitropic Response.

**Supplemental Figure 6.** *lax1* and *lax2* Mutants Exhibit a Normal Response to 2,4-D.

**Supplemental Figure 7.** *lax1* and *lax2* Mutants Exhibit Normal Root Growth and Lateral Root Growth.

**Supplemental Figure 8.** *lax1* and *lax2* Mutants Do Not Enhance *aux1* Mutant Phenotypes.

**Supplemental Figure 9.** *ProAUX1:AUX1* and *ProAUX1:LAX2* Seedlings Exhibit Comparable Transgene Expression Levels.

**Supplemental Data Set 1.** Alignment Used to Generate the Phylogeny Presented in Supplemental Figure 1A Online.

## AUTHOR CONTRIBUTIONS

R.S. and B.P. designed the research, performed research, analyzed data, wrote, and edited the article. K.S., A.F., M.S., Y.Y., S.D., N.J., I.C., P.P., A.S., H.Y., and J.R. performed research and analyzed data. E.V., C.H., M.A.P.-A., J.Y., and J.A. contributed new genetic tools (recombineering technology). L.L., A.M., G.T.S.B., and E.N. analyzed data. M.J.B. designed the research and edited the article.

## REFERENCES

**Bainbridge, K., Guyomarc'h, S., Bayer, E., Swarup, R., Bennett, M., Mandel, T., and Kuhlemeier, C.** (2008). Auxin influx carriers stabilize phyllotactic patterning. Genes Dev. **22:** 810–823.

**Bennett, M.J., Marchant, A., Green, H.G., May, S.T., Ward, S.P., Millner, P.A., Walker, A.R., Schulz, B., and Feldmann, K.A.** (1996). *Arabidopsis* AUX1 gene: A permease-like regulator of root gravitropism. Science **273:** 948–950.

**Carrier, D.J., Bakar, N.T., Swarup, R., Callaghan, R., Napier, R.M., Bennett, M.J., and Kerr, I.D.** (2008). The binding of auxin to the Arabidopsis auxin influx transporter AUX1. Plant Physiol. **148:** 529–535.

**Cho, M., Lee, S.H., and Cho, H.T.** (2007). P-glycoprotein4 displays auxin efflux transporter-like action in *Arabidopsis* root hair cells and tobacco cells. Plant Cell **19:** 3930–3943.

**Dharmasiri, S., Swarup, R., Mockaitis, K., Dharmasiri, N., Singh, S.K., Kowalchyk, M., Marchant, A., Mills, S., Sandberg, G., Bennett, M.J., and Estelle, M.** (2006). AXR4 is required for localization of the auxin influx facilitator AUX1. Science **312:** 1218–1220.

**Geisler, M., et al.** (2005). Cellular efflux of auxin catalyzed by the *Arabidopsis* MDR/PGP transporter AtPGP1. Plant J. **44:** 179–194.

**Grebe, M., Friml, J., Swarup, R., Ljung, K., Sandberg, G., Terlou, M., Palme, K., Bennett, M.J., and Scheres, B.** (2002). Cell polarity signaling in *Arabidopsis* involves a BFA-sensitive auxin influx pathway. Curr. Biol. **12:** 329–334.

**Jones, A.R., Kramer, E.M., Knox, K., Swarup, R., Bennett, M.J., Lazarus, C.M., Leyser, H.M., and Grierson, C.S.** (2009). Auxin transport through non-hair cells sustains root-hair development. Nat. Cell Biol. **11:** 78–84.

**Kleinboelting, N., Huep, G., Kloetgen, A., Viehoever, P., and Weisshaar, B.** (2012). GABI-Kat SimpleSearch: New features of the *Arabidopsis thaliana* T-DNA mutant database. Nucleic Acids Res. **40:** D1211–D1215.

**Kleine-Vehn, J., Dhonukshe, P., Swarup, R., Bennett, M., and Friml, J.** (2006). Subcellular trafficking of the *Arabidopsis* auxin influx carrier AUX1 uses a novel pathway distinct from PIN1. Plant Cell **18:** 3171–3181.

**Marchant, A., Bhalerao, R., Casimiro, I., Eklöf, J., Casero, P.J., Bennett, M., and Sandberg, G.** (2002). AUX1 promotes lateral root formation by facilitating indole-3-acetic acid distribution between sink and source tissues in the *Arabidopsis* seedling. Plant Cell **14:** 589–597.

**Moore, R.C., and Purugganan, M.D.** (2005). The evolutionary dynamics of plant duplicate genes. Curr. Opin. Plant Biol. **8:** 122–128.

**Péret, B., Swarup, R., Jansen, L., Devos, G., Auguy, F., Collin, M., Santi, C., Hocher, V., Franche, C., Bogusz, D., Bennett, M., and Laplaze, L.** (2007). Auxin influx activity is associated with Frankia infection during actinorhizal nodule formation in *Casuarina glauca*. Plant Physiol. **144:** 1852–1862.

**Petrásek, J., and Friml, J.** (2009). Auxin transport routes in plant development. Development **136:** 2675–2688.

**Petrásek, J. et al** (2006). PIN proteins perform a rate-limiting function in cellular auxin efflux. Science **312:** 914–918.

**Reinhardt, D.** (2003). Vascular patterning: More than just auxin? Curr. Biol. **13:** R485–R487.

**Reinhardt, D., Pesce, E.R., Stieger, P., Mandel, T., Baltensperger, K., Bennett, M., Traas, J., Friml, J., and Kuhlemeier, C.** (2003). Regulation of phyllotaxis by polar auxin transport. Nature **426:** 255–260.

**Swarup, R., Friml, J., Marchant, A., Ljung, K., Sandberg, G., Palme, K., and Bennett, M.** (2001). Localization of the auxin permease AUX1 suggests two functionally distinct hormone transport pathways operate in the *Arabidopsis* root apex. Genes Dev. **15:** 2648–2653.

**Swarup, R., Kramer, E.M., Perry, P., Knox, K., Leyser, H.M., Haseloff, J., Beemster, G.T., Bhalerao, R., and Bennett, M.J.** (2005). Root gravitropism requires lateral root cap and epidermal cells for transport and response to a mobile auxin signal. Nat. Cell Biol. **7:** 1057–1065.

**Swarup, R., et al.** (2004). Structure-function analysis of the presumptive *Arabidopsis* auxin permease AUX1. Plant Cell **16:** 3069–3083.

**Swarup, K., et al.** (2008). The auxin influx carrier LAX3 promotes lateral root emergence. Nat. Cell Biol. **10:** 946–954.

**Tursun, B., Cochella, L., Carrera, I., and Hobert, O.** (2009). A toolkit and robust pipeline for the generation of fosmid-based reporter genes in *C. elegans*. PLoS One **4:** e4625.

**Vandenbussche, F., Petrásek, J., Zádníková, P., Hoyerová, K., Pesek, B., Raz, V., Swarup, R., Bennett, M., Zazímalová, E., Benková, E., and Van Der Straeten, D.** (2010). The auxin influx carriers AUX1 and LAX3 are involved in auxin-ethylene interactions during apical hook development in *Arabidopsis thaliana* seedlings. Development **137:** 597–606.

**Vanneste, S., and Friml, J.** (2009). Auxin: A trigger for change in plant development. Cell **136:** 1005–1016.

**Vieten, A., Sauer, M., Brewer, P.B., and Friml, J.** (2007). Molecular and cellular aspects of auxin-transport-mediated development. Trends Plant Sci. **12:** 160–168.

**Vieten, A., Vanneste, S., Wisniewska, J., Benková, E., Benjamins, R., Beeckman, T., Luschnig, C., and Friml, J.** (2005). Functional redundancy of PIN proteins is accompanied by auxin-dependent cross-regulation of PIN expression. Development **132:** 4521–4531.

**Wisniewska, J., Xu, J., Seifertová, D., Brewer, P.B., Ruzicka, K., Blilou, I., Rouquié, D., Benková, E., Scheres, B., and Friml, J.** (2006). Polar PIN localization directs auxin flow in plants. Science **312:** 883.

**Yang, H., and Murphy, A.S.** (2009). Functional expression and characterization of *Arabidopsis* ABCB, AUX 1 and PIN auxin transporters in *Schizosaccharomyces pombe*. Plant J. **59:** 179–191.

**Yang, Y., Hammes, U.Z., Taylor, C.G., Schachtman, D.P., and Nielsen, E.** (2006). High-affinity auxin transport by the AUX1 influx carrier protein. Curr. Biol. **16:** 1123–1127.

**Young, G.B., Jack, D.L., Smith, D.W., and Saier, M.H. Jr.** (1999). The amino acid/auxin:proton symport permease family. Biochim. Biophys. Acta **1415:** 306–322.

**Zhou, R., Benavente, L.M., Stepanova, A.N., and Alonso, J.M.** (2011). A recombineering-based gene tagging system for *Arabidopsis*. Plant J. **66:** 712–723.

Appendix B

## ARTICLE

# ER-localized auxin transporter PIN8 regulates auxin homeostasis and male gametophyte development in *Arabidopsis*

Zhaojun Ding[1,2], Bangjun Wang[3], Ignacio Moreno[4], Nikoleta Dupláková[5], Sibu Simon[1], Nicola Carraro[6], Jesica Reemmer[6], Aleš Pěnčík[7], Xu Chen[1], Ricardo Tejos[1], Petr Skůpa[5], Stephan Pollmann[8], Jozef Mravec[1], Jan Petrášek[5], Eva Zažímalová[5], David Honys[5], Jakub Rolčík[7], Angus Murphy[6], Ariel Orellana[4], Markus Geisler[3] & Jiří Friml[1,9]

Auxin is a key coordinative signal required for many aspects of plant development and its levels are controlled by auxin metabolism and intercellular auxin transport. Here we find that a member of PIN auxin transporter family, PIN8 is expressed in male gametophyte of *Arabidopsis thaliana* and has a crucial role in pollen development and functionality. Ectopic expression in sporophytic tissues establishes a role of PIN8 in regulating auxin homoeostasis and metabolism. PIN8 co-localizes with PIN5 to the endoplasmic reticulum (ER) where it acts as an auxin transporter. Genetic analyses reveal an antagonistic action of PIN5 and PIN8 in the regulation of intracellular auxin homoeostasis and gametophyte as well as sporophyte development. Our results reveal a role of the auxin transport in male gametophyte development in which the distinct actions of ER-localized PIN transporters regulate cellular auxin homoeostasis and maintain the auxin levels optimal for pollen development and pollen tube growth.

[1] Department of Plant Systems Biology, VIB and Department of Plant Biotechnology and Genetics, Ghent University, B-9052 Gent, Belgium. [2] The Key Laboratory of Plant Cell Engineering and Germplasm Innovation, Ministry of Education, School of Life Sciences, Shandong University, Shanda Nanlu 27, Jinan 250100, China. [3] Department of Biology, Plant Biology, University of Fribourg, 1700 Fribourg, Switzerland. [4] Center for Genome Regulation, Center of Plant Biotechnology, Facultad de Ciencias Biologicas, Universidad Andres Bello, Santiago, Chile. [5] Institute of Experimental Botany ASCR, 16500, Praha 6, Czech Republic. [6] Department of Horticulture, Purdue University, West Lafayette, Indiana, USA. [7] Laboratory of Growth Regulators, Centre of the Region Haná for Biotechnological and Agricultural Research, Faculty of Science, Palacký University, 78371 Olomouc, Czech Republic. [8] Ruhr-Universität Bochum, Lehrstuhl für Pflanzenphysiologie, 44801 Bochum, Germany. [9] Department of Functional Genomics and Proteomics, Faculty of Science, and CEITEC, Masaryk University, Kamenice 5, CZ-62500 Brno, Czech Republic. Correspondence and request for materials should be addressed to J.F. (e-mail: jiri.friml@psb.vib-ugent.be).

The plant hormone auxin has a crucial role in plant development[1–6]. On account of its differential distribution within plant tissues, it acts as a versatile coordinative signal mediating a multitude of processes, including female gametophyte patterning, embryogenesis, organogenesis, meristem activity, growth responses to environmental stimuli and others[7–10]. High auxin concentration in germinating pollen and active auxin responses in developing pollen[11–13] implicated auxin also in male gametophyte development and function, but its role there remained elusive.

A crucial aspect of auxin action is its graded distribution (auxin gradients) that depends on local auxin biosynthesis[14–16] and directional, intercellular auxin transport[7,17,18]. The polar auxin transport has an essential role in most auxin-regulated processes and is mediated by auxin influx proteins from the AUX1/LAX family[19], by PIN auxin efflux proteins[20] and by homologues of the ABCB multiple drug resistance transporters[21,22]. These auxin transporters typically localize to the plasma membrane (PM) and facilitate auxin flow across the membrane in and out of the cell[23]. Recently, the *Arabidopsis thaliana* PIN5 auxin transporter has been shown to localize to the endoplasmic reticulum (ER) and its activity is important for the regulation of auxin metabolism[24]. These findings suggest the existence of auxin transport across the ER membrane, although a demonstration of such transport has not been provided yet and its role in auxin biology and plant development is still largely unclear.

Here we identify and functionally characterize PIN8, an auxin transporter preferentially expressed in male gametophyte. PIN8 transports auxin across the ER membrane and antagonistically to PIN5 regulates intracellular auxin homoeostasis and metabolism for male gametophyte function.

## Results

**PIN8 is expressed and functions in the male gametophyte.** To assess a potential role for the auxin transport in male gametophyte development, we examined the expression patterns of PIN auxin transporters by using available transcriptome data[25]. Among the eight members of the PIN protein family in the *Arabidopsis* genome, a so-far uncharacterized member PIN8 was the only one predominantly expressed in pollen (Supplementary Fig. S1a). Reverse transcription PCR confirmed the highly enriched expression of PIN8 in reproductive tissues (Supplementary Fig. S1b) and lines comprising the *PIN8* coding region fused with green fluorescent protein (GFP) under the control of its native promoter (*PIN8::PIN8-GFP*) showed strong signal in developing and germinating pollen (Supplementary Fig. S1a).

To analyse the potential role of PIN8 in pollen development, we isolated two insertion mutant alleles, *pin8-1* and *pin8-2*, disrupting the first and fifth exon of the *PIN8* gene, respectively (Supplementary Fig. S1c,d). No obvious phenotypic defects were observed in seedlings and adult plants in both alleles (data not shown), which was consistent with very low *PIN8* expression in most sporophytic tissues. However, *pin8* mutants showed a decreased transmission ability through male gametophyte (38%) for *pin8-1* versus the expected 50% for the wild-type (Col-0) pollen (Fig. 1a). The complementation of this phenotype confirmed that the described pollen transmission defects are due to the loss of PIN8 function (Supplementary Fig. S2). 4′,6-Diamidino-2-phenylindole (DAPI) staining of pollen revealed a high frequency of aborted and misshaped pollen grains in *pin8* (Fig. 1b,c, Supplementary Table S1) and transmission electron microscopy analyses showed that *pin8* mutant pollen has a reduced density of rough ER (10–15%, n > 150 pollen grains) in comparison to the wild-type pollen (Fig. 1d,e). Next, we examined transgenic lines overexpressing *PIN8* under strong pollen-specific promoter LAT52 (ref. 24). *LAT52::PIN8* also showed strongly reduced transmission through the male gametophyte (below 10% for *LAT52::PIN8* versus expected 50% for the wild-type control; Fig. 1a and Supplementary Fig. S1e). In addition, *in vitro*
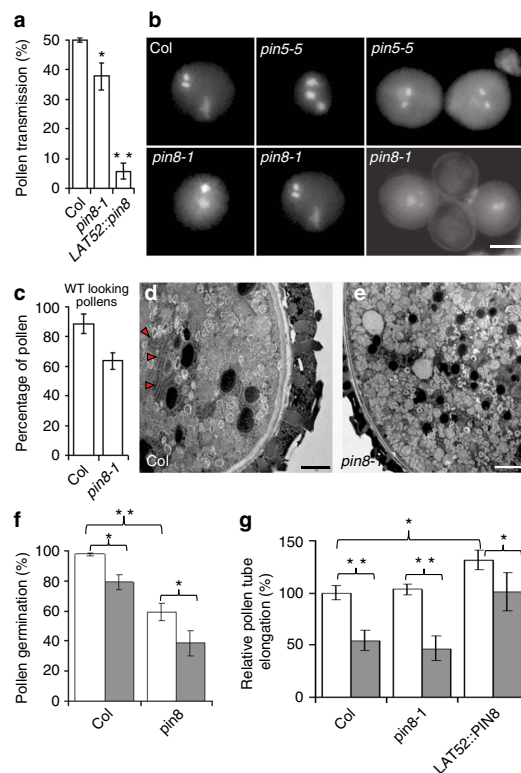


**Figure 1 | PIN8 is involved predominantly in the male gametophyte development.** (**a**) The *pin8* mutant and the *LAT52::PIN8* line showed reduced pollen transmission ability. Error bars represent the standard error of more than ten independent crosses (Student's *t*-test, *P < 0.05). (**b,c**) DAPI staining analysis showing defects in the morphology of *pin8* and *pin5* mutant pollen. Both mutants showed distorted and/or misplaced male germ unit and less frequently also exhibit pollen mitosis defects. Sometimes, collapsed pollen grains were observed. Scale bar, 10 μm. Error bars represent the standard error of more than 23 independent plants (Student's *t*-test, **P < 0.01). (**d,e**) Typical ER clusters in wild-type (WT) pollen (**d**) were not observed in 10–15% *pin8* pollen (observed 150 pollen grains) (**e**) by transmission electron microscope analysis. Scale bar, 10 μm. Red arrows mark ER clusters. (**f**) *pin8* (2256 pollen were analysed) shows reduced *in vitro* pollen germination abilities (2,814 Col pollens were analysed as the control) and increased sensitivity to auxin treatment (100 nM NAA) with a 35% reduction of pollen germination in *pin8* (5,017 pollens were analysed) compared with the 19% reduction in Col (1,131 pollens were analysed). Error bars represent the standard error of more than ten independent plants (Student's *t*-test, *P < 0.05; **P < 0.01). White and grey columns represent without and with NAA treatment, respectively. (**g**) Overexpression of *PIN8* in pollen in the *LAT52::PIN8* line strongly increased the resistance (with a 24% inhibition of pollen tube length compared with the 46% inhibition in Col) of *in vitro* pollen germination to NPA (100 μM NPA) treatment. Error bars represent the standard error of more than six independent plants (Student's *t*-test, *P < 0.05; **P < 0.01). White and grey column represent without and with NPA treatment, respectively, in Col, *pin8* or *LAT52::PIN8*.

pollen germination assays revealed a decreased pollen germination in *pin8* (40% decrease, Fig. 1f) and increased pollen tube elongation in *LAT52::PIN8* lines (30% increase, Fig. 1g) with a normal pollen

tube morphology (Supplementary Fig. S1f). Thus, the loss-of-function and ectopic expression analyses revealed a specific role of PIN8 in male gametophyte development and function.

As PIN8 is a member of the auxin transporter family, it is presumably involved in auxin transport. However, a role of auxin transport in male gametophyte development and function is far from being clear. To address this issue, we pharmacologically manipulated auxin levels and auxin transport during pollen germination and pollen tube growth. Auxin treatments (100 nM α-naphthaleneacetic acid (NAA)) reduced the pollen germination rate in wild type (19% reduction) and *pin8-1* pollen showed increased sensitivity to such auxin treatment (35% reduction) (Fig. 1f). Furthermore, the auxin transport inhibitor 1-*N*-naphthylphthalamic acid (NPA) strongly inhibited pollen tube growth and, notably, *LAT52::PIN8* pollen showed increased resistance to this NPA effect (Fig. 1g). The inhibition of the *in vitro* pollen tube growth by NPA was apparent only at high concentrations (100 μM) indicating that it might occur through APM1-regulated functions of PIN and ABCB auxin transport proteins, as APM1 is the target at high concentrations of NPA treatment[26,27]. The change in sensitivity in pollen tubes overexpressing auxin transport-related protein PIN8 suggests that it is auxin transport-related effect of NPA that affects pollen tube growth. Collectively, these findings hint at an important role of auxin and auxin transport for male gametophyte function and identified the pollen-specific putative auxin transporter PIN8 as an important factor regulating these processes.

**PIN8 overexpression affects many aspects of plant growth and development**. To further characterize the function of PIN8, we generated lines overexpressing PIN8 in sporophytic tissues under the control of the strong cauliflower mosaic virus 35S promoter (*PIN8OX*). *PIN8OX* lines flowered much earlier than wild-type plants (Fig. 2a,b), showed enhanced leaf margin serration, especially under short-day growth conditions (Fig. 2c) and had much longer hypocotyls than the control (Fig. 2d,e), which can be attributed to the increased cell elongation (Fig. 2f and Supplementary Table S2). All these plant growth and development phenotypes in *PIN8OX* suggest a capacity of PIN8 to influence different aspects of plant development, preferentially those where auxin is involved.

**PIN8 and PIN5 localize to the ER**. In *Arabidopsis,* the PIN auxin transporter family can be divided in two subclades: one represented by PIN1, PIN2, PIN3, PIN4 and PIN7, which all localize to the PM[23], and the other subclade represented by PIN5, PIN8 and possibly PIN6, which are characterized by a reduced middle hydrophilic loop[23] and for which PIN5 has been shown to localize to the ER in *Arabidopsis*[24]. To investigate the subcellular localization of PIN8, we examined *Arabidopsis* transgenic lines expressing a functional *PIN8::PIN8-GFP* construct. In *PIN8::PIN8-GFP* (Supplementary Fig. S2), a specific intracellular signal was observed only in pollen and growing pollen tubes (Fig. 3a–c and Supplementary Fig. S1a) consistent with the PIN8 expression data (Supplementary Fig. S1a). The *PIN8-GFP*-expressing cells showed intracellular signals, but no localization to the PM (Fig. 3a–c). A pronounced co-localization with the ER-tracer dye[24] suggested the association of PIN8-GFP with the ER (Fig. 3a–c).

To examine the PIN8 localization in more detail and in different sporophytic cell types, we ectopically expressed *PIN8* fused with GFP under the control of 35S promoter. Similar to what was observed in pollen, we detected a consistent, intracellular PIN8-GFP signal co-localized with ER markers, such as BIP2 (ref. 28) in root cells (Fig. 3d–f, p). On the other hand, we did not observe any co-localization of PIN8 with endosomes or Golgi apparatus (Fig. 3g–i, p and Supplementary Fig. S3) and also we did not observe any co-localization with labelled PM (Fig. 3j–l, p). Furthermore, PIN8 co-localized with PIN5 at the ER (Fig. 3m–p) and this
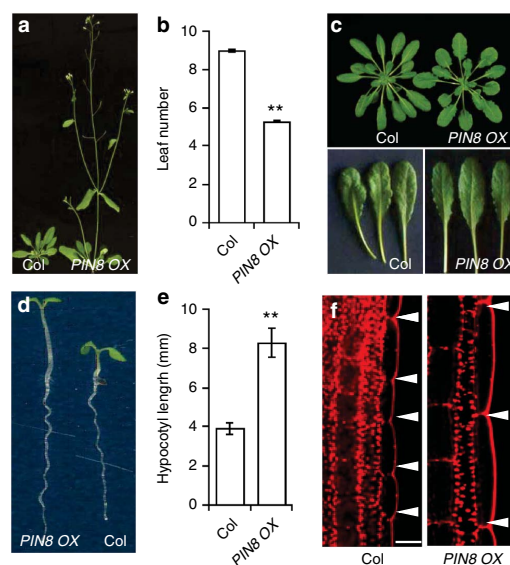


**Figure 2 | *PIN8OX* lines showed defects in many aspects of plant growth and development.** (**a,b**) *PIN8OX* lines flower earlier than the wild-type controls measured under long-day growth conditions. Error bars represent the standard error of the mean from three independent experiments (*n* = 48, Student's *t*-test, **P < 0.01). (**c**) *PIN8OX* lines showed strongly enhanced leaf margin serration under short-day growth conditions. (**d,e**) *PIN8OX* lines showed long hypocotyls compared with the control. Hypocotyl length was measured with 5-day-old seedlings grown under short days. Error bars represent the standard error of the mean from three independent experiments (*n* = 30, Student's *t*-test, **P < 0.01). (**f**) The cell length in *PIN8OX* lines is more than two times longer than that in the control (see the quantification data in Supplementary Table S2). The arrows indicate the intercellular space. Scale bar, 10 μm.

localization was, similar to that of PIN5 (ref. 24), insensitive to the treatment with the vesicle trafficking inhibitor brefeldin A (Supplementary Fig. S4). These results strongly suggest that PIN8, similar to PIN5, localizes to the ER and that these proteins might have related functions.

**PIN8 transports auxin and regulates cellular auxin homoeostasis**. The ER-localized PIN5 was found, in contrast to PM-localized PIN proteins, not to act in intercellular auxin transport, but to be involved in regulating cellular auxin homoeostasis, presumably by compartmentalizing auxin between the ER and the cytosol[24]. Therefore, we tested the role of PIN8 in regulating auxin homoeostasis. The visualization of auxin responses with the auxin-responsive reporter *DR5::GUS*[29] revealed no changes in *pin8* mutants (data not shown), consistent with a very low expression of *PIN8* in sporophytic tissues. In contrast, *PIN8OX* lines showed a markedly increased DR5 activity, both in the root and in the aerial parts of the seedling (Fig. 4a) suggesting elevated auxin levels.

To directly test the role of PIN8 in regulating auxin levels, we measured free auxin (indole-3-acetic acid (IAA)) levels in the *pin8* mutant and *PIN8OX* lines. Unfortunately, free IAA measurements directly in pollen were technically impossible, therefore, we used extraction and gas chromatography/mass spectroscopy detection of IAA in root tips, hypocotyls and rosette leaves. These measurements revealed that loss-of-function *pin8* mutants had similar levels
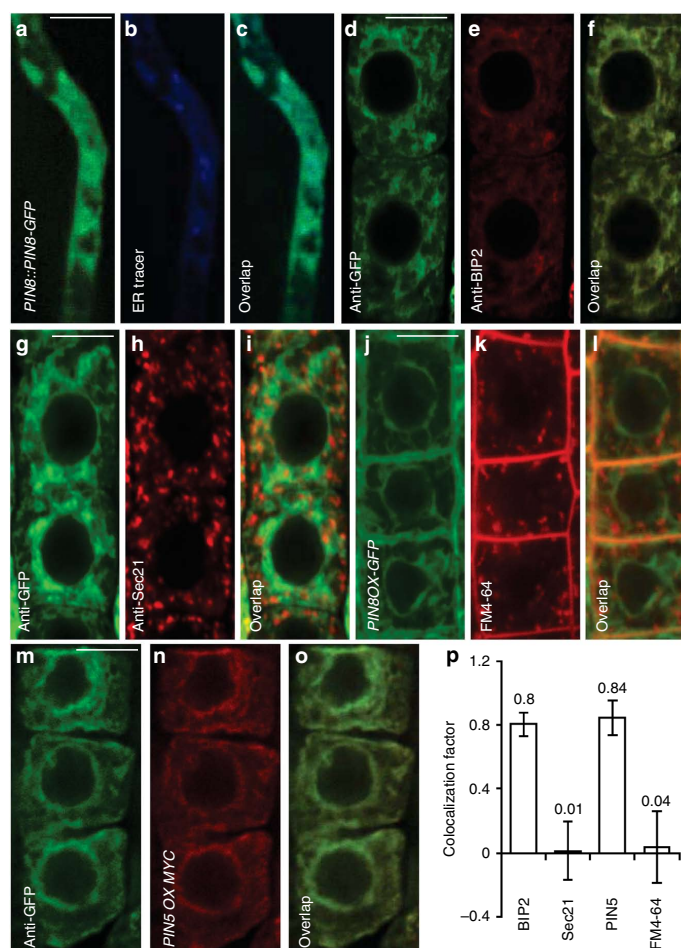
**Figure 3 | PIN8 localizes to the ER.** (**a–c**) PIN8 localization in the pollen tube of *PIN8::PIN8-GFP* line and co-localization of PIN8-GFP (green) with the ER-tracker dye (blue). (**d–f**) PIN8 localization in the root of *35S::PIN8-GFP* line and co-localization of PIN8-GFP (green) with ER marker BIP2 staining (red). (**g–i**) PIN8-GFP (green) does not co-localize with Golgi apparatus (GA) marker Sec21 (red). (**j–l**) PIN8-GFP (green) does not co-localize with endosomes stained with FM4-64 traced (red). (**m–o**) PIN8-GFP (green) and PIN5-myc (red) co-localize at the ER. (**p**) The quantification of PIN8 co-localization with ER (anti-BIP2), GA (anti-Sec21), PIN5 (anti-myc) and endosome (FM4-64 staining) markers confirms localization of PIN8 to the ER but not to the GA, endosomes or plasma membrane. The co-localization factor (the highest is 1.0) was calculated by Zeiss software. For microscope observation, 3-day-old seedlings ($n = 6$) and at least five areas were analysed for each seedling. Scale bar, 5 μm. Error bars represent the standard error. Live cell imaging (**a–c**, **j–l**) and immunostainings (**d–f**, **g–i**, **m–o**).

of free auxin as the control (Fig. 4b), whereas *PIN8OX* lines showed strongly increased free IAA levels in root tips, hypocotyls and rosette leaves (Fig. 4b). Thus, both DR5-monitored auxin response and direct auxin measurements revealed overall elevated auxin levels in plants overexpressing *PIN8*.

Next, we quantified the auxin efflux from mesophyll protoplasts isolated from rosette leaves of *PIN8* loss-of-function and overexpression lines. Consistent with the changes in auxin levels and *PIN8* expression data, protoplasts prepared from *pin8* mutants exhibited a comparable IAA and NAA efflux as wild-type controls, whereas in protoplasts isolated from *PIN8OX,* the efflux of IAA and NAA was increased (Fig. 4c and Supplementary Fig. S5), suggesting the

auxin transport competence of PIN8. The ER localization of PIN8 in protoplasts (Supplementary Fig. S6) is also consistent with a notion that PIN8 increases efflux of auxin from the ER into the cytoplasm and then presumably out of the protoplast.

To directly assess the ability of PIN8 at the ER membranes, we grew *PIN8OX*-etiolated plants in liquid culture and ER-enriched membrane fractions were prepared using sucrose gradient centrifugation as described[30]. This fraction was well separated from non-ER fractions including Golgi membranes and other organelles. PIN8-GFP was detected in the ER-enriched fraction with an anti-GFP antibody, but no PIN1 was detected with anti-PIN1 (not shown) confirming no or very low PM contamination. Transport assays with
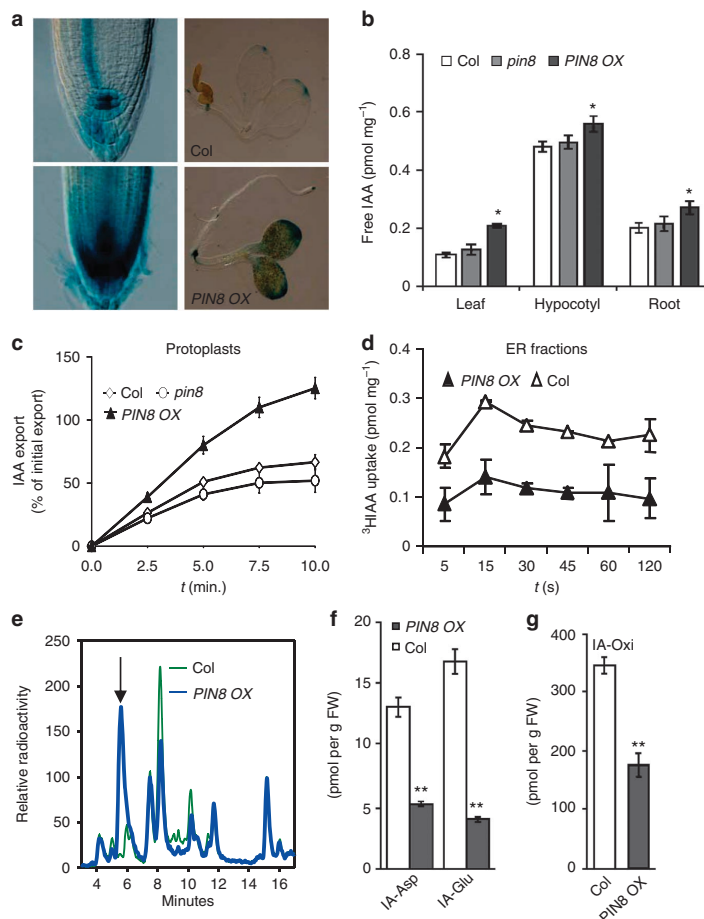
**Figure 4 | PIN8 regulates cellular auxin homoeostasis and auxin transport.** (**a**) *PIN8OX* exhibits enhanced auxin response as shown by the increased *DR5::GUS* activity in the root and in the aerial parts of the seedling. (**b**) Changes in free IAA levels in *PIN8OX* in young leaves/cotyledons, hypocotyls and root tips. Error bars represent the standard error of the mean, $n=5$ (Student's $t$-test, $*P<0.05$). (**c**) Protoplasts of *PIN8OX* showed a higher rate of IAA export. Error bars represent the standard error of the mean, $n=3$. (**d**) $^3$H-IAA uptake time course in ER-enriched membrane fractions from Col and *PIN8OX* plants. Transport assays were performed as described in Methods. ER-enriched membranes were incubated in 50 nM $^3$H-IAA fractions. Aliquots were taken at different times, filtered and washed. The radioactivity present in the filters was estimated by liquid scintillation counting and expressed as pmol of $^3$H-IAA/mg of total proteins. The experiment was performed two biological repeats, and the error bars represent the standard error of the mean. (**e**) The HPLC chromatogram of IAA metabolic profile changes noticeably in the *PIN8OX* line compared with the wild-type control (2.5-h incubation with $^3$H-IAA). (**f**,**g**) Liquid chromatography/mass spectrometry detected strongly decreased levels of IAA conjugates (indole-3-acetyl-aspartate, IA–Asp; indole-3-acetyl-glutamate, IA–Glu) (**f**), and oxindole-3-acetic acid (OxIAA) (**g**) in *PIN8OX* line. White and grey column represent Col and *PIN8OX*, respectively. Error bars represent the standard error of the mean, $n=3$ (Student's $t$-test, $**P<0.01$). FW, fresh weigh.

radiolabelled IAA showed increased auxin accumulation capacity of the ER fractions from the *PIN8OX* lines as compared with the control (Fig. 4d). In addition, competitive uptake assays with ER-enriched fraction from *PIN8OX* revealed that synthetic auxins NAA,2,4-D and auxin analogue indole-3-butyric acid can compete with radiolabelled IAA uptake, whereas the biologically inactive analogue benzoic acid (1 mM) did not compete with PIN8-mediated uptake of radiolabelled IAA (Supplementary Fig. S7a). Our auxin transport assays in mesophyll protoplasts from transiently transfected nicotiana benthamiana also indicated that IAA, not benzoic acid, was the preferred substrate of PIN8 action (Supplementary Fig. S7b).

These results show that IAA and other biologically active auxins are preferred substrates of PIN8 action. In an independent set of experiments, lighter ER membranes from *PIN8OX* seedlings, exhibited acidification after addition of ATP and accumulation of $^3$H-IAA in short-term (60 s) uptake assays, whereas denser ER vesicles, tonoplast vesicles and PM vesicles did not show auxin transport activity (Supplementary Fig. S8). The overall increase in auxin responses and free auxin levels in *PIN8OX* as well as changed auxin transport capacity of *PIN8OX* protoplasts and ER-derived membranes altogether suggested that PIN8 is an ER-localized auxin transporter involving in the regulation of auxin homoeostasis.
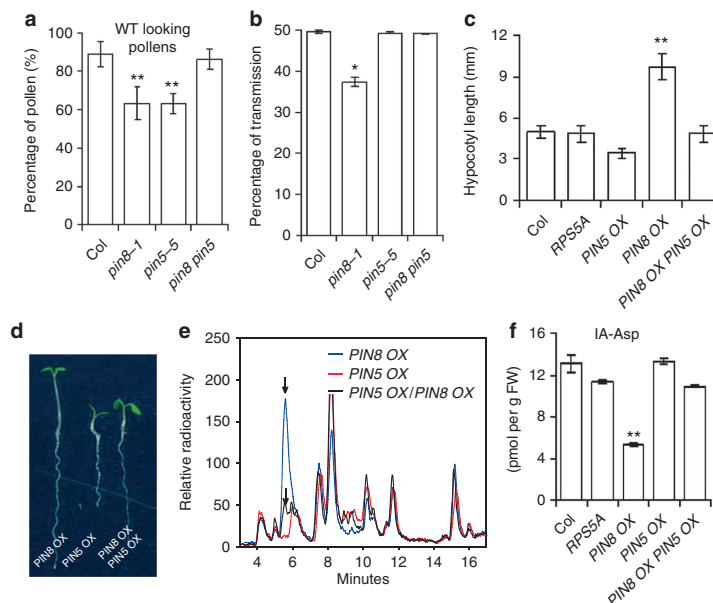
**Figure 5 | PIN8 and PIN5 act antagonistically.** (**a**) Morphological defects in pollen of *pin5* (2,400) and *pin8* (2,400) single mutants were rescued in *pin5 pin8* (3,300) double mutants as shown by DAPI staining. A total of 7,100 wild-type (WT) pollens were counted as the control. Error bars represent the standard error of more than 23 independent plants (Student's *t*-test, **P < 0.01). (**b**) The reduced pollen transmission ability in the *pin8* mutant was rescued in the *pin5 pin8* double mutant. Error bars represent the standard error of more than ten independent crosses (Student's *t*-test, *P < 0.5). (**c,d**) The long hypocotyl phenotype of the *PIN8OX* line was rescued in the *PIN8OX PIN5OX* line. Error bars represent the standard error of three independent experiments (*n* = 60, Student's *t*-test, **P < 0.01). (**e**) Specific HPLC chromatogram of IAA metabolic profile of *PIN8OX* was largely rescued in the *PIN8OX PIN5OX* line (2.5-h incubation with ^{3}H-IAA). Arrows indicate the notable changes in the IAA metabolic profile. (**f**) The decreased IA-Asp of the *PIN8OX* line was rescued in the *PIN8OX PIN5OX* line. Error bars represent the standard error of the mean, *n* = 3 (Student's *t*-test, *P < 0.05).

To assess the role of PIN8 in IAA metabolism, we analysed the IAA metabolic profile of *PIN8OX* transgenic seedlings through high-performance liquid chromatography (HPLC). *PIN8* over-expression remodelled the IAA metabolism as demonstrated by the pronounced changes in the HPLC profile (Fig. 4e). Direct analysis by ultra-high-performance liquid chromatography coupled to tandem mass detection of the selected IAA conjugates confirmed the changes in the IAA metabolic profile and showed that the *PIN8OX* line had a decreased capacity to produce amino-acid conjugates, such as IA-Asp (indole-3-acetyl-aspartate), IA-Glu (indole-3-acetyl-glutamate) or OxIAA (oxindole-3-acetic acid; Fig. 4f,g). These results demonstrated that the ER-localized PIN8 auxin transporter, similar to PIN5, is also involved in the regulation of auxin homoeostasis.

**PIN8 and PIN5 act antagonistically**. To gain additional insights into the roles of PIN5 and PIN8, we systematically compared the loss-of-function and overexpression lines and also generated the *pin5 pin8* double mutants and the *PIN8OX PIN5OX* double trans-genic plants. Similar to *pin8*, *pin5* was also defective in pollen morphology (Figs 1b, 5a), but, in contrast to the single *pin5* mutant, the *pin5 pin8* double mutant largely rescued the pollen morphology defects and the *pin8* defect in transmission through the male gametophyte (Fig. 5a,b). Thus, the *pin5* and *pin8* loss-of-function mutants compensated to a large extent each other in male gametophyte development and function.

Regarding the overexpression lines, *PIN5OX* seedlings had shorter hypocotyls[24], whereas *PIN8OX* seedlings had strikingly longer hypocotyls than the wild-type control (Fig. 5c,d). These overexpression effects were also rescued in the *PIN8OX PIN5OX* double overexpressing line (Fig. 5c,d). In addition, we also observed that *pin5* significantly enhanced the long hypocotyl phenotype of *PIN8OX* further supporting the antagonistic roles of PIN5 and PIN8 (Supplementary Fig. S9a). The same could be observed for the flowering time. Under long-day conditions, *PIN8OX* plants flowered earlier than the control, whereas *PIN5OX* plants flowered significantly later (Supplementary Fig. S9b,c) and the *PIN8OX PIN5OX* plants flowered at a time that was comparable to the control plants (Supplementary Fig. S9b,c). These different observations are also consistent with previous observations on the opposite action of PIN5 and PIN8 in root hair development[31]. Thus, both the loss-of-function mutants and overexpression lines of *PIN5* and *PIN8* can largely compensate each other in regulating different developmental processes, suggesting antagonistic roles of these two ER-localized PIN proteins.

Next, we tested genetic interaction between PIN5 and PIN8 in regulating auxin homoeostasis. In the *PIN8OX* line, both free IAA measurements and enhanced *DR5::GUS* activity consistently suggested increased free IAA levels (Fig. 4), whereas *PIN5OX* had been shown to have decreased auxin levels[24]. To test the possible antagonistic roles of PIN5 and PIN8 in the regulation of auxin metabolism, we measured free IAA levels in *PIN8OX PIN5OX* double transformants. This analysis revealed that, similar to morphological phenotypes, the increased free IAA levels in *PIN8OX* were largely rescued in the *PIN8OX PIN5OX* line that exhibited free IAA levels

comparable to those of the control lines (Supplementary Fig. S10a). The increased IAA export in protoplasts prepared from *PIN8 OX* also phenocopies *pin5* mutant (Supplementary Fig. S10b). Moreover, notable changes in the IAA metabolic profile of *PIN8OX* seedlings as demonstrated by the HPLC spectrum were also largely rescued in *PIN8OX PIN5OX* lines (Fig. 5e). Accordingly, liquid chromatography–tandem mass spectroscopeanalysis confirmed that the decreased capacity of *PIN8OX* seedlings to conjugate IAA to amino acids was rescued in the *PIN8OX PIN5OX* lines (Fig. 5f).

Overall, the opposite and mutual compensatory effects of *pin5* and *pin8* loss-of-function and overexpression alleles on male gametophyte and sporophyte phenotypes as well as on auxin homoeostasis and metabolism revealed that PIN5 and PIN8 act antagonistically. This strongly suggests that PIN5 and PIN8 localized both at the same subcellular compartment (ER) can have distinct roles.

## Discussion

In conclusion, this study identified auxin transporter PIN8 with a strong expression in a male gametophyte and revealed a role for auxin transport in regulating pollen development and function. Our results, including localization, auxin transport as well as genetic and physiological analyses, showed that, although both PIN8 and PIN5 auxin transporters are localized at the ER, they can have antagonistic roles in regulating gametophyte and sporophyte development, cellular auxin homoeostasis and metabolism. PIN5 has been proposed to transport auxin intracellularly from the cytoplasm into the ER, where enzymes involved in IAA metabolism are compartmentalized[6], thus reducing the auxin availability for the PM-based auxin efflux[24]. It is unclear how PIN8 localized to the same intracellular compartment, namely ER, can act antagonistically but it suggests more complex functional interaction between PIN proteins than anticipated so far. A possible scenario would envision transient or more stable interaction of PIN5 and PIN8 negatively regulating each other transport capabilities. Notably, PIN8 activity in *Arabidopsis* is required only in male gametophyte. It is known that developing and germinating pollen has high levels of auxin[32], but the auxin role there is unclear. Thus, it is possible that specifically during pollen development, the ER-localized PIN transporters regulate the release of auxin from the internal stores in the ER to drive auxin-mediated pollen tube elongation.

The finding that some PIN proteins localize to the ER and other to the PM brings about an interesting question, namely, which of these functions and cellular localizations is ancestral and which physiological and developmental role did this ancestral PIN protein play. In the moss *Physcomitrella*, the most typical member of PIN clade localizes to ER, when expressed in BY-2 tobacco cells[24]. As in most ancestral land plants, the gametophyte generation is predominant, the male gametophytic PIN8 might represent a more ancestral form of auxin transporters that were at the ER involved in regulating subcellular auxin homoeostasis, before they acquired PM localization and new function in mediating auxin transport between cells for mediating development of higher plants. Nonetheless, also in higher plants, different ER-localized PIN proteins, including *Arabidopsis* PIN5, PIN8 and possibly also PIN6, have spatially and/or temporally distinct expression patterns[24] that can fine-tune the cellular free IAA levels optimal for plant growth and reproduction.

## Methods

**Plant material and DNA constructs**. For all experiments, we used *Arabidopsis thaliana* ecotype Columbia (Col). Insertion mutant lines were *pin5-5* (ref. 24), *pin8-1* (Salk_107965) and *pin8-2* (Salk_044651). Transgenic lines were *DR5::GUS*[29], *DR5rev::GFP*[33], *RPS5A::GAL4* (ref. 34) and *RPS5A > >PIN5-myc* (*PIN5 OX*)[24]. *pin5 pin8* double mutants and the *PIN8OX PIN5OX* double transgenic plants were generated through crossing *pin5-5* with *pin8-1* or crossing *PIN8OX* with *PIN5OX*. All SALK lines were obtained from the Nottingham Arabidopsis Stock Center. The *35S::PIN8-GFP* (*PIN8 OX*) line was generated by

transformation of the ecotype Columbia (Col) with the *35S::PIN8-GFP* (*PIN8OX*) construct[24]. The *LAT52ΔPIN8* line was generated via replacing the *35S* promoter with the *LAT52* promoter and transformed to the Colecotype. The primers used for cloning the *LAT52* promoter are described in Supplementary Table S3.

**Growth conditions**. Seeds were sterilized with chlorine gas and stratified at 4°C for 3 days in the dark. Seedlings were grown vertically on half Murashige and Skoog (MS) medium supplemented with 1% sucrose and respective drugs. Drugs were purchased from Sigma-Aldrich. Plants were grown under the stable long-day (16 h light/8 h dark) or short-day (8 h light/16 h dark) conditions at 19°C in growth chambers.

**Phenotype analyses and GUS (β-glucuronidase) staining**. Plates were scanned on a flat-bed scanner and hypocotyl lengths were measured with the ImageJ (http://rsb.info.nih.gov/ij/) software. GUS staining was done as described[35].

**Microscopy analysis**. The immunological analyses were done as previously described[36]. Details on antibodies and dilutions can be found in the later section. GFP samples were scanned without fixation. For confocal microscopy images, Zeiss LSM 510 or Olympus FV10 ASW confocal scanning microscopes were used.

**Pollen transmission assays**. We used the *PIN3::PIN3-GFP* line for the transmission wild-type controls. Pollen from the hetero *PIN3::PIN3-GFP*, hetero *pin8-1* or hetero *LAT52::PIN8* was used as a pollen donor, and crossed with Col female. Wild-type control–here is the hetero *PIN3::PIN3-GFP* line–showing around 50% transmission that was confirmed via antibiotic selection of the resulted seedlings. *pin8-1*and *LAT52::PIN8* transmission was assessed by PCR analysis or antibiotic selection of the resulted seedlings.

**Auxin measurements and transport assays**. Free IAA measurements and IAA metabolic profiling were done as described[24]. For protoplast transport assays, protoplasts prepared from loss-of-function mutant and overexpression lines were loaded under controlled conditions (loading is performed on ice in order to minimize transport processes with identical amounts of cells and radioactivity) leading to highly comparable loading of cells[22]. Loaded cells were then temperature shifted to 25°C enabling catalysed auxin transport (of course both over the ER and PM membrane), and after defined time-points supernatants (containing effluxed radioactivity) were separated from cells by silicon oil centrifugation and quantified. For IAA conjugate quantification, ~10 mg of plant material was taken for analysis. The samples were processed as described[37] and quantified by ultra-high-performance liquid chromatography coupled to tandem mass detection.

**Auxin transport assays in ER-enriched microsomal fractions**. *Arabidopsis* plants grown in liquid culture were homogenized using razor blade in 5 ml of 0.5 M sucrose, 0.1 M $KH_2PO_4$ (pH 6.65), 5 mM $MgCl_2$ and 1 mM dithiothreitol (freshly added). Membranes were separated following the procedure described by Muñoz *et al.*[38,39]. Briefly, the homogenate was filtered through miracloth (Calbiochem) and centrifuged at 3,000 *g* for 3 min. The supernatant was then layered on 5 ml of a 1.3 M sucrose cushion and centrifuged at 108,000 *g* for 90 min. The upper phase was removed without disturbing the interface fraction and sucrose layers of 1.1, 0.7 and 0.25 M were overlaid on the membrane pad. The discontinuous sucrose gradient was then centrifuged at 108,000 *g* for 90 min. The 1.1/1.3 M interface enriched in ER membranes was collected, diluted and centrifuged separately at 108,000 *g* for 50 min, the pellet was resuspended in 200 µl of 0.5 M sucrose, 0.1 M $KH_2PO_4$ (pH 6.65) and 5 mM $MgCl_2$ and stored at −80°C until use.

ER-enriched membranes, obtained as described above, were used to perform [3H]-IAA uptake assays, based on a filtration method previously described[39]. A total of 50 µg of protein from the ER-enriched membrane fraction were resuspended in a buffer containing 250 mM sucrose, 20 mM KCl, 25 mM Tris–HCl (pH 7). The reaction was initiated by adding 100 µl of 50 nM [3H]-IAA (20 nCi), to reach 1 ml, final volume. Aliquots were taken at different times and filtered through 0.45-µm cellulose–ester filters (Millipore), previously treated with 250 mM sucrose, 20 mM KCl, 25 mM Tris–HCl (pH 7) and 1 mM IAA. The reaction was stopped by filtering and immediate wash using 5 ml of ice-cold 250 mM sucrose, 20 mM KCl, 25 mM Tris–HCl (pH 7) and 1 mM IAA. The filters were air-dried and the remaining radioactivity was measured in a liquid scintillation counter. The uptake of 3H-IAA is reported in 'nmol of [3H]-IAA/mg of protein'.

**Whole-mount immunolocalization and lifetime confocal microscopy**. Whole-mount immunological staining on 4-day-old seedlings was done in an Intavis robot. Antibodies were used at the following dilutions: rabbit anti-BIP2 (Hsc70), 1:200 (Stressgen Bioreagents); mouse anti-GFP, 1:600 (Roche); rabbit anti-myc, 1:600 (Sigma-Aldrich). Anti-rabbit and anti-mouse antibodies conjugated with Cy3 or fluorescein isothiocyanate (Dianova, Germany) were used at 1:600 dilutions. For ER-tracker dye labelling, *PIN8::PIN8–GFP* seedlings were mounted in water with a 1:1,000 dilution of ER-tracker dye (Invitrogen). Brefeldin A treatment for 2 h was performed by incubation of 4-day-old etiolated seedlings on solid MS medium supplemented with brefeldin A (50 µM), counterstaining of cell walls was achieved by mounting seedling roots in 10 µM propidium iodide.

# ARTICLE

**Quantitative PCR analysis**. RNA was extracted with the Plant RNeasy kit (Qiagen). Poly(dT) complementary DNA was prepared from flower total RNA. Superscript III reverse transcription (Invitrogen) and quantification were done on a LightCycler 480 apparatus (Roche Diagnostics) with the SYBR Green I Master kit (Roche Diagnostics), according to the manufacturer's instructions. All individual reactions were done in triplicate. Data were analysed as described before[40]. The primers used to quantify gene expression levels are provided in Supplementary Table S3.

**Light and fluorescent microscopy**. For pollen phenotype observations, flowers from *pin* or Col-0 plants were collected to GUS buffer (0.1 M phosphate buffer, pH 7.0; 10 mM EDTA, pH 8.0; 0.1% triton X-100) supplemented with $100 \, ng \, ml^{-1}$ DAPI as described[41]. After 30-min incubation at room temperature in the dark, samples were analysed by bright-field and fluorescence microscopy with Nikon TE2000-E microscope (objective Nikon CFI Plan Fluor ELWD 10×/0.60, eyepiece Nikon CFI 10×/22, intermediate magnification ×1–×1.5; Nikon).

**Pollen germination *in vitro***. Pollens were collected from flowers opened day (day 0) of Col and *pin8-1* plants. Subsequently they were germinated on a germination medium on a microscope slide according to Boavida and McCormick[42]. Pollen germination medium was always prepared fresh from 0.5 M stock solutions of the main components (5 mM KCl, 0.01% $H_3BO_3$, 5 mM $CaCl_2$, 1 mM $MgSO_4$) using autoclaved water. Sucrose (10%) was added and pH was adjusted to 7.5 with NaOH. Low-melting agarose (Amresco, Solon, OH) was added to final 1.5% concentration and melted in a microwave oven. Pollen grains from three flowers were spread on the surface of 250 μl agarose germination pads on microscope slides covered by polypropylene foil by inverting the flower with the help of tweezers and gently bringing it onto agarose surface. The whole flower was used as a 'brush' to spread pollen uniformly. The slides were incubated upside down in a moisture incubation chamber for 16 h in the dark at 22 °C and 100% humidity. The samples were examined by bright-field microscopy using Nikon TE2000-E microscope (objective Nikon CFI Plan UW 2×/0.06, eyepiece Nikon CFI 10×/22, intermediate magnification ×1–×1.5). The germinating pollen was defined as a pollen with a clearly visible pollen tube with length at least 1 diameter of pollen grain. The germination was carried out overnight (16 h). The percentage of germinated pollen was scored manually from captured image. From each microscope slide, five to six individual areas were taken. For NAA pollen germination test, 1 μM NAA was dissolved in the germination medium to 100 nM final concentration.

## References

1. Leyser, O. The power of auxin in plants. *Plant Physiol.* **154**, 501–505 (2010).
2. Leyser, O. Auxin distribution and plant pattern formation: how many angels can dance on the point of PIN? *Cell* **121**, 819–822 (2005).
3. Santner, A. & Estelle, M. Recent advances and emerging trends in plant hormone signalling. *Nature* **459**, 1071–1078 (2009).
4. Kepinski, S. & Leyser, O. Plant development: auxin in loops. *Curr. Biol.* **15**, R208–210 (2005).
5. Chapman, E. J. & Estelle, M. Mechanism of auxin-regulated gene expression in plants. *Annu. Rev. Genet.* **43**, 265–285 (2009).
6. Woodward, A. W. & Bartel, B. Auxin: regulation, action, and interaction. *Ann. Bot.* **95**, 707–735 (2005).
7. Grunewald, W. & Friml, J. The march of the PINs: developmental plasticity by dynamic polar targeting in plant cells. *EMBO J.* **29**, 2700–2714 (2010).
8. Vanneste, S. & Friml, J. Auxin: a trigger for change in plant development. *Cell* **136**, 1005–1016 (2009).
9. Pagnussat, G. C., Alandete-Saez, M., Bowman, J. L. & Sundaresan, V. Auxin-dependent patterning and gamete specification in the Arabidopsis female gametophyte. *Science* **324**, 1684–1689 (2009).
10. Wu, M.- F., Tian, Q. & Reed, J. W. Arabidopsis microRNA167 controls patterns of ARF6 and ARF8 expression, and regulates both female and male reproduction. *Development* **133**, 4211–4218 (2006).
11. Feng, X.- L. *et al.* Auxin flow in anther filaments is critical for pollen grain development through regulating pollen mitosis. *Plant Mol. Biol.* **61**, 215–226 (2006).
12. Cecchetti, V., Altamura, M. M., Falasca, G., Costantino, P. & Cardarelli, M. Auxin regulates *Arabidopsis* anther dehiscence, pollen maturation, and filament elongation. *Plant Cell* **20**, 1760–1774 (2008).
13. Chen, D. & Zhao, J. Free IAA in stigmas and styles during pollen germination and pollen tube growth of Nicotiana tabacum. *Physiol. Plant* **134**, 202–215 (2008).
14. Zhao, Y. Auxin biosynthesis and its role in plant development. *Annu. Rev. Plant Biol.* **61**, 49–64 (2010).
15. Stepanova, A. N. *et al.* TAA1-mediated auxin biosynthesis is essential for hormone crosstalk and plant development. *Cell* **133**, 177–191 (2008).
16. Ikeda, Y. *et al.* Local auxin biosynthesis modulates gradient-directed planar polarity in Arabidopsis. *Nat. Cell Biol.* **11**, 731–8 (2008).
17. Petrášek, J. & Friml, J. Auxin transport routes in plant development. *Development* **136**, 2675–2688 (2009).
18. Swarup, R. & Bennett, M. Auxin transport: the fountain of life in plants? *Dev. Cell* **5**, 824–826 (2003).
19. Swarup, K. *et al.* The auxin influx carrier LAX3 promotes lateral root emergence. *Nat. Cell Biol.* **10**, 946–954 (2008).
20. Petrášek, J. *et al.* PIN proteins perform a rate-limiting function in cellular auxin efflux. *Science* **312**, 914–918 (2006).
21. Noh, B., Murphy, A. S. & Spalding, E. P. Multidrug resistance-like genes of Arabidopsis required for auxin transport and auxin-mediated development. *Plant Cell* **13**, 2441–2454 (2001).
22. Geisler, M. *et al.* Cellular efflux of auxin catalyzed by the Arabidopsis MDR/PGP transporter AtPGP1. *Plant J.* **44**, 179–94 (2005).
23. Křeček, P. *et al.* The PIN-FORMED (PIN) protein family of auxin transporters. *Genome Biol.* **10**, 249–256 (2009).
24. Mravec, J. *et al.* Subcellular homeostasis of phytohormone auxin is mediated by the ER-localized PIN5 transporter. *Nature* **459**, 1136–1140 (2009).
25. Dupáková, N. *et al.* Arabidopsis Gene Family Profiler (aGFP)—user-oriented transcriptomic database with easy-to-use graphic interface. *BMC Plant Biol.* **7**, 39: 10.1186/1471-2229-7-39 (2007).
26. Peer, W. A. *et al.* Mutation of the membrane-associated M1 proteaseAPM1 results in distinct embryonic and seedling developmental defects in *Arabidopsis*. *Plant Cell* **21**, 1693–1721 (2009).
27. Sánchez-Morán, E. *et al.* A puromycin-sensitive aminopeptidase is essential for meiosis in *Arabidopsis thaliana*. *Plant Cell* **16**, 2895–909 (2004).
28. Ishikawa, F., Suga, S., Uemura, T., Sato, M. H. & Maeshima, M. Novel type aquaporin SIPs are mainly localized to the ER membrane and show cell-specific expression in *Arabidopsis thaliana*. *FEBS Lett.* **579**, 5814–5820 (2005).
29. Ulmasov, T., Liu, Z. B., Hagen, G. & Guilfoyle, T. J. Composite structure of auxin response elements. *Plant Cell* **7**, 1611–1623 (1995).
30. Reyes, F., León, G., Donoso, M., Brandizzí, F., Weber, A. P. & Orellana, A. The nucleotide sugar transporters AtUTr1 and AtUTr3 are required for the incorporation of UDP-glucose into the endoplasmic reticulum, are essential for pollen development and are needed for embryo sac progress in *Arabidopsis thaliana*. *Plant J.* **61**, 423–35 (2010).
31. Ganguly, A. *et al.* Differential auxin-transporting activities of PIN-FORMED proteins in Arabidopsis root hair cells. *Plant Physiol.* **153**, 1046–1061 (2010).
32. Aloni, R., Aloni, E., Langhans, M. & Ullrich, C. I. Role of auxin in regulating Arabidopsis flower development. *Planta* **223**, 315–328 (2006).
33. Friml, J. *et al.* Efflux-dependent auxin gradients establish the apical-basal axis of Arabidopsis. *Nature* **426**, 147–153 (2003).
34. Weijers, D. *et al.* Maintenance of embryonic auxin distribution for apical-basal patterning by PIN-FORMED-dependent auxin transport in Arabidopsis. *Plant Cell* **17**, 2517–2526 (2005).
35. Benková, E. *et al.* Local, efflux-dependent auxin gradients as a common module for plant organ formation. *Cell* **115**, 591–602 (2003).
36. Sauer, M., Paciorek, T., Benková, E. & Friml, J. Immunocytochemical techniques for whole mount *in situ* protein localization in plants. *Nat. Protoc.* **1**, 98–103 (2006).
37. Pencik, A. *et al.* Isolation of novel indole-3-acetic acid conjugates by immunoaffinity extraction. *Talanta* **80**, 651–655 (2009).
38. Munoz, P., Norambuena, L. & Orellana, A. Evidence for a UDP-glucose transporter in Golgi apparatus-derived vesicles from pea and its possible role in polysaccharide biosynthesis. *Plant Physiol.* **112**, 1585–1594 (1996).
39. Liang, F. & Sze, H. A high-affinity Ca2+ pump, ECA1, from the endoplasmic reticulum is inhibited by cyclopiazonic acid but not by thapsigargin. *Plant Physiol.* **118**, 817–825 (1998).
40. Ding, Z. J. *et al.* Auxin regulates distal stem cell differentiation in Arabidopsis roots. *Proc. Natl Acad. Sci. USA* **107**, 12046–120 (2010).
41. Park, S. K., Howden, R. & Twell, D. The *Arabidopsis thaliana* gametophytic mutation gemini pollen disrupts microspore polarity, division asymmetry and pollen cell fate. *Development* **125**, 3789–3799 (1998).
42. Boavida, L. C. & McCormick, S. Temperature as a determinant factor for increased and reproducible *in vitro* pollen germination in *Arabidopsis thaliana*. *Plant J.* **52**, 570–582 (2007).

## Acknowledgements

## ARTICLE

**Author contributions**

J.F., Z.D., A.M. and M.G. planned experiments. B.W., N.D., S.S., P.S., A.P., S.P., J.M., X.C., I.M., N.C., J.R. (Jesica Reemmer) and Z.D. performed experiments. J.F., Z.D., M.G., D.H., J.P., J.R. (Jakub Rolčík), X.C., I.M., A.O., R.T. and E.Z. analysed the data. J.F. and Z.D. wrote the paper. All authors discussed the results and commented on the manuscript.

**Additional information**

**Supplementary Information** accompanies this paper at http://www.nature.com/naturecommunications

**Competing financial interests**: The authors declare no competing financial interests.

**Reprints and permission** information is available online at http://npg.nature.com/reprintsandpermissions/

**How to cite this article:** Ding, Z. *et al.* ER-localized auxin transporter PIN8 regulates auxin homoeostasis and male gametophyte development in *Arabidopsis. Nat. Commun.* 3:941 doi: 10.1038/ncomms1941 (2012).

VITA

VITA

I am originally from Leo, Indiana, and I received my Bachelors of Science in both Plant Sciences and Biochemistry and Biotechnology with high honors at Michigan State University. While at Purdue, I was a graduate student in the Interdisciplinary Life Science (PULSe) program, and my major advisor was Angus Murphy. My Master's thesis concerns the characterization the ABCB transporter B11 and its effects on auxin transport, at both the subcellular and whole plant level. I also worked with *twd1-3* and related mutants of auxin transport to serve as comparative models.

Before starting on my thesis project, I worked on a number of projects to expand my repertoire of techniques. During my rotation in the Murphy-Peer lab, I assisted Dr. Haibing Yang in the determination of auxin transport capacity of the LAX (LIKE AUXIN1) proteins of the small AUX/LAX family. Through this project, I gained essential experience in the growth and preparation of *S. pombe* yeast for use in $^{3}$H-IAA transport assays, and the interpretation of the resultant data. I also contributed to an ongoing investigation of the subcellular localization of PIN auxin family transporters PIN5 and PIN8. Of particular use, I learned how to precisely prepare sucrose density gradients and analyze the resultant fractions via immunochemistry and western blotting. Both projects resulted in authorship on published articles (found in appendix).